Reply to Anonymous Referee #1 comments

We thank the Reviewer#1 for her/his valuable comments that greatly contributed to the improvement and readability of the present manuscript.

In the revised version of the manuscript the replies to the comments from Reviewer#1 are highlighted with the green color.

General Comments:

> **This manuscript deals with the evaluation of the relative contribution of rural and urban sources for the urban aerosol measured in 5 countries of Europe, by using PMF source apportionment of aerosol samples collected in parallel in rural and urban areas.**
> **The evaluation methodology and the results are interesting and the results merit to be published.**
>
> **Unhappily the manuscript is not well written. It is too long and with several sections too descriptive, making the paper difficult to follow and repeating the reasoning and conclusions in various sections. The data has the problem of being taken from several research initiatives with methodologies of sampling, analysis and data treatment that are different, which makes more difficult to intercompare the results between the various European regions. For some of the sites and data the source apportionment results have already been published and it is not worthwhile to repeat the simple source apportionment results and discussion. There is also an important fraction of the text that mostly repeats the information that already is given in figures and tables.**

Thanks to the comments raised by the Reviewers the text has been considerably shortened compared to the original version. Comment #2 below addresses the Reviewer question about the comparability of the results despite the use of different methodologies for uncertainties calculation.

> **In my opinion the present manuscript should concentrate and put most of the effort in the spatial increments using the Lenschow's approach to evaluate in each country the incremented contributions of urban areas in relation to regional contributions, of the aerosol mass and aerosol source groups. Sections such as Section 3.3 should be reduced and if possible integrated in the spatial increments approach sections.**

We agree with the Reviewer that the Section 3.3 was too long. Consequently, this Section was considerably shortened in the revised version of this manuscript. We shortened the text and removed Figures 3, 4, and S7 (annual cycle of source contributions). Following the Reviewer's comment #9 below, we moved from the Supporting material to this Section Figures S8 and S9 in order to better follow the discussion about primary emissions of sulfate from ships.

Specific Comments:

1) **Line 28- Abstract- the Abstract is too long and too descriptive of results- reduce and concentrate in the more prominent outcomes from spatial increment conclusions.**

We have attempted to reduce and consolidate it. This paper is multifaceted and provides much information. We need to provide the reader with a sufficient amount of information that they can make an informed decision about reading it.

2) **Line133 and following- Quite different methodologies were used for calculating uncertainties in the data base used for PMF in each country. Which is the influence of these variable approaches in the uncertainty of the final results? This subject should be discussed in the manuscript. How were estimated the uncertainties for EC, OC and sugars?**

The treatment of uncertainties has a significant effect on the outputs of PMF results. For this reason, it is important to perform some tests which help understanding if the uncertainties are properly estimated. These tests can be performed for example studying if the scaled residuals are within the range of −3 and +3 of the standard deviation and if the bootstrap results can be mapped for all the factors. However, there is not just only one rule to estimate the species uncertainties in the PMF. In fact, the uncertainties calculation depends on the information available for each database and the techniques used for the determination of chemical species concentration. For this reason, different formulas are reported in literature (and in the present manuscript) and considered equally valid. What is important is that the applied formulas allow weighting the uncertainties as function of the specie concentrations. So higher uncertainties are given to species with low concentrations and the data with more information content has a greater weight in determining the results. In the present manuscript, the different methodologies we used for uncertainties calculation were based on sensitivity studies performed by the data providers (and published in previous publications). For example, the uncertainties used here for the French database were based on sensitivity studies performed by Waked et al. (2014). Based on this sensitivity study, Waked et al. (2014) selected the uncertainties providing the best and stable PMF solution. Similarly, the uncertainties used in the Spanish database were based on the sensitivity studies performed by Amato et al. (2009) and Escrig et al. (2009). These different schemes used for uncertainties calculation led to stable PMF results and can be considered as equally valid. Thus, we assume that the influence on the final results of the variable approaches applied here for uncertainties estimation is minimal because the formulas we applied were tested and were demonstrated to provide stable and robust PMF outputs. Also, as long as the uncertainties err on the side of being too large (greater downweighting), there is little probability of serious errors in the analysis. Downweighting rarely perturbs the solution. The bigger issue is having too small uncertainties. That is generally easily observed through seeing a variable be placed in many profiles, often where it would not be expected to be present in order to provide the fit to the specified level of precision.

For EC and OC, expanded relative uncertainties were calculated to account for the uncertainty in the split point position of the thermo-optical technique used to determine the concentrations of OC and EC. For the French, Spanish and Swiss databases 10%-15% for OC and EC (Cavalli et al., 2010) were added (e.g. Waked et al., 2014). Moreover, a 15% uncertainty was added for monosaccharide sugars (French database) such as levoglucosan, arabitol, sorbitol and mannitol (e.g. Piot et al., 2012; Waked et al., 2014). Again such downweighting is not going to undermine the quality of the results.

The following sentence was added to the Section 2.1:

"For EC and OC, expanded relative uncertainties were calculated to take into account for the uncertainty in the split point position of the thermo-optical technique used to determine the concentrations of OC and EC. For the French, Spanish and Swiss databases 10%-

15% for OC and EC (Cavalli et al., 2010) were added (e.g. Waked et al., 2014). Moreover, a 15% uncertainty was added for monosaccharide sugars (French database) such as levoglucosan, arabitol, sorbitol and mannitol (e.g. Piot et al., 2012; Waked et al., 2014). The different schemes used here for uncertainties calculation were tested by data providers and their robustness demonstrated in previous publications. Thus, despite the different methodologies, the presented final PMF results were stable and their robustness estimated using bootstrapping resampling and studying the distribution of the scaled residuals for each variable (e.g. Paatero et al., 2002)."

3) **Line 281 and following- The description of sampling sites characteristics is too long. Try to reduce the length of the text referring to other publications where these descriptions have already been done.**

Following the Reviewer comment, the Section 2.3 was considerably reduced.

4) **Line 413 and following- Most of the discussion presented here is repeated in the following sections.**

Following the Reviewer comment the Section 3.1 (PMF sources) was shortened in order to avoid repetitions in the text.

5) **Line 456- WISC (water insoluble carbon; sum of EC and WISC). ??- The second WISC shouldn't be WIOC (water insoluble organic carbon)?**

This was a mistake. The sentence was changed, as presented in van Pinxteren et al. (2016), as follows:
"….high mass contributions of WISC (water insoluble carbon; i.e. EC + hydrophobic organics)"

6) **Line 491 and following- this subsection is difficult to follow because it is the result of previous studies and possibly not all information is provided here. For example "Cooking" can't be characterised only by WISC and WSOC.**

We agree with the reviewer that the sentence is difficult to follow as it is. Consequently, we changed the text presenting only the list (with a very short description were necessary) of the six additional sources found in DE and providing the reference to the original paper were these sources were better described (i.e. van Pinxteren et al. (2016)). In this way we further reduce the length of the text. Moreover, these sources were grouped together in the following of the manuscript and a detailed description is not needed here.
Accordingly, the sentence was changed as follows:
"Six additional sources were detected only in DE, namely: sea salt/road salt (SSRS; an SS source with influence of road salt for de-icing), Coal combustion (CC) and Local coal combustion (this latter contributing mostly at the EIB site, which was removed from this analysis),

Photochemistry (PHO; with high mass contributions of NH_4^+ and SO_4^{2-} and WSOC), Cooking, and Fungal spores. A detailed description of these additional sources can be found in van Pinxteren et al. (2016)."

7) **Line 543- Table 1- Why in Spain the "Sea Salt" source is not considered "Aged Sea Salt"? Even in Barcelona more than 50% of the CL- has already been evaporated and substituted by SO4/NO3-.**

We agree with the reviewer that a better definition of sea salt source in Spain is "*Aged sea salt*". The text and Table1 were accordingly changed.
Moreover, in order to further shorten the text and following the Reviewer's comments #9 AND 10 (below), we moved the Table 1 to the Supporting Material leaving more room in the main text to discuss the theme of ship emissions of sulphur and primary sulphate. The Section 3.2 "Feasibility of the multi-site PMF" was accordingly changed.

8) **Lines 589-590- Did not understood the objective of this sentence.**

Following some Reviewer comments, i.e. avoiding repetitions and shortening the text and especially Section 3.3, the sentence has been removed from the text.

9 AND 10) Line 592- Here the theme of ship emissions of sulphur and primary sulphate is initiated. This interesting theme is discussed in various parts of the paper which makes difficult to fully understand the relative importance of the emission source. If Ship emissions are so relevant in Europe why PMF could not separate a ship emission source, at least for coastal areas?

10) **Line 699 and following – Here and throughout the text Figures and Tables in the Annex Section are used in the discussion of results. In my opinion Figures and Tables in the Annex should exist only as complementary information. If these figures and Tables need to be used to follow a discussion and to demonstrate a statement in the text they have to be added to the main part of the paper.**

Maritime shipping can potentially be an important source of pollutant especially in port towns. As explained in the present manuscript (cf. Section 3.3 and Conclusion section), the fundamental tracers of ship emissions, i.e. V and Ni, must be measured (especially the V) to properly detect this source thorough application of PMF. In the present work, both V and Ni were available in Spain and The Netherlands (where the shipping source was detected), whereas only V was available in Switzerland (where the shipping source was not detected). In France and Germany the concentrations of V were not available thus preventing the detection of the maritime shipping source. The concentrations of V in the Zurich (Switzerland) were about one order of magnitude lower compared to the V concentrations measured in Barcelona, mostly because the distance of Zurich from shipping emissions (coastline and major ports) or other sources of residual oil combustion. For this reason, the shipping source was not detected in Switzerland.

For example in Gianini et al. (2012), the Ni was excluded from PMF analysis because of its very low signal-to-noise ratio, demonstrating the small effect of residual oil combustion sources (such as shipping) at the Swiss sites.

To address the Reviewer's comment, we moved Figures S8 and S9 in supporting material to the main text. Moreover, Table 1 (feasibility of multi-site PMF) was moved to supporting material.

11) Line 729- "showed" instead of "slowed"?

Is "slowed". We meant that for the four additional sites included in this work (where more recent (2013-2014) data were available) the primary SSA produced for every 1 $\mu g/m^3$ of residual oil was lower compared to 2007-2008.

12) Line 782 and following- Some information should be provided about the precision/ accuracy of urban and regional estimations of aerosol mass and source classes.

Estimating the accuracy of urban and regional estimations from application of the Lenschow's approach is extremely difficult if not even unmanageable. There are important sources of errors such as meteorology on a daily base that are difficult to manage. For this reason, we selected chemically speciated PM datasets covering at least one year and presented average values to reduce all possible sources of error. The comparability of the calculated estimations among the selected countries and the agreement with previous studies is used here to prove the robustness of the analysis.
In order to further demonstrate the feasibility of the of the present work, we report in supporting material the results of the bootstrapping resampling from PMF which is used to prove the robustness of the detected sources.

13) Line 815 and following.- In the paper the word "increment" is used both for urban and regional/continental contributions to the aerosol. The use of the term for R+C is somehow confusing (increment in relation to what?). Substitute by contribution?

The main motivation to prefer the term "increment" to "contribution" is that "contribution" implies a univocal link to a given source. Referring to the increased concentration levels over the city as "urban contribution", implies that the city sources only contribute to air pollutant concentrations over the city, whereas they also contribute to background levels outside of the city, because of advection/diffusion referred to as "City Spread" in Thunis (Atmospheric Environment 173 (2018) 210–222).
Similarly, R+C is an increment compared to a clean background, we considered that referring to an R+C contribution, would ignore the fact that regional background also contributes to urban levels.

14) Lines 950-960- SSA does not need the NH3 in order to be high! NH3 merely neutralices the already formed sulphuric acid.

The sentence: "…and the high concentrations of NH3 measured in the city." Was removed from the text.

Long range and local air pollution: what can we learn from chemical speciation of particulate matter at paired sites?

Marco Pandolfi [a,*], Dennis Mooibroek [b], Philip Hopke [c], Dominik van Pinxteren [d], Xavier Querol [a], Hartmut Herrmann [d], Andrés Alastuey [a], Olivier Favez [e], Christoph Hüglin [f], Esperanza Perdrix [g], Véronique Riffault [g], Stéphane Sauvage [g], Eric van der Swaluw [b], Oksana Tarasova [h], and Augustin Colette [e]

[a] Institute of Environmental Analysis and Water Research (IDAEA-CSIC), c/ Jordi-Girona 18-26, Barcelona, Spain

[b] Centre for Environmental Monitoring, National Institute of Public Health and the Environment (RIVM), A. van Leeuwenhoeklaan 9, P.O. Box 1, 3720 BA, Bilthoven, The Netherlands

[c] Center for Air Resources Engineering and Science, Clarkson University, Potsdam, NY, USA

[d] Leibniz Institute for Tropospheric Research (TROPOS), Atmospheric Chemistry Department (ACD), Permoserstr. 15, 04318 Leipzig, Germany

[e] National Institute for Industrial Environment and Risks (INERIS), Verneuil-en-Halatte, 60550, France

[f] Empa, Swiss Federal Laboratories for Materials Science and Technology, 8600 Dübendorf, Switzerland

[g] IMT Lille Douai, Univ. Lille, SAGE – Département Sciences de l'Atmosphère et Génie de l'Environnement, 59000 Lille, France

[h] World Meteorological Organization, Research Department, Geneva, Switzerland

* Corresponding author: Marco Pandolfi (marco.pandolfi@idaea.csic.es)

Abstract

We report here results of a detailed analysis of the urban and non-urban contributions to PM concentrations and source contributions in 5 European cities, namely: Shiedam (The Netherlands; NL), Lens (France; FR), Leipzig (Germany; DE), Zurich (Switzerland; CH) and Barcelona (Spain; ES). PM chemically speciated data from 12 European paired monitoring sites (1 traffic, 5 urban, 5 regional and 1 continental background) were analyzed by Positive Matrix Factorization (PMF) and Lenschow's approach to assign measured PM and source contributions to the different spatial levels. Five common sources were obtained at the 12 sites: *sulfate-rich* (SSA) and *nitrate-rich* (NSA) aerosols, *road traffic* (RT), *mineral matter* (MM), and *aged sea salt* (SS). These sources explained from 55% to 88% of PM mass at urban low-traffic

impact sites (UB) depending on the country. Three additional common sources were identified at a subset of sites/countries, namely: *biomass burning* (BB) (FR, CH, and DE), explaining an additional 9-13% of PM mass, *residual oil combustion* (V-Ni), and *primary industrial* (IND) (NL and ES), together explaining an additional 11-15% of PM mass. In all countries, the majority of PM measured at UB sites was of regional+continental (R+C) nature (64-74%). The R+C PM increments due to anthropogenic emissions in DE, NL, CH, ES and FR represented around 66%, 62%, 52%, 32% and 23%, respectively, of UB PM mass. Overall, the R+C PM increments due to natural and anthropogenic sources showed opposite seasonal profiles with the former increasing in summer and the latter increasing in winter, even if exceptions were observed. In ES, the anthropogenic R+C PM increment was higher in summer due to high contributions from regional SSA and V-Ni sources, both being mostly related to maritime shipping emissions at the Spanish sites. Conversely, in the other countries, higher anthropogenic R+C PM increments in winter were mostly due to high contributions from NSA and BB regional sources during the cold season. On annual average, the sources showing higher R+C increments were SSA (77-91% of SSA source contribution at urban level), NSA (51-94%), MM (58-80%), BB (42-78%), IND (91% in NL). Other sources showing high R+C increments were *photochemistry* and *coal combustion* (97-99%; identified only in DE). The highest regional SSA increment was observed in ES, especially in summer, and was related to ship emissions, enhanced photochemistry and peculiar meteorological patterns of the Western Mediterranean. The highest R+C and urban NSA increments were observed in NL and associated with high availability of precursors such as NO_x and NH_3. Conversely, on average, the sources showing higher local increments were RT (62-90% at all sites) and V-Ni (65-80% in ES and NL). The relationship between SSA and V-Ni indicated that the contribution of ship emissions to the local sulfate concentrations in NL strongly decreased from 2007 thanks to the shift from high-sulfur to low-sulfur content fuel used by ships. An improvement of air quality in the 5 cities included here could be achieved by further reducing local (urban) emissions of PM, NO_x and NH_3 (from both traffic and non-traffic sources) but also SO_2 and PM (from maritime ships and ports) and giving high relevance to non-urban contributions by further reducing emissions of SO_2 (maritime shipping) and NH_3 (agriculture) and those from industry, regional BB sources and coal combustion.

1. Introduction

In the last scientific assessment report from the Convention on Long-Range Transboundary Air Pollution (CLRTAP) "Toward Cleaner Air", it is stated that because non-urban sources (i.e. regional+continental sources) are often major contributors to urban pollution, many cities will be unable to meet WHO guideline levels for air pollutants through local action alone. Consequently, it is very important to estimate how much the local and regional+continental (R+C) sources (both natural and anthropogenic) contribute to urban pollution in order to design global strategies to reduce the levels of pollutants in European cities.

There are various modelling approaches to disentangle the local/remote contribution to urban air pollution. But it is also relevant to investigate how in-situ measurements can be used for that purposed. The Task Force on Measurements and Modeling (TFMM-CLRTAP) therefore initiated an assessment of the added value of paired urban and regional/remote sites in Europe. Experimental data from paired sites were used to allocate urban pollution to the different spatial scale sources. The paired sites selected for this study provided chemically speciated PM_{10} or $PM_{2.5}$ data simultaneously measured at urban/traffic and regional/remote sites. In some cases, (e.g. Spain; ES) these measurements were continuously performed over long periods, whereas in other cases the measurements were performed for a limited time period. The periods presented here were comparable in Switzerland (CH; 2008-2009) and the Netherlands (NL; 2007-2008), whereas more recent data were used for Spain (ES; 2010 – 2014), Germany (DE; 2013-2014) and France (FR; 2013 – 2014).

The approach proposed and described in this paper aimed at identifying the urban and non urban (R+C) contributions (or a mix of both) to the PM mass measured at urban level and at calculating the urban increments that corresponds to the concentration difference between the city and the regional locations (Lenschow's approach; Lenschow et al., 2001). This method, detailed in Sect. 2.2 and developed by Lenschow et al. (2001), is based on measurements of atmospheric pollutants at sites of different typologies (i.e. rural and urban background) and has been widely used to discriminate the local and non-local increments (e.g. Pope et al., 2018; Petetin et al., 2014; Gianini et al., 2012 among others).

The uniqueness of the present work is that we were able to allocate urban and non-urban pollution to major primary sources by activity sector or to main secondary aerosol fractions thanks to the application of Positive Matrix Factorization (PMF) (described in Sect. 2.1) that quantitatively groups species emitted from the same source. The PMF is a widely used receptor model to perform PM source apportionment studies, identifying main sources of pollution and estimating their contributions to PM concentrations in ambient air (e.g. Hopke P.K., 2016; Liao et al., 2015; Amato et al., 2009; Kim and Hopke, 2007; Kim et al., 2003 among others). This information is useful for devising opportune abatement/mitigation strategies to tackle air pollution.

Chemistry Transport Models (CTMs) are regularly used to design air pollution mitigation strategies and a recurring question regards the identification of the main activity sectors and geographical areas that produce the pollutants. The performances of CTMs in this identification must therefore be compared to measurements. A first step consists in comparing the chemical composition of PM between models and observations. Such comparison has been performed before for specific areas or overall for Europe (Bessagnet et al., 2016), but the synthesis presented in the present paper will be particularly relevant to identify the main characteristics of the diversity of sites in terms of both chemical composition and urban/regional gradients. In a second step, a comparison with the models that provide a direct quantification of activity sectors is also relevant. Whereas CTMs focus essentially on chemical composition, some models (e.g. the TNO LOTOS-EURO; Kranenburg et al., 2013) include a tagging or source apportionment information (also referred to as source oriented models). However, we can also include Integrated Assessment Models such as GAINS (Amann et al., 2011; Kiesewetter et al., 2015) or SHERPA (Pisoni et al., 2017) or even the Copernicus Atmosphere Monitoring Service (CAMS) Policy Service (http://policy.atmosphere.copernicus.eu). In various ways, these tools propose a quantification of the priority activity sectors and scale for actions that must be targeted when designing air quality policies, although these models are challenging to compare with observations.

The scientific questions we are tackling here are distributed over two topics. The first one relates to the relative importance of local and remote air pollution sources. This aspect is of course the most directly connected to the policy expectations, but is also raises a number of scientific challenges that we address in an innovative manner by differentiating primary/secondary particulate matter of different types. The second one is more related to methodological developments. The approach we use here has already been explored for a given city/region. However, for the first time we intend to compare very different European regions, with also different monitoring strategies, which induce specific scientific questions in terms of consistency that were addressed throughout this work.

2. Methodology

The proposed methodology consists in the application of Lenschow's approach (Lenschow et al., 2001) to the source contributions calculated by means of PMF at appropriately paired sites to assess the increments of air pollution.

2.1 PMF model

PMF (EPA PMFv5.0) was applied to the collected daily PM speciated data for source identification and apportionment. PMF was applied to the PM chemically speciated data from ES, CH, and FR. For NL and DE, we used the PMF analysis already presented in Mooibroek et al. (2011) and van Pinxteren et al. (2016), respectively, and then applying the Lenschow approach to the PMF outputs.

Detailed information about PMF can be found in the literature (e.g. Paatero and Tapper, 1994; Paatero, 1999; Paatero and Hopke, 2003; Paatero and Hopke, 2008; Hopke, 2016). PMF is a factor analytical tool that reduces the dimension of the input matrix (i.e. the daily chemically speciated data) to a limited number of factors (or sources). It is based on the weighted least squares method and uses the uncertainties of the input data to solve the chemical mass balance equations. In the present study, individual uncertainties and detection limits were calculated in different ways, depending on the available information about analytical uncertainties.

One approach (applied to the Spanish database) was based on the use of both the analytical uncertainties and the standard deviations of species concentrations in the blank filters for uncertainties calculations. This approach was described in Escrig et al. (2009) and Amato et al. (2009). For the French sites, the uncertainty calculations for the trace elements was performed using the expanded relative uncertainties for each species and the total uncertainties were calculated by multiplying these relative uncertainties by the concentration of each species (Waked et al., 2014 and references herein). These relative uncertainties included variability from contamination, sampling volume, repeatability and accuracy (through the digestion recovery rate determinations). For the Swiss and Dutch sites, the uncertainties were estimated using information about the minimum detection limit (MDL) of the techniques used for chemical analysis. In this approach, data below the MDL were replaced by half the MDL and the corresponding uncertainty was set to 5/6 times the MDL (Polissar et al., 1998; Kim et al., 2003; Kim and Hopke, 2008). For the German sites, the uncertainty matrix was constructed from 3 components: (i) uncertainty of the instrumental limit of detection (LOD), defined as 5/6 of the LOD, (ii) analytical uncertainty, obtained from relative standard deviations of signal intensities from repeated standard measurements, and (iii) uncertainty of the mean field blank concentration, defined as 3 times the standard deviation of the field blank. Total uncertainty was calculated from these components applying Gaussian error propagation (details in van Pinxteren et al., 2016). For EC and OC, expanded relative uncertainties were calculated to take into account for the uncertainty in the split point position of the thermo-optical technique used to determine the concentrations of OC and EC. For the French, Spanish and Swiss databases 10%-15% for OC and EC (Cavalli et al., 2010) were added (e.g. Waked et al., 2014). Moreover, a 15% uncertainty was added for monosaccharide sugars (French database) such as levoglucosan, arabitol, sorbitol and mannitol (e.g. Piot et al., 2012; Waked et al., 2014).

The different schemes used here for uncertainties calculation were tested by data providers and their robustness demonstrated in previous publications. Thus, despite the different methodologies, the presented final PMF results were stable and their robustness estimated using bootstrapping resampling and studying the distribution of the scaled residuals for each variable (e.g. Paatero et al., 2002).

The signal-to-noise ratio (S/N) was estimated starting from the calculated uncertainties and used as a criterion for selecting the species used within the PMF model. In order to avoid any bias in the PMF results, the data matrix was uncensored (Paatero, 2004). The PMF was run in robust mode (Paatero, 1997). The optimal number of sources was selected by inspecting the variation of the objective function Q (defined as the ratio between residuals and errors in each data value) with a varying number of sources (e.g., Paatero et al., 2002).

2.1.1 Multi-site PMF

In this work, we used the chemically speciated data from 24h samples collected at the paired sites available in a country combining together the datasets from the available site pairs (multi-site PMF) as the PMF input. Thus, the hypothesis is that the chemical profiles of the sources are similar at the paired sites. If this hypothesis is not satisfied, then the multi-site PMF could lead to undesired uncertainties in the estimation of the source contributions. In the following sections, we demonstrate the feasibility of the multi-site PMF for each country. However, it is important to consider that we can only apply the Lenschow approach to exactly the same variables (same pollutant sources in this case) that can be only obtained through the application of the multi-site PMF.

To demonstrate the feasibility of the multi-site PMF, we compared the source profiles from the multi-site PMF with the source profiles from the individual single-site PMF results (Sofowote et al., 2015). This procedure was applied to the PMF outputs obtained for ES, FR, and CH. For NL and DE, as stated before, the multi-site PMF was already published. Thus, we did not perform the sensitivity study for Dutch and German databases.

The feasibility of the multi-site PMF depends on the degree of similarity of the source profiles among the PMF runs. For the comparison, we calculated the ratio between specific tracers in each chemical profile for each PMF run and then we calculated the coefficient of variation (CV) of the obtained ratios. As an example, for the *sulfate-rich* source we compared the $[NH_4^+]/[SO_4^{2-}]$ ratios. Sofowote et al. (2015) suggested that if CV of the ratios for each chemical profile is lower than 20-25%, multi-site PMF is applicable. If this condition is satisfied, we can assume that the chemical profiles of the obtained sources are similar at the paired sites. For this sensitivity test, the number and types of sources from each PMF run (single and multi-site) should be the same.

The robustness of the identified sources in each PMF run can be estimated using some of the tools available in the EPA PMF version 5.0 such as the bootstrapping resampling and the displacement of factor elements or both (Paatero et al., 2014; Brown et al., 2015). Bootstrapping resampling results for ES, FR and CH were reported in Table S1.

The main advantage of the multi-site PMF is that a larger dataset is used in the PMF model compared to the separate single-site PMFs. Thus, multi-site PMF is more likely to include low contribution (edge point) values and produce more robust results. Moreover, by combining the datasets, the analysis will provide insight into the sources affecting both receptor sites, and will most likely tend to focus on the general phenomena instead of the unique local variations (Escrig et al., 2009).

Additionally, pooling the concentrations of PM constituents collected at the paired sites into one dataset allows the application of the Lenschow's approach detailed below. To obtain the net local source impacts, the source contributions estimated at the regional station are subtracted from the source contributions estimated at the urban station. Thus, we need that the sources identified at the paired sites are exactly the same and for this reason, multi-site PMF was performed.

2.2 The Lenschow's approach

Lenschow's approach (Lenschow et al., 2001) is a simple technique that aims at assessing the contribution of pollutants from different spatial scales (i.e. local, regional, continental) into the urban concentration.

Depending on the country, different paired sites were available for this analysis (traffic/urban/regional/remote). The descriptions of the sites are given in the next section. Lenschow's approach implies some important assumptions to assess the increments at various sites in terms of actual contributions:

- The differences of source contributions between a traffic station (TS) and a urban low-traffic impact sites (UB) station can be attributed to the very local influence of traffic (and other very local sources) on the adjacent street/district. This difference is called *traffic increment*.
- The differences between an UB station and a rural background (RB) station can be attributed to the sources of the agglomeration such as building heating or the dispersed traffic increment. This difference is called *urban increment*.

If a remote (i.e. mountain top station/continental background station (CB)) is also available, then we assume that:

- The differences of the source contributions between the RB and CB stations can be attributed to the regional sources with little contribution from the urban agglomeration. This difference is called *regional increment*.
- The source contributions at the CB station can be attributed to continental sources. This contribution is called *continental increment*.

If only the RB station is available we cannot separate the regional and continental contributions, therefore we assume that:

- The source contributions at the RB station can be attributed to both regional and continental sources (without the possibility to separate the two contributions) with little contribution from the urban agglomeration.

The important hypothesis behind Lenschow's approach is that the emissions from the city should not directly affect the regional/remote site, otherwise this approach will lead to an underestimation of the urban increment. The city contribution to the measured RB levels (called "city spread" in Thunis et al., 2018) also depends on the distance between the city and the RB station. The larger the distance between the UB and RB sites, the lower should be the city impacts. Moreover, as suggested by Thunis et al. (2018), the size of the city is also a parameter that can affect the city effect. Another consideration is that: a) specific meteorological conditions favoring the transport of the city emissions to the RB site can also contribute to the city spread, and b) even if the city emissions do not influence the RB site, nearby rural emissions might increase RB levels of PM. This issue is made even more complex when considering the different lifetime of chemical species. Whereas the dispersion of primary species will be primarily constrained by the geometry of the sources, the topography of the areas and the meteorological dispersion patterns, for secondary species, the chemical formation process introduces a substantial complexity.

2.3 Paired sites and measurements

In the following, we provide a brief description of the paired sites included in this analysis and the PM chemically speciated data available in each country. Figure 1 shows the location of the paired sites, whereas the main statistics of the chemical species used in the PMF model is provided in Tables S1-S4.

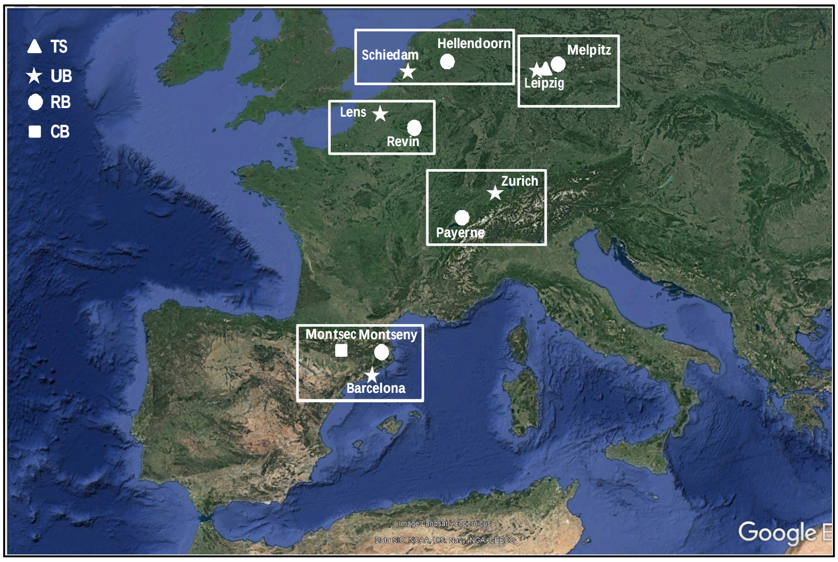

Figure 1: Paired sites included in this work. TS: Traffic station (DE). UB: Urban background (NL, DE, FR, CH, ES); RB: Regional background (NL, DE, FR, CH, ES); CB: Continental background (ES);

- *Spain (ES)*

Three sites were available in ES, namely: the *Barcelona* UB station (BCN; 41°23’24.01’’ N, 02°6’58.06’’ E, 64 m a.s.l.), the *Montseny* RB station (MSY; 41°46’45.63’’ N, 02°21’28.92’’ E, 720 m a.s.l.) located about 50 km to the NNE of BCN and the *Montsec* CB (MSA; 42°3’ N, 0°44’ E, 1570 m a.s.l.) located 140 km southeast of BCN. These stations are run by the EGAR Group of the Institute of Environmental Assessment and Water Research (IDAEA-CSIC) in Barcelona. Detailed descriptions of the measuring sites can be found in Querol et al. (2008), Amato et al. (2009) and Pandolfi et al. (2014) for BCN, Pérez et al. (2008), Pey et al. (2010) and Pandolfi et al.

(2011; 2014) for MSY, and Ripoll et al. (2014) and Pandolfi et al. (2014) for MSA. Both MSY and MSA stations are part of the ACTRIS (Aerosol, Clouds, and Trace gases Research Infrastructure, www.actris.net) and GAW (Global Atmosphere Watch Programme, www.wmo.int/gaw) networks and of the measuring network of the government of Catalonia.

Measurements of PM_{10} chemically speciated data from the three Spanish sites used here covered the period 2010 – 2014. Details on the analytical methods used can be found for example in Querol et al. (2007) and Pandolfi et al. (2016). A total of 2115 samples were used in the PMF model. Table S2 in Supporting Materials reports the chemical species included in PMF analysis and the main statistics (mean, median, SD) for each species for the three Spanish sites.

- *Switzerland (CH)*

Two measuring sites were available in CH: a UB station in Zurich (*Zurich-Kaserne,* ZUE; 47°22'36.42'' N, 8°31'44.70'' E, 410 m a.s.l.) and the RB station of Payerne (PAY; 46°49'12'' N, 06°57' E, 491 m a.s.l.) located about 130 km west of ZUE. A detailed description of ZUE (which is part of the Swiss National Air Pollution Monitoring Network – NABEL) and PAY stations (part of the EMEP and GAW networks) was provided by Gehrig and Buchmann (2003), Gianini et al. (2012), Hueglin et al. (2005), Szidat et al. (2006), Bukowiecki et al. (2010) and Lanz et al. (2008).

Measurements of PM_{10} chemically speciated data were available at the two sites during the period August 2008 – July 2009 (Gianini et al., 2012). A total of 178 samples (89 collected at ZUE and 89 collected at PAY) and 31 species (listed in Table S3) were used in the PMF analysis. Table S3 reports the summary statistics for these chemical species .

- *The Netherlands (NL)*

The measuring sites and the $PM_{2.5}$ chemically speciated data available in NL were presented by Mooibroek et al. (2011) where data from 5 stations (one TS, one UB and three RB sites) were simultaneously used in the PMF model in order to document the variability of the $PM_{2.5}$ source contributions in NL. Among the five stations presented in Mooibroek et al. (2011), we only used data from Schiedam (SCH; UB) and Hellendoorn (HEL; RB) located around 150 km from SCH.

Measurements of $PM_{2.5}$ chemically speciated data were available at the two sites during the period September 2007 – August 2008. A total of 479 samples were used in Mooibroek et al. (2011) for PMF analysis using data from 5 sites. 87 and 82 samples were collected at UB and RB, respectively. Table S4 reports the mean concentrations of $PM_{2.5}$ chemical species at these two sites.

- Germany (DE)

The PM chemically speciated data and the PMF source apportionments used here were published by van Pinxteren et al. (2016). Data from four stations (Leipzig-Mitte (LMI; TS), Leipzig Eisenbahnstrasse (EIB; TS), Leipzig TROPOS (TRO; UB), and Melpitz (MEL; RB) were collected during summer 2013 and winters 2013/14 and 2014/15. A total of 172 samples were used in the PMF model by van Pinxteren et al. (2016). In order to apply the PMF+Lenschow's approach, we excluded the TS (Leipzig-Eisenbahnstrasse) located in a residential area, approx. 2 km east of LMI. The three measuring sites used in this work, LMI, TRO, and MEL located approximately 50 km north-east of TRO and described in van Pinxteren et al. (2016).

- France (FR)

Two sites were used: a UB site in *Lens* (LEN; 50°26'13''N, 2°49'37''E, 47 m a.s.l.) and the RB station of *Revin* (REV; 49°54'28.008''N, 4°37'48''E, 395 m a.s.l.). The distance between Lens and Revin is around 140 km. A description of the French measuring sites can be found in Waked et al. (2014).

Measurements of PM_{10} chemically speciated data were available at the two sites during the period January 2013 – May 2014. A total of 335 samples (167 from LEN, and 168 from REV) were analyzed with PMF. The number of 24h samples simultaneously collected at the two sites and used for Lenschow's approach was 104. Table S5 reports the statistics of the chemical species measured at the French paired sites.

3. Results

This section is organized as follows: Section 3.1 presents the PMF sources calculated for each group of paired sites. Some of these sources were common for all the sites included in this work, whereas other sources were obtained only for a subset of paired sites. The chemical profiles of the sources calculated for ES, CH and FR are reported in Supporting Material (Figures S1, S2, and S3, respectively). The source chemical profiles for NL and DE can be found in Mooibroek et al. (2011) and van Pinxteren et al. (2016), respectively. In Section 3.2, we present a sensitivity study that aimed at demonstrating the feasibility of the multi-site PMF analyses. In Section 3.3, we present the PMF source contributions, and in Section 3.4, we present and discuss the results of the Lenschow approach applied to PM concentrations and PMF source contributions.

3.1 PMF sources

Sources identified at all paired sites

- *Secondary inorganic aerosol* (SIA) source traced mostly by inorganic species ammonium (NH_4^+), sulfate (SO_4^{2-}) and nitrate (NO_3^-). At all sites included here, with the exception of DE, the contribution of SIA was separated between *sulfate-rich aerosols* (SSA) and *nitrate-rich aerosols* (NSA). The origin of SSA and NSA is, respectively, the atmospheric oxidation of SO_2 (mostly from combustion of sulfur-containing fuels) and NO_x (from combustion processes such as traffic, power generation, industry and domestic sector). At all sites the SSA and to a lesser extent NSA source profiles (and consequently the SIA source profile in DE) showed enrichments in organic carbon (OC), which was attributed to both the condensation of semi-volatile compounds on the high specific surface area of ammonium sulfate and nitrate (Amato et al., 2009) and photochemistry causing similar temporal variation of these constituents of atmospheric PM (Kim et al., 2003; Kim and Hopke, 2004; Petit et al., 2019).
- The *Mineral* source (MM) was traced by typical crustal elements such as Al, Ca, Fe, and Mg and accounted for a large mass fraction of crustal trace elements such as Ti, Rb, Sr, Y, La, Ce and Nd. This factor also included a variable fraction of OC, an indication of mixing of inorganic and organic matter during aging or by entrainment of soils including their associated organic matter (Kuhn, 2007). At the German sites, this source (named *Urban dust* in van Pinxteren et al. (2016)) consisted of NO_3^- and WSOC (water soluble organic carbon) with high mass contributions of Ca and Fe indicating a mixture of mineral dust with urban pollution. A MM factor (enriched in Si, Al, Ti, Ca and Fe) was also found by Mooibroek et al. (2011) in $PM_{2.5}$ at the Dutch sites.
- The *Primary road traffic* (RT) source included both exhaust and non-exhaust primary traffic emissions and was traced by EC and OC and a range of metals such as Fe, Cu, Ba, Mo and Sb from brakes and tires abrasion (i.e. Amato et al., 2009). Only for DE it was possible to separate the contributions from exhaust and non-exhaust traffic emissions (van Pinxteren et al., 2016) whereas in the other cases, the two sources were jointly apportioned. In van Pinxteren et al. (2016), the vehicle exhaust emissions were identified by high mass contributions of WISC (water insoluble carbon; i.e. EC + hydrophobic organics), as well as contributions of hopanes with increasing species contributions toward either lower chain length (<C25) n-alkanes (for ultrafine particles) or larger (≥C25) chain length n-alkanes with a predominance of even C

compounds (coarse particles). The contributions from exhaust and non-exhaust traffic sources in DE were summed to obtain the RT source contribution.

- The *Aged sea salt* (SS) source was traced mostly by Na^+, Cl^- and Mg^{2+} with variable contributions from SO_4^{2-} and NO_3^- suggesting some aging of the marine aerosol. In CH, this source contributed to high fractions of Na^+ and Mg^{2+} and did not show a clear annual cycle with elevated values during winter, thus suggesting a low contribution from the de-icing road salt. In Gianini et al. (2012), this source was named *Na-Mg-rich* factor and it was related to the transport of sea spray aerosol particles in Zurich. In DE, the calculated SS factor consisted mainly of NO_3^- and Na^+ with no mass contribution of Cl^-, indicating efficient Cl^- depletion during transport over the continent. In FR, two SS sources were calculated: a fresh SS source (traced by Na^+ and Cl^-), and an aged SS source with lack of Cl^- and presence of Na^+ and NO_3^-.

Sources identified only at a subset of paired sites

- The *biomass burning* (BB) source, mostly traced by K^+ and levoglucosan together with EC and OC, was resolved for three paired sites (in FR, DE, and CH).
- The *residual oil combustion* source (V-Ni) was identified at two paired sites (in ES and NL). This source contained significant fractions of the measured V and Ni concentrations together with EC, OC and SO_4^{2-} that are the tracers for residual oil combustion sources such as ocean shipping, municipal district heating power plants, and industrial power plants using residual oil.
- The *primary industrial* (IND) source, also resolved only in ES and NL. In ES, it was identified by Pb and Zn along with As and Mn mostly from metallurgical operations (e.g. Amato et al., 2009). In NL, different trace metals appeared indicating a mixture of many different sources, including waste incineration, (coal) combustion, metallic industrial activities, and fertilizer production. Mooibroek et al. (2011) summarized the profile as industrial activities and incineration.

Sources identified at only one set of paired sites

- Two sources were identified only in FR, namely: a *marine biogenic* source identified by methanesulfonic acid, a product of DMS oxidation, and a *Land* (or *primary*) *biogenic* source, traced by alcohols (arabitol and mannitol).
- Six additional sources were resolved only in DE, namely: *sea salt/road salt* (SSRS; an SS source with influence of road salt for de-icing), *Coal combustion* and *Local coal combustion* (this latter contributing mostly at the EIB site, which was removed from this analysis), *Photochemistry* (with high mass contributions of NH_4^+ and

SO_4^{2-} and WSOC), *Cooking*, and *Fungal spores.* As reported in van Pinxteren et al. (2016), photochemistry factor concentrations (Fig. 4 and S11 in van Pinxteren et al. (2016)) tended to be higher in summer and showed no clear site-dependent trend. In contrast to the general secondary aerosol, the photochemistry factor thus seems to be more related to radiation-driven formation processes. A detailed description of these additional sources can be found in van Pinxteren et al. (2016).

3.2 Feasibility of the multi-site PMF

The results of the sensitivity test performed to demonstrate the feasibility of the multi-site PMF were reported in Table S6 in supporting material. Table S6 shows the main features of the sources from both the single-site PMF and the multi-site PMF for ES, CH, and FR reporting for each source and country: 1) the explained variation (EV) of the main markers of the source for each PMF run (i.e. how much each source explains in % the concentration of a given tracer), 2) the ratio values (K) between specific tracers in each source for each PMF run, and 3) the coefficient of variation (CV) of the ratios for each source (calculated as the ratio between the standard deviation and the mean of the K values obtained from the single-site PMF). This sensitivity test was not performed for NL and DE because the multi-site PMF was not applied here but directly taken from Mooibroek et al. (2011) and van Pinxteren et al. (2016), respectively. Given the encouraging results shown below for ES, CH, and FR, it seems valid to assume that the multi-site PMF results for DE and NL can be used, even without the single-site validation. As reported in Table S6, the calculated CVs are below 20-25% for the majority of the sources (cf. Section 2.1.1).
The exceptions were *IND* in ES (CV=48.8%), *SS* in ES (CV=35.9), *marine biogenic* in FR (CV=31.9%) and *RT* in CH (CV=31.1%). As shown below, the contribution of the *IND* source to the measured PM_{10} in BCN was very low and consequently the uncertainty associated to the high CV for this source was minimal. The high CV for the SS source in ES is due to the progressive depletion of Cl^- when moving from UB to RB and to CB. In fact, as reported in Table S6, the $[Na^+]/[Cl^-]$ ratio correspondingly increased when moving from the UB site to the CB site. However, the SS source, and the *marine biogenic* source, were considered as natural sources without separating the urban and regional increments. Thus, the contribution from these two sources can be totally attributed to regional natural sources. On the other side, the RT source in CH was, as shown below, mostly local. For all other sources, the CVs are quite low indicating the similarity in the chemical profiles at the three sites, thereby allowing the application of the multi-site PMF.

3.3 PMF source contributions and seasonal patterns

Figure 2 shows the mean annual PMF source contributions calculated for the considered paired sites. The mean winter (DJF) and summer (JJA) source contributions are presented in Figures S4 and S5, respectively, in the Supporting Material. Figure S6 in Supporting Material reports the same information as in Figure 2 but using box-and-whisker plots to show the data variability.

At all stations, the secondary inorganic aerosol (SIA = SSA + NSA) was among the most abundant components of PM. At UB sites the SIA contribution ranged between 5.7-5.8 μg/m^3 (29-35%) in DE and FR, where the sampling periods were similar, to around 8.2-9.8 μg/m^3 (33-58%) in ES, CH and NL, where the sampling periods were also similar. A decreasing gradient was observed for SIA concentrations when moving from UB (or TR) sites to RB (or CB) sites.

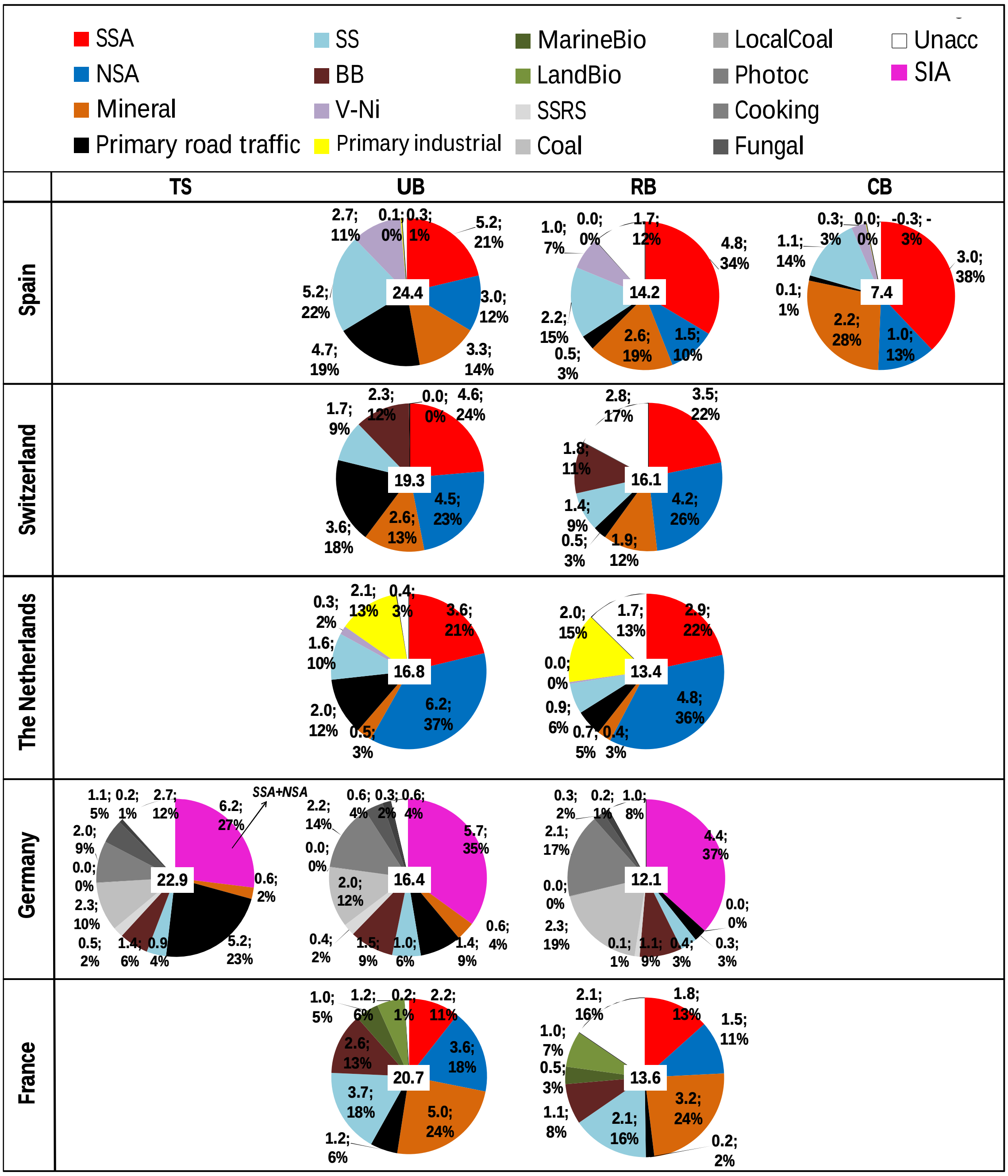

Figure 2: Mean annual source contributions to PM_{10} ($PM_{2.5}$ for NL) from the multi-site PMF for each country. The number in the white box at the center of the pie chart is the measured mass of PM (in $\mu g/m^3$). TS: traffic site; UB: urban background; RB: regional background; CB: continental background.

This gradient was mostly driven by NSA contributions which showed higher decreasing gradients compared to SSA suggesting a regional character of this latter source. The spatial gradients will be discussed in more details in the next section.

The contribution from the MM source to PM_{10} at UB sites ranged from 5.0 μg/m^3 (24%) in FR to 0.6 μg/m^3 (4%) in DE. Low MM contribution was observed at UB station in NL (0.5 μg/m^3; 3%) where $PM_{2.5}$ was measured. These regional differences could be related to the intensity and regional impact of Saharan dust outbreaks which can be very different from one year to the other, thus also contributing to explain the observed regional variation of the MM source contributions (Alastuey et al., 2016). The high MM source contribution in FR was mostly due to the period March-April 2014 (not shown), when the MM contribution reached daily means of more than 40 μg/m^3. Low dust concentration in DE compared to other European countries was also reported by Alastuey et al. (2016). Moreover, van Pinxteren et al. (2016) reported that the contribution from the MM source at the German sites is much lower in winter compared to summer. For the German sites, we used data collected during one summer and two winters, thus also explaining the low annual average contribution from this source reported here. A clear decreasing gradient from UB/TR to RB/CB was also observed for the MM source contributions.

The mean annual contribution from the RT source at UB stations ranged from 4.7 μg/m^3 (19% of PM_{10} mass) in ES to 1.2 μg/m^3 (6% of PM_{10} mass) in FR. The highest contribution from this source was observed at the TS in DE (5.2 μg/m^3; 23%). The absolute contributions at the RB sites were similar in all countries at around 0.2-0.7 μg/m^3 (2-5%). Thus, the RT source showed a clear gradient indicating that this source was local at all TS/UB sites.

The contributions from the SS source were highest at the paired sites close to the sea such as in ES and FR were the mean annual contributions were around 5.2 μg/m^3 (22%) and 3.7 μg/m^3 (18%), respectively, at the UB stations. In both countries, the mean annual contribution calculated at RB stations was lower compared to the contribution at UB stations, because of the larger distance of RB stations to the sea compared to the UB stations. At UB sites in NL, CH and DE the SS source contributed 1.6 μg/m^3 (10%), 1.7 μg/m^3 (9%) and 1.0 μg/m^3 (6%), respectively. The low SS contribution in NL was due to the coarse mode prevalence of SS whereas $PM_{2.5}$ was sampled in NL. In the following, we will not apply Lenschow's approach to the SS source contributions and we will consider this source as totally natural and R+C in origin.

The contribution from the BB source was identified only in FR (2.6 μg/m^3; 13% at UB site), DE (1.5 μg/m^3; 9%), and CH (2.3 μg/m^3; 12%). Previous study in Barcelona using aerosol mass spectrometer data reported a small BB contribution to OA and PM (around 11% and 4%, respectively) in winter in BCN (Mohr et al., 2012). Therefore, it was not possible to identify the BB source in BCN based on the PM_{10} chemical speciated data used here. The BB source contributions reported here for LEN site were very similar to the values reported by Waked et al. (2014) for LEN despite the differences in periods studied. A slight gradient is observed moving from TS/UB to RB stations indicating the presence of both local and R+C increments for this source.

The contribution from the IND source at UB stations in NE and ES was 2 $\mu g/m^3$ (13% of $PM_{2.5}$ mass) and 0.1 $\mu g/m^3$, respectively. The low IND source contribution in ES was probably due to the implementation of the IPPC Directive (Integrated Pollution Prevention and Control) in 2008 in ES (Querol et al., 2007). As reported in Figure 2, a very small gradient was observed when moving from UB to RB station suggesting a regional character for this source.

The V-Ni source contributions were higher in ES (2.7 $\mu g/m^3$, 11% at UB site) compared to NL (0.3 $\mu g/m^3$, 2% at UB site). This factor was not apportioned in the other countries. In FR because the measurements of V and Ni were not available; in DE only the measurements of Ni were available (whereas V, as important tracer of residual oil combustion was not available); in CH, despite the fact that the measurements of V were available, the V-Ni source was not resolved likely because the distance of Swiss sites from important residual oil combustion sources. The contribution from this source in ES showed a clear gradient when moving from UB to CB station. The high V-Ni source contribution at UB in ES was related to ship emissions from both the intense vessel traffic from the Mediterranean Sea and the port of Barcelona. Figure 3 shows the Concentration Weighted Trajectory (CWT) plots for the V-Ni source contributions in Barcelona (2010-2014) and Schiedam (2007-2008). The use of computed concentration fields to identify source areas of pollutants, referred as CWT, was first proposed by Siebert et al. (1994). Here, we used the CWT function available in the Openair package (Carslaw and Ropkins, 2012; Carslaw, 2012). In Figure 3, contributions higher than the 90th percentile were used to look at the origin of high contributions from the V-Ni source. As shown in Figure 3, the V-Ni source in ES and NL was mostly linked to maritime shipping emissions.

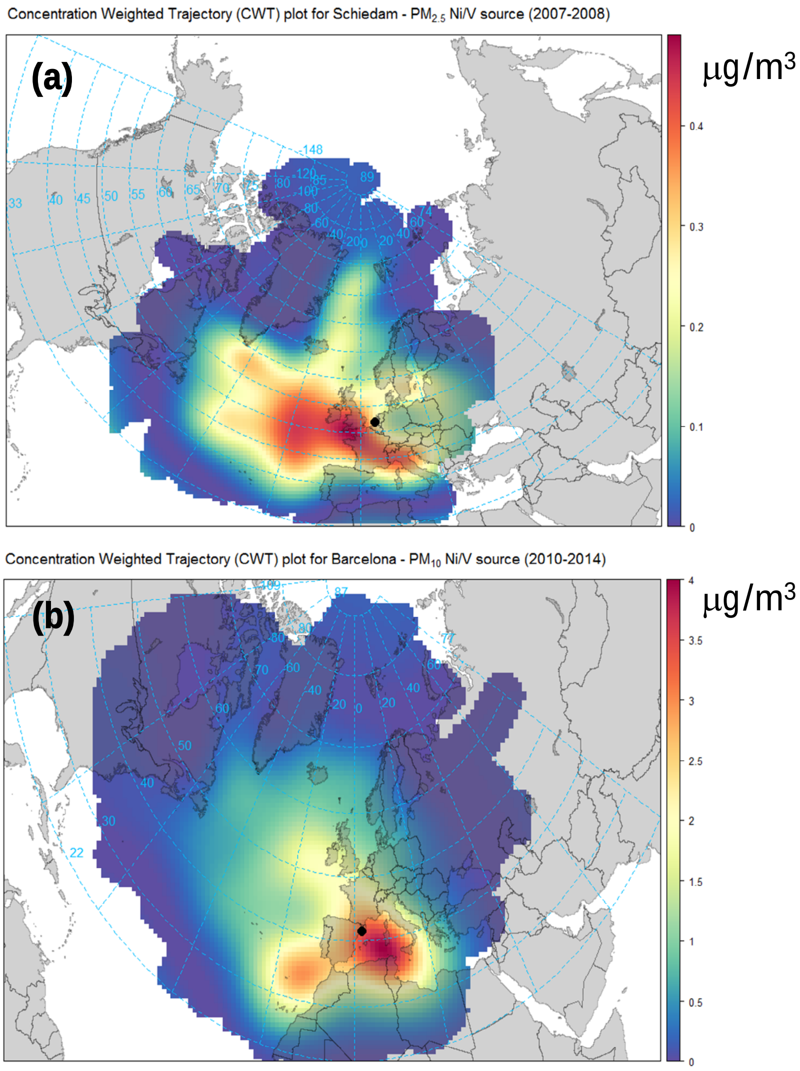

Figure 3: Concentration Weighted Trajectory (CWT) plots of the V-Ni source contributions for: (a) Schiedam (NL; $PM_{2.5}$; 2007-2008) and (b) Barcelona (ES; PM_{10}; 2010-2014).

Figure 4 shows the scatter-space plots of the V-Ni and SSA source contributions for BCN (PM_{10}; 2007-2008 and 2010-2014) (Figure 4c and d, respectively) and SCH ($PM_{2.5}$; 2007-2008; Figure 4a). Data from Rotterdam ($PM_{2.5}$; 2007-2008; Figure 4b) were also used for the V-Ni vs. SSA comparison. Figure 4 also shows the analogous plots for 4 additional sites in NL, Belgium, and FR for a more recent period (2013-2014), namely: Wijk aan zee and Amsterdam in NL (Figure 4e,f), Antwerp (Belgium, Figure 4g) and Lille (FR, Figure 4h). Details on the measurements performed at these 4 additional sites, the PM_{10} chemically speciated data, and PMF analyses can be found in Mooibroek et al. (2016). In all of the g-space plots in Figure 4, an edge was observed (highlighted with red color) that can be used to estimate the amount of SSA produced for every 1 $\mu g/m^3$ of residual oil burned by ships (e.g. Kim and Hopke, 2008; Pandolfi et al., 2011a). This sulfate represents direct SO_3 emissions from the ship that appear as particulate sulfate at the sampling sites (e.g. Agrawal et al., 2008; 2010).

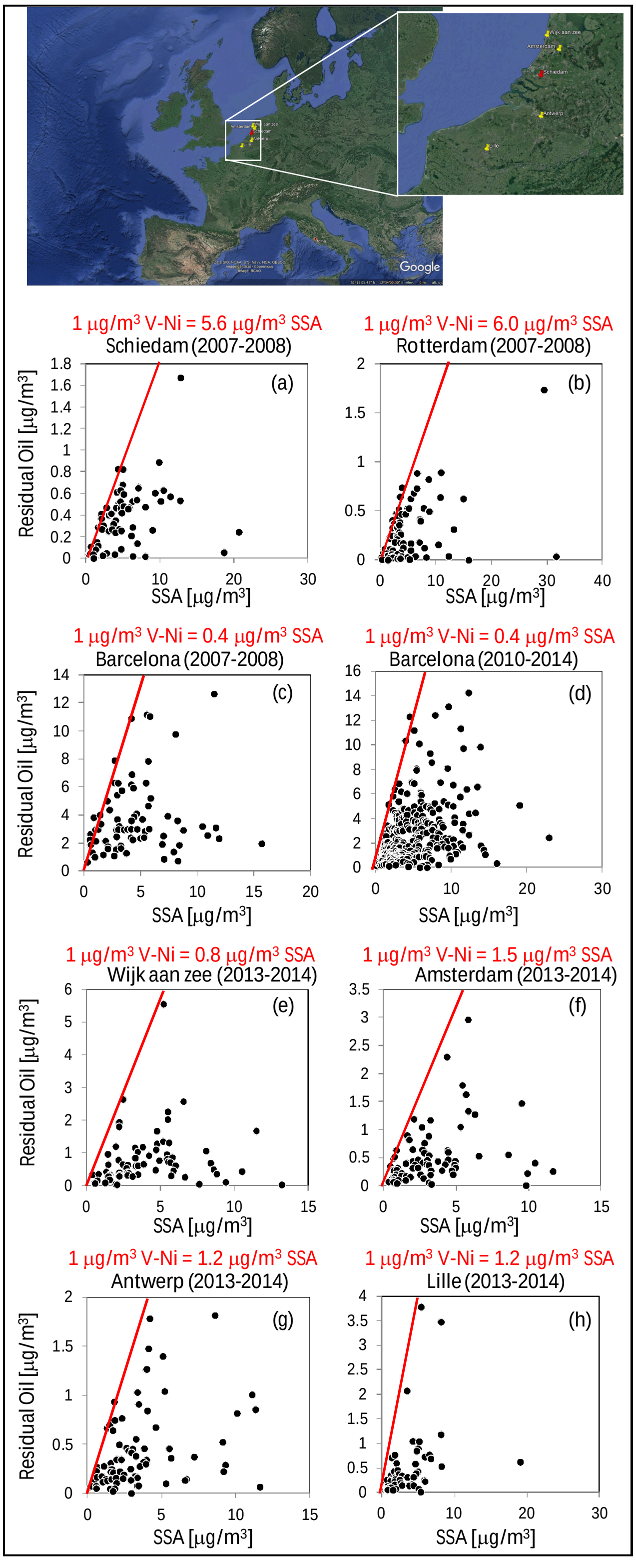

Figure 4: Contributions (μg/m^3) of the V/Ni-bearing particles from shipping and SSA particles to PM at Schiedam (a), Rotterdam (b), Wijk aan zee (e), Amsterdam (f) in the Netherlands, Barcelona (c and d; Spain), Antwerp (g; Belgium) and Lille (h; France). The red lines represent the edges of the scatter plots.

Ship diesels typically burn high sulfur content residual oil (Bunker-C), and thus primary sulfate emissions can be anticipated (Kim and Hopke, 2008). In BCN we found that around 0.4 μg/m^3 of SSA were produced for every 1 μg/m^3 of V-Ni PM_{10} contribution (during both 2007-2008 and 2010-2014), whereas in SCH and Rotterdam the amount of SSA was much higher, around 5.6-6.0 μg/m^3, suggesting the use of a residual oil with high sulfur content during 2007-2008. Kim and Hopke (2008) and Pandolfi et al. (2011a) reported that around 0.8 μg/m^3 of SSA were produced for every 1 μg/m^3 of V-Ni $PM_{2.5}$ in Seattle (US) and of V-Ni PM_{10} in the Bay of Gibraltar (ES), respectively. The difference between BCN and SCH and Rotterdam was high during the same period (2007-2008). However, recent data (2013-2014) from the four additional sites slowed lower primary SSA produced (around 0.8 – 1.5 μg/m^3) for every 1 μg/m^3 of residual oil, indicating a reduction of sulfur content in fuels (cf. Figure 4). Indeed, Figure S7 in supporting material shows the strong reduction of SO_2 emitted from maritime shipping in Rotterdam from 2007 to 2014 despite the rather constant number of ships registered in port (Environmental Data Compendium, Government of the Netherlands, https://www.clo.nl/en). A similar result was reported by Zhang et al. (2019). In their study, Zhang et al. (2019) showed the significant reduction in ambient SO_2, EC, V, and Ni concentrations at both port sites and urban sites in Shanghai after the implementation of the Chinese DECA (Domestic Emission Control Areas) despite increasing ship traffic activity. Moreover, a report of the Netherlands Research Program on Particulate Matter (Denier van der Gon and Hulskotte, 2010) reported that in the port of Rotterdam in 2003 the dominant energy source for ships in berth was high-sulfur content heavy fuel oil (HFO). The use of HFO in berth was a surprising result, as it is often thought that ships use distilled fuels while in berth (Denier van der Gon and Hulskotte, 2010). The observed reduction in primary SSA from ships in NL from 2007-2008 to 2013-2014 could be also due to the change of fuel used by ships in berth, from HFO to low-sulfur content marine diesel oil. The type of fuel used by ships while in berth could also explain the difference observed between BCN and SCH during 2007-2008.

The *marine biogenic* and *land biogenic* sources, assessed only in FR, contributed around 1.0 μg/m^3 and 1.2 μg/m^3, respectively, at the UB station. These two sources were not identified in the other countries mostly because the measurements of methanesulfonic acid and traced alcohols (arabitol and mannitol) were not available. Analogously to the SS source, Lenschow's approach was not applied to the contributions from these two sources that were considered as totally R+C and natural.

Finally, in DE, the contributions from the six sources assessed only in this country summed to mean values of 5.6 μg/m^3 (34%) at UB site. Among these six sources, the contribution from *coal combustion* was the highest in winter (suggesting the influence of buildings heating), explaining around 60-70% of the total contributions from these six sources. In summer, *photochemistry* was the source contributing mostly to the total from the six sources (50-80%). Among these six sources, only the contribution from the *fungal spores* source was considered as totally R+C and natural.

3.4 Spatial increments: Lenschow`s approach results

The results of Lenschow's approach applied to the PM mass concentrations and to the PMF source contributions for each country are presented in Figure 5 and Table S7 and Figure 6 and Table S8, respectively. Figures 5 and 6 show the annual average values. Allocation of PM concentrations and source contributions for winter (DJF) and summer (JJA) are presented in Figures S8 and S9 and Table S7, for PM concentrations, and in Figures S10 and S11 and Table S9 and Table S10, for the PMF source contributions.

An attempt was made to separate the natural and anthropogenic R+C increments whereas the urban increment was considered to be totally anthropogenic. We considered some sources such as *Aged sea salt*, *fresh sea salt*, *marine biogenic*, *land biogenic* as totally natural without allocating their contributions to the different spatial levels. Thus, for example, we assumed that there were no local (traffic/urban) sources of *fresh sea salt*. For the *Aged sea salt* source the presence of SIA in the chemical profile suggests that this source was not entirely natural. However, we cannot estimate the relative natural and anthropogenic contributions to this source using data available here. The urban MM increment was associated with resuspended dust from passing vehicles and local demolition/construction activities. Consequently, it was considered anthropogenic in origin. Conversely, the R+C MM increment was considered to be as of natural origin from both wind-blown dust and Saharan dust episodes, the latter being most important in the Mediterranean region and especially in summer compared to other European countries (Pey et al., 2013; Alastuey et al., 2016). Nevertheless, regional suspended soil could be the result of anthropogenic activities such as farming. However, it is impossible based on the available information to estimate the relative contributions of natural and anthropogenic sources to the R+C MM increments. Other sources such as SSA and NSA, RT, IND, V-Ni, and BB, were considered anthropogenic in origin. Finally, the gradients of PM concentrations reported in Figure 5 and Table S7 were calculated by summing the increments calculated from the different source contributions, and not as the difference between the gravimetric measurements performed at the paired sites.

3.4.1 Urban and regional-continental PM allocation

As reported in Figure 5, the sum of the annual natural and anthropogenic R+C PM increments in all countries were higher compared to the urban increments, therefore confirming the statement of the 2016 LRTAP Assessment Report about the importance of long range air pollution, even in urban areas. On annual basis, the relative R+C PM_{10} increments were similar in all countries and ranged between around 64% in ES to 74% in DE (cf. Table S7), For this comparison, the R+C PM increment in ES was calculated as the sum of regional and continental increments and in DE it was calculated as relative to the PM_{10} concentration measured at the UB site (not at the LMI traffic site). If the relative R+C PM_{10} increment in DE is calculated with respect to the PM_{10} mass measured at LMI traffic site, then the R+C increment can be estimated to be around 55% in close agreement with the R+C PM_{10} increment reported by van Pinxteren et al. (2016). For NL, the relative R+C $PM_{2.5}$ increment was around 74%, whereas in CH and FR, the relative R+C PM_{10} increments were around 67-69%.

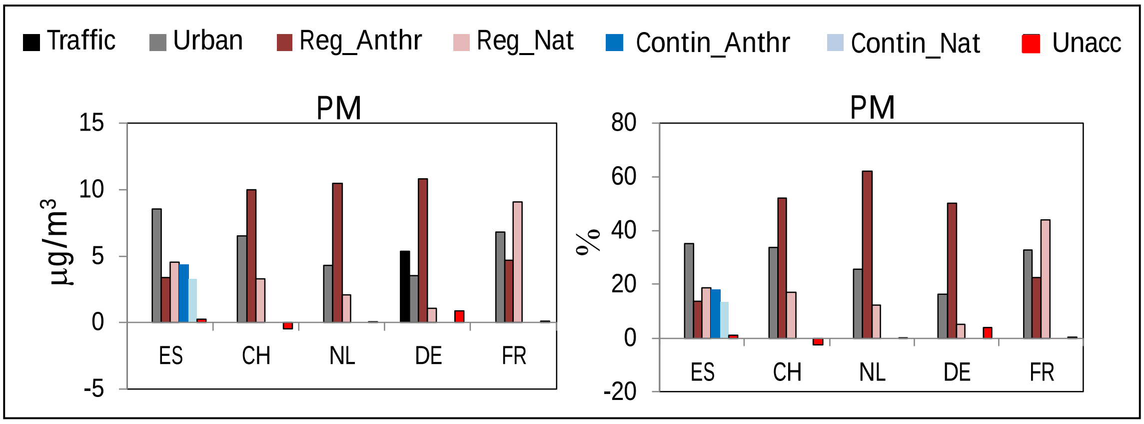

Figure 5: Lenschow's approach applied to the concentrations of PM_{10} in the different countries ($PM_{2.5}$ in the Netherlands). Annual means are reported. ES: Spain; CH: Switzerland; NL: The Netherlands; DE: Germany; FR: France. In all countries with the exception of Spain, Reg_Anthr and Reg_Nat are the sum of regional+continental.

In terms of absolute values, the lowest PM urban and R+C (anthropogenic and natural) increments were observed in DE (3.5 µg/m^3 and 11.9 µg/m^3 of PM_{10} mass measured at the UB TRO site) where the PM_{10} concentrations were also lower compared to the other cities included in this work. The highest urban and R+C PM increments were instead observed in ES (8.5 μg/m^3 and 15.6 μg/m^3 of PM_{10} mass measured in BCN) where the PM_{10} concentrations were higher. For DE, the local PM increment measured at the traffic site (LMI) was 5.4 μg/m^3 (cf. Table S7) and contributed around 25% to the PM mass measured at LMI.

Overall (annual means; cf. Table S7 and Figures 5, S8, and S9), the R+C PM increments due to anthropogenic activities in CH, NL, and DE were higher compared to the R+C PM increment due to natural sources. In these countries, the R+C anthropogenic PM increments were very similar (10-10.8 μg/m^3) and explained around 52%, 62%, and 66%, respectively, of the PM mass measured at the UB stations. Conversely, in these three countries, the R+C PM increments due to natural sources varied more (1.1-3.3 μg/m^3) and explained around 17%, 12% and 7%, respectively, of the UB PM mass. In ES, the anthropogenic and natural R+C PM increments were similar (around 8 μg/m^3) and both explained around 32-33% of the PM mass measured at BCN. Conversely, in FR, the R+C natural PM increment was the highest (around 9.1 μg/m^3) and explained around 44% of the PM mass measured in LEN, whereas the R+C anthropogenic PM increment was around 4.6 μg/m^3 (23%). As shown later, the high R+C natural PM increment observed in FR and ES was mostly related to regional emissions from SS and MM sources. Moreover, in FR, *marine biogenic* and *land biogenic* source emissions also contributed to the high R+C natural PM increment.

In all countries, with the exception of DE, the absolute and relative PM urban increments were higher in winter compared to summer (cf. Table S7). This result suggested that in winter, the typical atmospheric conditions in these countries of lower wind speeds and lower mixed layer heights favored the accumulation of locally emitted pollutants compared to summer. The winter-to-summer PM urban increment ratios ranged between 1.5 in CH up to 3.5 in FR. The lack of a clear seasonal profile for the PM urban increment at TRO (DE) could be due to the overall effect that the two main air mass inflows have on pollutant concentrations at the German sites during both seasons (van Pinxteren et al., 2016). As shown in van Pinxteren et al. (2016), the source contributions to PM at the German sites differed considerably depending on the sources, seasons, and air mass inflows.

The natural and anthropogenic R+C PM increments showed different seasonal patterns. Those due to natural sources were higher in summer at all sites with the exception of NL where the R+C natural PM increment was higher in winter. As shown later, the observed higher summer R+C PM natural increments were due to MM and

SS source emissions that were higher on average during the warm season. Conversely, as also shown in Waked et al. (2014), the high R+C PM natural increment in NL in winter was due to SS emissions that were higher during the cold season (cf. Tables S8 and S9).

The R+C PM increments due to anthropogenic sources showed an opposite seasonal profile compared to the R+C natural PM increments. In fact, the anthropogenic R+C PM increments were lower in summer compared to winter in all countries, with the exception of ES where it was higher in summer compared to winter. As shown later, the higher anthropogenic R+C PM increment in summer in ES was mostly driven by high contributions from regional SSA sources, mostly related to ship emissions at the Spanish sites, and the peculiar meteorological patterns in the Western Mediterranean inducing vertical recirculation of air masses (i.e. Millán et al., 1997). The relatively lower anthropogenic R+C PM increment observed in the other countries in summer compared to winter were mostly related to high winter contributions from NSA and BB regional sources.

3.4.2 Allocation of PMF source contribution

- Sources identified at all paired sites

SIA source (anthropogenic)

In all countries, the majority of SIA calculated from PMF was of R+C origin (Figure 6). On annual average, the lowest relative R+C SIA increment was around 57% in FR (where 43% of *SIA* was of local origin). In the other countries, the relative R+C SIA increment was similar and ranged between around 76% and 85% in ES and CH, respectively. In absolute values, the highest R+C SIA increment (around 7.7 $\mu g/m^3$; cf. Table S8) was observed in CH and NL, followed by ES (6.2 $\mu g/m^3$), DE (4.4 $\mu g/m^3$) and FR (3.3 $\mu g/m^3$). The relative R+C SIA increments were similar in winter and summer in all countries with the exception of ES where in summer the relative R+C SIA increment (around 88%; cf. Figure S11 and Table S10) was much higher compared to winter (51%; cf. Figure S10 and Table S9). In summer, the Western Mediterranean Basin is characterized by regional recirculation episodes driven by strong insolation and the orography of the area. These conditions in summer favor the formation of cells of meso-to-regional scales (i.e. Millan et al., 1997; 2000) and air mass recirculate over the region causing dispersion and aging of pollutants. Furthermore, the high summer insolation favors a faster oxidation of SO_2 and, accordingly, higher SO_4^{2-} concentrations (i.e. Querol et al., 1999). During these summer conditions, the SIA concentrations were similar at the three Spanish sites, thus leading to high relative R+C SIA contributions in summer compared to winter in ES (cf. Figures S4 and S5).

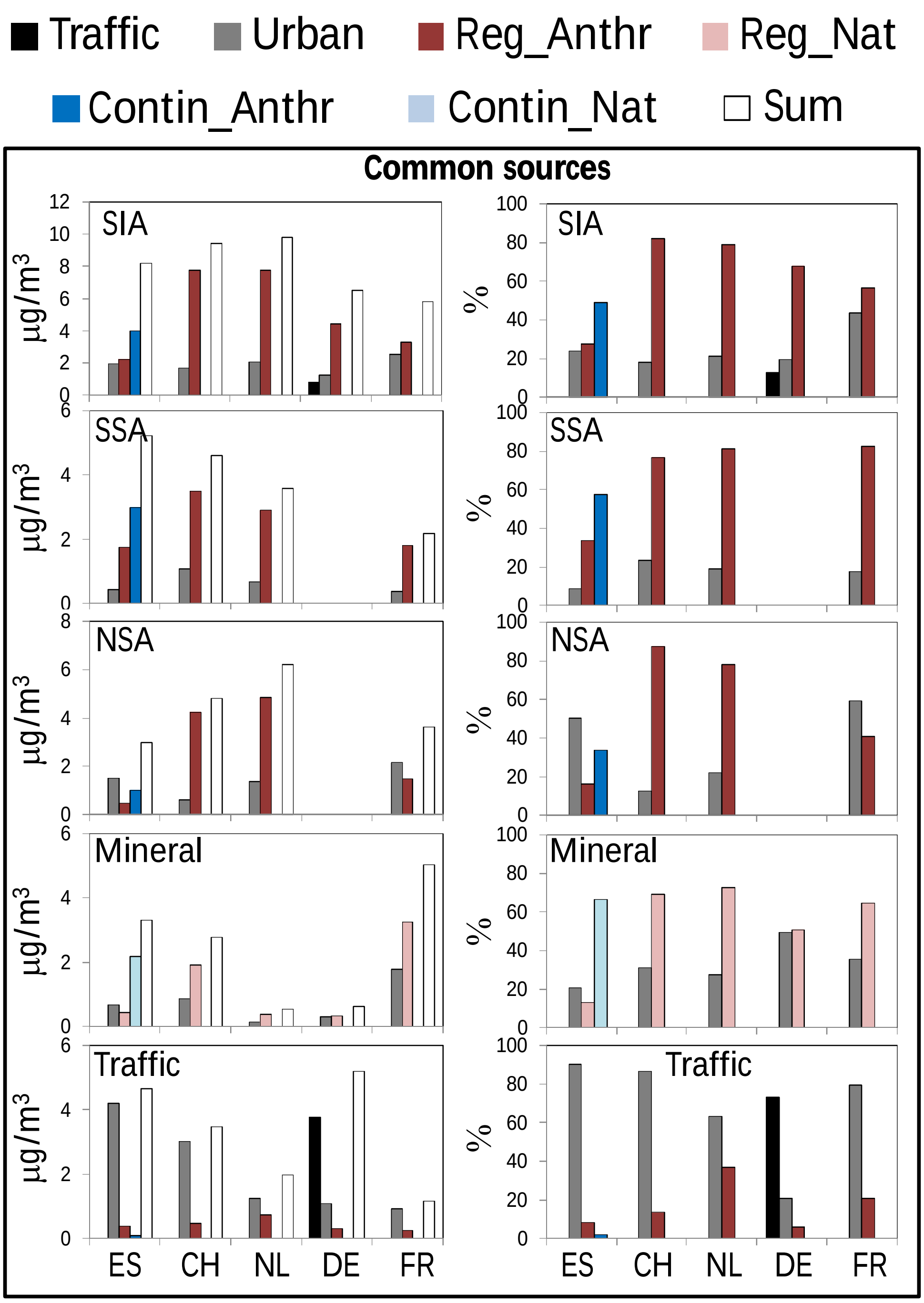

Figure 6: Lenschow's approach applied to the PM_{10} ($PM_{2.5}$ in the Netherlands) PMF source contributions. Annual means are reported. ES: Spain; CH: Switzerland; NL: The Netherlands; DE: Germany; FR: France. In all countries, with the exception of Spain, Reg_Anthr and Reg_Nat are the sum of regional+continental.

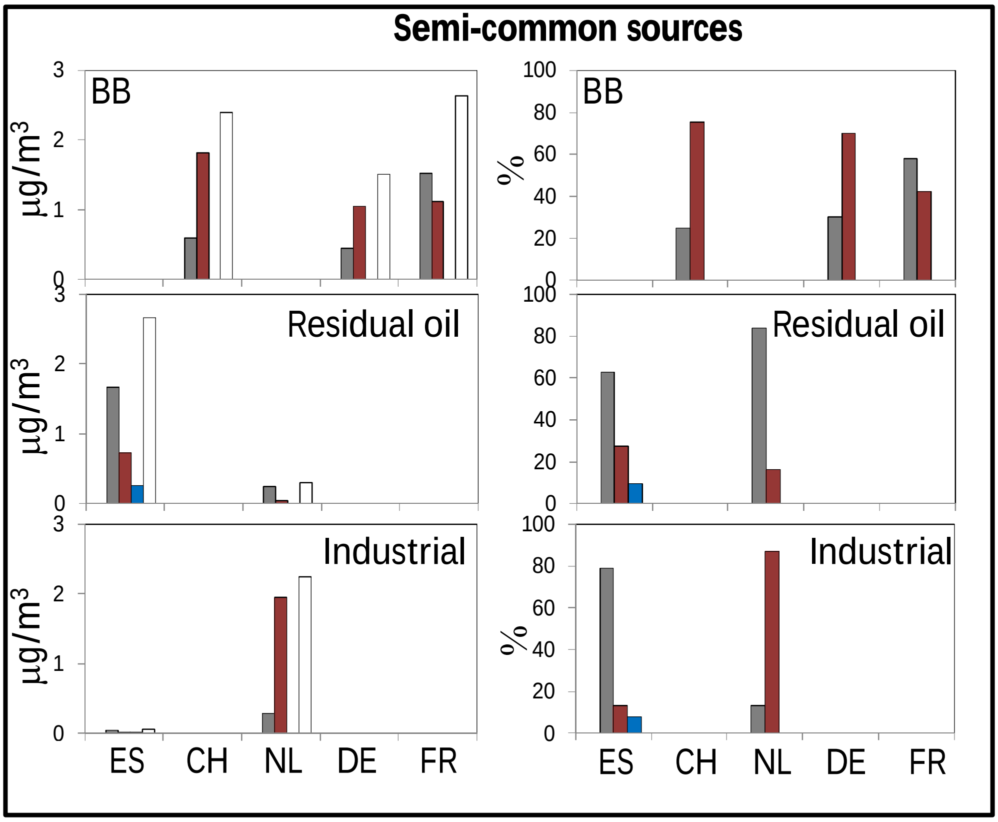

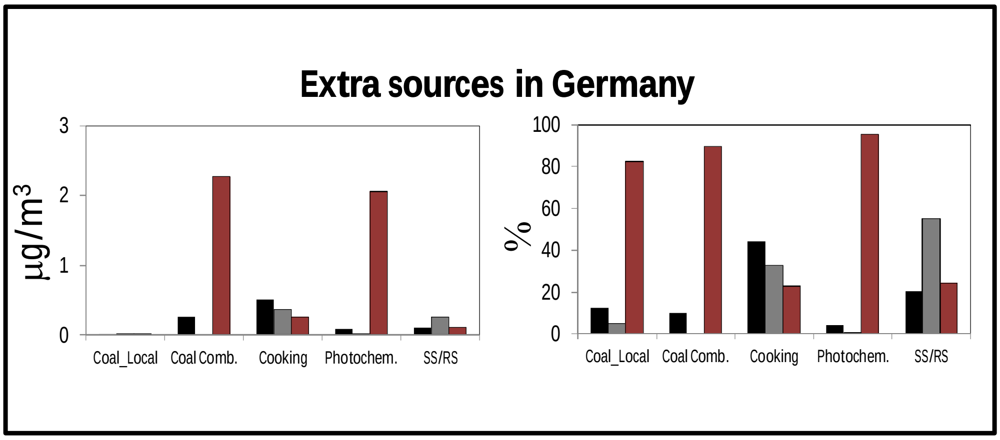

Figure 6 (continue): Lenschow's approach applied to the PM_{10} ($PM_{2.5}$ in the Netherlands) PMF source contributions. Annual means are reported. ES: Spain; CH: Switzerland; NL: The Netherlands; DE: Germany; FR: France. In all countries, with the exception of Spain, Reg_Anthr and Reg_Nat are the sum of regional+continental.

In absolute values, the R+C SIA increments were higher in winter compared to summer in all countries, with the exception of ES. The winter-to-summer R+C SIA increment ratios (using absolute values) ranged between 1.5 in FR to around 5 in DE. In ES it was 0.7. As shown later, the difference observed between ES and the other countries was due to the different effects that SSA and NSA have on the seasonal SIA profile. In ES, the higher relative and absolute R+C SIA increments in summer compared to winter were due to the increase of the R+C SSA increment during the warm season. In the other European countries, the higher winter R+C SIA increment compared to summer was due mostly to the strong increase of the NSA regional increment during the cold season. The very high winter-to-summer R+C SIA increment ratio observed in DE were likely related to the air mass transport at the German sites. As reported by van Pinxteren et al. (2016), in DE during both summer and winter two air mass origins prevail: western and eastern inflow. Particle mass concentrations in Leipzig were typically higher during eastern than during western inflow and especially during the winter period, thus explaining the high winter-to-summer ratio of the R+C SIA increment in DE. This trend has been commonly observed in the area of Leipzig and can be explained with a more continental character of eastern air masses (western air masses typically spend considerable time above the Atlantic Ocean) and higher PM pollution in Eastern European countries (e.g. Pokorná et al., 2013; 2015).

SSA source (anthropogenic)

As expected, the majority of SSA measured in the selected cities was of R+C origin. On annual basis, the highest R+C SSA increment was observed in ES (4.8 $\mu g/m^3$, 91% of *SSA* source contribution in BCN). Thus, in BCN the local SSA increment was low (0.5 $\mu g/m^3$; 9%). The high R+C SSA increment in ES was likely due to shipping emissions in the Mediterranean Sea, whereas the very local SSA increment could be linked to the emissions of primary sulfate from ships in the port of Barcelona. Recently, Van Damme et al. (2018) identified Catalonia (NE Spain) as one of the major hotspots in terms of NH_3 emissions. In all other countries, the annual R+C SSA increment was lower and ranged between 3.5 $\mu g/m^3$ (77% of SSA source contribution) in CH and 1.8 $\mu g/m^3$ (83%) in FR where the lowest absolute R+C SSA increment was observed. The R+C SSA increment in NL, where the NH_3 emissions are high (Van Damme et al., 2018), was estimated to be around 2.9 $\mu g/m^3$ (81% of SSA), being the remaining SSA associated with primary emissions from ships. The relatively high annual urban SSA increment observed at ZUE (CH; 1.1 $\mu g/m^3$; 24% of SSA contribution in ZUE; cf. Figure 6 and Table S8) could be related to local road traffic and wood combustion emissions which in addition contribute to NSA and SSA through emissions of gaseous precursors of SIA (Gianini et al., 2012). In the other cities included in this analysis, the local SSA increment ranged between 0.4 (LEN, FR) and 0.7 (SCH, NL) $\mu g/m^3$ (0-18%).

In absolute values, the R+C SSA increment in summer was higher compared to winter in all countries with the exception of NL where a higher R+C SSA increment was observed in winter (4.0 μg/m^3) compared to summer (2.6 μg/m^3). Mooibroek et al. (2011) reported a flat seasonal pattern of the SSA source contributions in NL that resembled the long-term average of SO_4^{2-}. Moreover, the low SSA summer-to-winter ratio in the Netherland could be also associated with emissions of primary sulfate from ships, which, as shown before, was high in SCH during the period considered. In ES, the R+C SSA increment in summer (cf. Table S10) was related to long-range transport of SSA, which accumulated over the region due to the summer regional recirculation described above, and the photochemistry which enhances the SO_2 oxidation. .

Finally, in all countries the *SSA* absolute local increments did not show clear seasonal cycles likely resembling the effect of local sources on SSA.

<u>NSA source (anthropogenic):</u>

On annual average, high and similar R+C NSA increments were observed in CH (annual mean: 4.2 μg/m^3; 94% of NSA contribution in ZUE) and NL (4.8 μg/m^3; 78% of NSA contribution in SCH). Conversely, lower R+C NSA increments were observed in ES (1.5 μg/m^3; 50% of NSA contribution in BCN) and FR (1.5 μg/m^3; 41% of NSA contribution in LEN). In BCN (ES), the high local NSA increment (around 50% or 1.5 μg/m^3 of NSA source contribution in BCN) was explained by the NO_x emissions from traffic and the availability of NH_3 in the city of Barcelona (e.g. Reche at al., 2012; Pandolfi et al., 2012). High NO_x emissions originating from road traffic could also be responsible for the high local NSA increment in LEN (FR; 2.1 μg/m^3; 59% of NSA contribution to PM_{10} in LEN). Agricultural emissions of NH_3 and NO_x emissions from road and maritime traffic and industry were the likely cause of the high R+C NSA increment observed especially in NL and CH.

In all countries, as a consequence of the thermal instability of ammonium nitrate, both local and R+C NSA increments were higher in winter compared to summer (Figures S10 and S11 and Tables S8 and S9). In both winter and summer, the highest local and R+C NSA increments were observed in NL. As reported in Mooibroek et al. (2011), the concentration of ammonia in the Dutch atmosphere is such that when sulfate is fully neutralized, a considerable amount is left to stabilize the ammonium nitrate even in summer. In this country, the mean R+C NSA increments were 10 μg/m^3 and 2.5 μg/m^3 in winter and summer, respectively. The high summer R+C NSA increment in NL (much higher compared to the other countries where it was around of 0-0.8 μg/m^3) was due to the high concentration of NH_3 in the Dutch atmosphere and NO_x emissions. NH_3 concentration is such that when SSA is fully neutralized, a considerable amount is left to stabilize the ammonium nitrate also in summer (Mooibroek et al., 2011).

Mineral (local anthropogenic; regional+continental natural):

On annual basis, the R+C MM increments were higher compared to the local increments at all sites with the exception of DE where the urban and R+C increments were similar. As reported in van Pinxteren et al. (2016), the MM factor identified in DE was characterized by high nitrate fraction and anthropogenic n-alkanes signature indicating a mixture of soil with urban pollution thus likely explaining the lower R+C increment compared to the other sites. Moreover, the seasonal and site dependencies of concentrations presented in van Pinxteren et al. (2016) suggested an urban background MM source without direct association to traffic. This could be the reason for the null traffic MM increment reported here for the German traffic site (Figure 6 and Table S8). The highest urban and R+C MM increments were observed in FR (1.8 $\mu g/m^3$ and 3.2 $\mu g/m^3$, respectively) followed by ES (0.7 $\mu g/m^3$ and 2.6 $\mu g/m^3$, respectively) and CH (0.9 $\mu g/m^3$ and 1.9 $\mu g/m^3$, respectively), whereas these values were much lower in NL (where $PM_{2.5}$ was sampled) and DE. For LEN (FR), Waked et al. (2014) showed a very similar trend for the MM factor and for primary traffic emissions in Lens, suggesting a major influence of road transport for particles resuspension. Alastuey et al. (2016) have shown that in the North of FR, the average mineral dust concentration and its relative contribution to PM_{10} was higher compared to DE and mostly in summer.

As shown in Figure 6, the majority of the R+C MM increments in ES were of continental origin (2.2 $\mu g/m^3$ continental and 0.4 $\mu g/m^3$ regional; cf. Table S8) and especially in summer (3.2 $\mu g/m^3$ continental and 0.1 $\mu g/m^3$ regional) whereas in winter the regional and continental contributions were lower and similar (0.4 $\mu g/m^3$ continental and 0.5 $\mu g/m^3$ regional). The seasonality of the MM increments observed in ES was also due to the long-range transport of mineral dust from the Saharan Desert during Saharan dust outbreaks (Querol et al., 2009; Pey et al., 2013). As shown in Alastuey et al. (2016), the contribution from desert dust to PM is expected to be higher in the Mediterranean region compared to Central/North of Europe. The higher R+C MM increments in summer compared to winter, observed also in the other countries, were linked to the enhanced regional resuspension of dust during the dry season together with Saharan dust outbreaks which are more sporadic in Central and North Europe (i.e. Gianini et al., 2102).

Road traffic (anthropogenic)

As expected, the majority of the RT source emissions were of local origin in all cities included in this analysis. The relative urban RT increments ranged between 62% in SCH (NL) to 90% in BCN. The relatively high R+C RT increment observed in NL (36% compared to 6-20% in the other countries) was in agreement with the value reported by Mooibroek et al. (2011). In winter, the local RT increments were higher than in summer in BCN (ES) and SCH (NL) by factors of 2 and 4, respectively. Conversely, similar winter and summer local RT increments were observed in ZUE (CH), LMI (DE) and LEN (FR). For DE, van Pinxteren et al. (2016) have shown that for coarse particles urban background and traffic increments were broadly similar in year-round averages. It is important to note that the identification of a clear RT source at regional level in the selected countries and, consequently, the possibility to resolve a regional RT increment, even if low, was due to the application of the multi-site PMF.

- ***Sources identified only at a subset of paired sites***

Biomass burning (anthropogenic)

On annual base the R+C BB increments were rather similar in CH (1.8 $\mu g/m^3$; 78% of *BB* contribution in ZUE), DE (1.1 $\mu g/m^3$; 77% of *BB* contribution in LMI/TRO) and in FR (1.1 $\mu g/m^3$; 42% of *BB* contribution in LEN). Notable difference was the relatively higher urban BB increment observed in LEN (1.5 $\mu g/m^3$; 58%) compared to LMI/TRO (0.3 $\mu g/m^3$; 23%) and ZUE (0.6 $\mu g/m^3$; 22%). Both the urban and R+C BB increments were much higher in winter compared to summer at the three paired sites where the BB source was found. In CH, the R+C BB increment in winter reached around 3.9 $\mu g/m^3$ (73% of winter *BB* contribution in ZUE), whereas it was around 1.7-1.9 $\mu g/m^3$ in DE and FR. In winter, the highest urban increment was observed in LEN (FR; 2.7 $\mu g/m^3$; 59%).

Residual oil combustion (V-Ni) and Industrial (anthropogenic)

In both ES and NL (cf. Figures 6, S10 and S11 and Tables S7, S8 and S9), the local V-Ni increments were higher compared to the R+C V-Ni increments likely because of the influence of emissions from the port of Barcelona and Schiedam. Both the urban and R+C V-Ni increments were much higher in ES (1.7 $\mu g/m^3$ urban and 1.0 $\mu g/m^3$ R+C) than in NL (0.2 $\mu g/m^3$ urban and 0.1 $\mu g/m^3$ R+C), especially in summer when the urban and R+C increments in ES reached around 1.9 $\mu g/m^3$ (56%) and 1.5

μg/m^3 (44%), respectively. Thus, the V-Ni and the SSA local/R+C increments strongly contributed to the observed seasonal profile of PM measured in Barcelona.

On annual average, the urban and R+C IND increments were almost negligible in ES (0.04 μg/m^3 and 0.01 μg/m^3, respectively) compared to NL (0.3 μg/m^3 and 2.0 μg/m^3, respectively). The R+C IND increments in NL were higher in summer (2.3 μg/m^3; 96%) compared to winter (1.7 μg/m^3; 95%). Mooibroek et al. (2011) showed that the IND source profile had slightly higher contributions during summer compared to the other seasons. Due to the lack of a pronounced seasonal pattern and the similar contribution at all Dutch receptor sites, Mooibroek et al. (2011) assumed the IND source was a common source representing negligible local contributions.

- ***Sources identified only at one paired site***

As already shown, two additional natural sources were identified in FR; *marine biogenic* and *land biogenic* sources. These sources can be considered as totally natural. Thus, Lenschow's approach was not applied.

In DE, six extra sources were resolved and among these sources the f*ungal* s*pores* source was considered as totally regional/natural. For the other five sources, the Lenschow approach was applied, and the results are shown in Figure 6 and Table S8. Among these five sources, the contributions from *coal combustion* and *photochemistry* sources were the highest. Both sources showed strong seasonal characters and were mostly of R+C origin. The R+C *coal combustion* increment was much higher in winter (3.9 μg/m^3; 90% of *coal combustion* source contribution to LMI) compared to summer (0.01 μg/m^3; 33%), whereas the R+C *photochemistry* increment was slightly higher in summer (2.2 μg/m^3; 83%) compared to winter (1.9 μg/m^3; 97%). As reported in van Pinxteren et al. (2016), coal combustion was a significant source only during easterly air mass inflow in winter and showed very similar concentrations at all sites included in van Pinxteren et al. (2016), highlighting the importance of trans-boundary air pollution transport in the study area. This, together with increased regional concentrations of biomass combustion (e.g. Hovorka et al., 2015) and secondary material, emphasizes the importance of transboundary pollution transport for regional air quality in the area of Leipzig.

4. CONCLUSIONS

This investigation aimed at discriminating local and R+C contributions from different sources to the concentrations of PM measured in five European cities. To accomplish this objective, we selected five paired sites in Europe (traffic/urban and regional/continental) providing PM chemically speciated data and applied the PMF model (EPA PMF v5.0). The obtained PM source contributions were then used to estimate the urban and non-urban (regional+continental; R+C) PM and source contributions increments through the application of Lenschow's approach. Urban increments were computed by withdrawing the rural source contributions to the local (urban) source contributions. In turn, regional increments were computed by withdrawing remote contributions (when available, i.e. in ES) to the regional contributions. For those countries where a remote site was not available, we did not separate the regional contributions from the continental contributions and the sum of the two (R+C) was calculated.

The results presented here provided a robust and feasible source allocation and estimation of the R+C increments to urban pollution. With the approach presented (multi-site PMF + Lenschow's approach), we were able to allocate urban pollution to major primary sources by activity sector or to main secondary aerosol fractions thanks to the application of the Positive Matrix Factorization (PMF) model that gathers together species emitted from the same source. Regarding source allocation for secondary aerosols, it is important to note that the sources such as shipping, agricultural activities, road transport, power generation, industry and domestic sector are important contributors of gaseous precursors and consequently to secondary aerosols. However, these separated contributions cannot be easily identified using PMF that tends to group in the same source (e.g. NSA) secondary nitrates formed from different sources. However, the PMF allocation for secondary aerosols presented here is extremely useful for models that can simulate, for example, NSA particles starting from emissions from different sectors. Moreover, this approach turns out to be useful in air quality management to assess both the sources and the relevance of local and regional emissions.

We have shown that we can use paired sites to estimate the relative contributions of local and R+C sources of PM. Sources of primary PM such as traffic dominate at the local scale while secondary PM like sulfate is mostly R+C in origin. However, NSA has a local component because of its rapid formation rates and the availability of NH_3 in urban settings. Other potentially important local sources of PM are emissions from ships, ports and industry especially in cities with harbors. We have shown that the amount of primary SSA emitted by ships depends on the amount of sulfur content in residual oil burned, and that it was much higher in NL compared to ES during 2007-2008. We have also shown that the primary SSA emitted by ships in NL was much lower in 2013-2014 compared to 2007-2008 due to change of fuel used by ships in berth and, in general, to the shift from high-sulfur to low-sulfur content fuels.

Finally, potentially important regional sources are biomass burning and coal combustion.

The last EMEP report on air pollution trends in the EMEP region (Colette et al., 2016), reported on the significant negative trends observed at 38% (for PM_{10}) and 55% (for $PM_{2.5}$) of the sites during the period 2002 - 2012, with a relative change over the decade of -29% ([-29,-19]) and - 31% ([-35,-25]) for PM_{10} and $PM_{2.5}$, respectively. The observed reductions were mostly driven by the decrease of SO_4^{2-}, NO_3^- and NH_4^+ particles because of the reduction of the concentrations of gaseous precursors such as SO_2, NO_2 and NH_3. SO_2 and sulfate particles showed the strongest decreasing trends with median relative changes over the period 2002 – 2012 of -48% [-53,-38] and -39% [-42,-27], respectively. These decreases were even stronger during the period 1990 – 2001 with median relative changes of -80% [-82,-72] and -52% [-56,-46], respectively. NO_2 and particulate nitrate, cumulated with gaseous nitric acid (NO_3^-+HNO_3), showed lower decreasing trends of -17% [-20,18] and -7.1% [-12,18], respectively, during 2002 – 2012, and -28% [-34,-19] and -24% [-39,-9.8], respectively, during 1990 – 2001. Particulate NH_4^+ cumulated with gaseous NH_3 (NH_3+NH_4^+) showed decreasing trend of -14% [-15,23] and -40% [-47,-19], during the period 2002 – 2012 and 1990 – 2001, respectively. Recently, Pandolfi et al. (2016) reported total reductions of around 50% for both PM_{10} and $PM_{2.5}$ in Barcelona (UB; NE ES) during the period 2004 – 2014 and around 8% and 21%, for PM_{10} and $PM_{2.5}$, respectively, at regional level in NE of Spain (RB Montseny station). The sources that mostly contributed to the observed PM reductions were secondary SO_4^{2-}, secondary NO_3^- and residual oil combustion. The contributions from these sources decreased exponentially over the decade, with the sharpest decrease observed for secondary SO_4^{2-} in Barcelona mostly, but not only, because of the ban of heavy oils and petroleum coke for power generation around Barcelona from 2007 and the EC Directive on Large Combustion Plants, which resulted in the application of flue gas desulfurization (FGD) systems in a number of large facilities spread regionally. The fact that the trend of the secondary SO_4^{2-} source contribution in NE Spain was exponential suggested the attainment of a lower limit, and indicated a limited scope for further reduction of SO_2 emissions in NE of Spain. In fact, it has been estimated that the maximum in EU will be a further 20% SO_2 reduction through measures in industry, residential and commercial heating, maritime shipping, and reduced agricultural waste burning (UNECE, 2016). Conversely, in eastern European countries the scope for reduction is much greater and around 60% (UNECE, 2016).

For the present work, we used data collected over variable periods depending on the country and covering the period 2007 – 2014. Based on the analysis presented here, an improvement of air quality in the 5 cities included in this study could be achieved by further reducing local (urban) emissions of PM, NO_x and NH_3 (from both traffic and non-traffic sources) but also of PM and SO_2 from maritime ships and ports. Moreover, improvements can be achieved by reducing non-urban emissions of NH_3 (agriculture), SO_2 (regional maritime shipping) and PM and gaseous precursors from regional BB sources, power generation, coal combustion and industries.

The possibility to identify pollutant sources is related to the PM chemical speciation available. We have shown here that BB emissions can be important contributors to PM, however, a clear determination of its contribution depends on the availability of specific BB tracers such as levoglucosan, or other specific polysaccharides, together with K^+. For the determination of residual oil combustion sources such as ships, whose emissions are projected to increase significantly if mitigation measures are not put in place swiftly, the determination of specific tracers such as V and Ni is necessary. Emissions from coal combustion, which we have seen to be important in central Europe, can be traced by using PAHs, As and Se, as important tracers of this source.

Data availability

The chemically speciated PM data used in this study are available upon request from the corresponding authors.

Code availability

The PMF model version 5.0 used in this study is available at https://www.epa.gov/air-research/positive-matrix-factorization-model-environmental-data-analyses.

Author contribution

AC, OT and MP developed the idea behind this study. MP performed the analysis, created the figures and wrote the manuscript. DM and EvdS applied the multi-site PMF on Dutch database. DvP and HH applied the multi-site PMF on German database. MP, DM and PH provided the analysis on primary sulfate emissions from ships in Spain and The Netherlands. XQ, AA, OF, CH, EP, VR, SS, provided guidance. All authors read and approved the final paper.

ACKNOWLEDGMENTS:

Measurements at Spanish sites (Montseny, Montsec and Barcelona) were supported by the Spanish Ministry of Economy, Industry and Competitiveness and FEDER funds under the project HOUSE (CGL2016-78594-R), and by the Generalitat de Catalunya (AGAUR 2014 SGR33, AGAUR 2017 SGR41 and the DGQA). Marco Pandolfi is funded by a Ramón y Cajal Fellowship (RYC-2013-14036) awarded by the Spanish Ministry of Economy and Competitiveness. The authors thank Cristina Reche, Noemi Pérez, and Anna Ripoll (IDAEA-CSIC) for providing chemically speciated PM data for Barcelona, Montseny, and Montsec stations (Spain). Measurements at French sites (Lens, Revin) were notably funded by the French Ministry of Environment ("Bureau de l'Air du Ministère de l'Ecologie, du Développement durable, et de l'Energie") and included in the CARA air quality monitoring and research project coordinated by the French reference laboratory for air quality monitoring (LCSQA), with technical support provided by the air quality monitoring networks Atmo Hauts-de-France and Atmo Grand-Est. IMT Lille Douai acknowledges financial support from the CaPPA project, which is funded by the French National Research Agency (ANR) through the PIA (Programme d'Investissement d'Avenir) under contract ANR-11-LABX-0005-01, and the CLIMIBIO project, both financed by the Regional Council "Hauts-de-France" and the European Regional Development Fund (ERDF). For the measurements at the German sites, financial support from the Saxon State Office for Environment, Agriculture and Geology (LfULG) is acknowledged. Gathering of in-situ data supporting this analysis was organized through the EMEP Task Force on Measurement and Modelling. The authors wish to thank D. C. Carslaw and K. Ropkins for providing the Openair software used in this paper.

BIBLIOGRAPHY:

Alastuey, A., Querol, X., Aas, W., Lucarelli, F., Pérez, N., Moreno, T., Cavalli, F., Areskoug, H., Balan, V., Catrambone, M., Ceburnis, D., Cerro, J. C., Conil, S., Gevorgyan, L., Hueglin, C., Imre, K., Jaffrezo, J.-L., Leeson, S. R., Mihalopoulos, N., Mitosinkova, M., O'Dowd, C. D., Pey, J., Putaud, J.-P., Riffault, V., Ripoll, A., Sciare, J., Sellegri, K., Spindler, G., and Yttri, K. E.: Geochemistry of PM10 over Europe during the EMEP intensive measurement periods in summer 2012 and winter 2013, Atmos. Chem. Phys., 16, 6107-6129, https://doi.org/10.5194/acp-16-6107-2016, 2016.

Amann, M., Bertok, I., Borken-Kleefeld, J., Cofala, J., Heyes, C., Höglund-Isaksson, L., Klimont, Z., Nguyen, B., Posch, M., Rafaj, P., Sander, R., Schöpp, W., Wagner, F., Winiwarter, W.: Cost-effective control of air quality and greenhouse gases in Europe: modeling and policy applications. Environmental Modelling and Software 26, 1489–1501. doi:10.1016/j.envsoft.2011.07.012., 2011.

Amato, F., Pandolfi, M., Escrig, A., Querol, X., Alastuey, A., Pey, J., Perez, N., and Hopke, P. K.: Quantifying road dust resuspension in urban environment by Multilinear Engine: A comparison with PMF2, Atmos. Environ., 43, 2770–2780, 2009.

Agrawal, H., Welch, W.A., Miller, J.W., Cocker III, D.R.: Emission Measurements from a Crude Oil Tanker at Sea, Environ. Sci. Technol., 42, 19, 7098-7103, https://doi.org/10.1021/es703102y, 2008.

Agrawal, H., Welch, W. A., Henningsen, S., Miller, J. W., Cocker III, D. R.: Emissions from main propulsion engine on container ship at sea, J. Geophys. Res., 115, D23205, doi:10.1029/2009JD013346, 2010.

Bessagnet, B., Pirovano, G., Mircea, M., Cuvelier, C., Aulinger, A., Calori, G., Ciarelli, G., Manders, A., Stern, R., Tsyro, S., García Vivanco, M., Thunis, P., Pay, M.-T., Colette, A., Couvidat, F., Meleux, F., Rouïl, L., Ung, A., Aksoyoglu, S., Baldasano, J. M., Bieser, J., Briganti, G., Cappelletti, A., D'Isidoro, M., Finardi, S., Kranenburg, R., Silibello, C., Carnevale, C., Aas, W., Dupont, J.-C., Fagerli, H., Gonzalez, L., Menut, L., Prévôt, A. S. H., Roberts, P., and White, L.: Presentation of the EURODELTA III intercomparison exercise – evaluation of the chemistry transport models' performance on criteria pollutants and joint analysis with meteorology, Atmos. Chem. Phys., 16, 12667–12701, https://doi.org/10.5194/acp-16-12667-2016, 2016.

Belis C. A., Pernigotti D., Pirovano G., Favez O., Jaffrezo J.L., Kuenen J., Denier van Der Gon H., Reizer M., Pay M.T., Almeida M., Amato F., Aniko A., Argyropoulos G., Bande S., Beslic I., Bove M., Brotto P., Calori G., Cesari D., Colombi C., Contini D., De Gennaro G., Di Gilio A., Diapouli E., El Haddad I., Elbern H., Eleftheriadis K., Ferreira J., Foret G., Garcia Vivanco M., Gilardoni S., Hellebust S., Hoogerbrugge R., Izadmanesh Y., Jorquera H., Karppinen A., Kertesz Z., Kolesa T., Krajsek K., Kranenburg R., Lazzeri P., Lenartz F., Liora N., Long Y., Lucarelli F., Maciejewska K., Manders A., Manousakas M., Martins H., Mircea M., Mooibroek D., Nava S., Oliveira D., Paatero P., Paciorek M., Paglione M., Perrone M., Petralia E., Pietrodangelo A., Pillon S., Pokorna P., Poupkou A., Pradelle F., Prati P., Riffault V., Salameh D., Samara C., Samek L., Saraga D., Sauvage S., Scotto F., Sega K., Siour G., Tauler R., Valli G., Vecchi R., Venturini E., Vestenius M., Yarwood G., Yubero E., 2018 Results of the first European Source Apportionment intercomparison for Receptor and Chemical Transport Models, EUR 29254 EN, Publications Office of the European Union, Luxembourg, 2018, ISBN 978-92-79-86573-2, doi: 10.2760/41815, JRC 111887.

Brown, S.G., Eberly, S., Paatero, P., Norris, G.A.: Methods for estimating uncertainty in PMF solutions: Examples with ambient air and water quality data and guidance on reporting PMF results, Sci. of Tot. Environ., 518–519, 626-635, https://doi.org/10.1016/j.scitotenv.2015.01.022, 2015.

Bukowiecki, N., Lienemann, P., Hill, M., Furger, M., Richard, A., Amato, F., Prévôt, A.S.H., Baltensperger, U., Buchmann, B., Gehrig, R.: PM10 emission factors for non-exhaust particles generated by road traffic in an urban street canyon and along a freeway in Switzerland, Atm. Env., 44, 2330-2340, 2010.

Carslaw, D. C.: The openair manual – open-source tools for analysing air pollution data, Manual for version 0.7-0, King's College, London, 2012.

Carslaw, D. C. and Ropkins, K.: openair – an R package for air quality data analysis, Environ. Modell. Softw., 27–28, 52–61, 2012.

Colette, A., Aas, W., Banin, L., Braban, C.F., Ferm, M., González Ortiz, A., Ilyin, I., Mar, K., Pandolfi, M., Putaud, J.-P., Shatalov, V., Solberg, S., Spindler, G., Tarasova, O., Vana, M., Adani, M., Almodovar, P., Berton, E., Bessagnet, B., Bohlin-Nizzetto, P., Boruvkova, J., Breivik, K., Briganti, G., Cappelletti, A., Cuvelier, K., Derwent, R., D'Isidoro, M., Fagerli, H., Funk, C., Garcia Vivanco, M., González Ortiz, A., Haeuber, R., Hueglin, C., Jenkins, S., Kerr, J., de Leeuw, F., Lynch, J., Manders, A., Mircea, M., Pay, M.T., Pritula, D., Putaud, J.-P., Querol, X., Raffort,V., Reiss, I., Roustan, Y., Sauvage, S., Scavo, K., Simpson, D., Smith, R.I., Tang, Y.S., Theobald, M., Tørseth, K., Tsyro, S., van Pul, A., Vidic, S., Wallasch, M., Wind, P., Air pollution trends in the EMEP region between 1990 and 2012, Joint Report of the EMEP Task Force on Measurements and Modelling (TFMM), Chemical Co-ordinating Centre (CCC), Meteorological Synthesizing Centre-East (MSC-E), Meteorological Synthesizing Centre-West (MSC-W), EMEP/CCC-Report 1/2016.

Escrig, A., Monfort, E., Celades, I., Querol, X., Amato, F., Minguillon, M. C., and Hopke, P. K.: Application of optimally scaled target factor analysis for assessing source contribution of ambient PM10, J. Air Waste Manage., 59, 1296–1307, 2009.

Lenschow, P., Abraham, H.-J., Kutzner, K., Lutz, M., Preu, J.-D., Reichenbacher, W.: Some ideas about the sources of PM10, Atm. Env., 35, 1, S23–S33, 2001.

EEA: European Environment Agency, Air quality in Europe, Report No 12/2018, ISSN 1977-8449, doi: 10.2800/777411, 2018.

Gehrig, R., and Buchmann, B.: Characterising seasonal variations and spatial distribution of ambient PM10 and PM2.5 concentrations based on long-term Swiss monitoring data, Atm. Env., 37(19), 2571-2580, https://doi.org/10.1016/S1352-2310(03)00221-8, 2003.

Gianini, M.F.D., Fischer, A., Gehrig, R., Ulrich, A., Wichser, A., Piot, C., Besombes, J.-L., Hueglin, C.: Comparative source apportionment of PM10 in Switzerland for 2008/2009 and 1998/1999 by Positive Matrix Factorisation, Atm. Env., 54, 149-158, 2012.

Godoy, M., Godoy, J.M., Artaxo, P.: Aerosol source apportionment around a large coal fired power plant e thermoelectric complex Jorge Lacerda, Santa Catarina, Brazil. Atm. Env., 39, 5307-5324, 2005.

Hopke, P.K.: Review of receptor modeling methods for source apportionment, Journal of the Air & Waste Management Association, 66:3, 237-259, DOI: 10.1080/10962247.2016.1140693, 2016.

Hovorka, J., Pokorná, P., Hopke, P.K., Křůmal, K., Mikuška, P., Píšová, M.: Wood combustion, a dominant source of winter aerosol in residential district in proximity to a large automobile factory in Central Europe, J., Atm. Environ., 113, 98- 107, 2015.

Hueglin, C., Gehrig, R., Baltensperger, U., Gysel, M., Monn, C., Vonmont, H.: Chemical characterisation of PM2.5, PM10 and coarse particles at urban, near city and rural sites in Switzerland, Atm. Env., 39, 637-651, 2005.

IPCC, 2013: Climate Change 2013: The Physical Science Basis. Contribution of Working Group I to the Fifth Assessment Report of the Intergovernmental Panel on Climate Change [Stocker, T.F., D. Qin, G.-K. Plattner, M. Tignor, S.K. Allen, J. Boschung, A. Nauels, Y. Xia, V. Bex and P.M. Midgley (eds.)]. Cambridge University Press, Cambridge, United Kingdom and New York, NY, USA, 1535, 2013.

Kiesewetter, G., Borken-Kleefeld, J., Schöpp, W., Heyes, C., Thunis, P., Bessagnet, B., Terrenoire, E., Fagerli, H., Nyiri, A., and Amann, M.: Modelling street level PM10 concentrations across Europe: source apportionment and possible futures, Atmos. Chem. Phys., 15, 1539-1553, https://doi.org/10.5194/acp-15-1539-2015, 2015.

Kim E., Hopke P.K., Edgerton E.S.: Source identification of Atlanta aerosol by positive matrix factorization Journal of the Air and Waste Management Association, 53, 731-739, 2003.

Kim, E. and Hopke, P.K.: Improving source identification of fine particles in a rural northeastern U.S. area utilizing temperature-resolved carbon fractions, J. Geophys. Res., 109: D09204, doi:10.1029/2003JD004199, 2004.

Kim, E. and Hopke, P.K.: Source characterization of ambient fine particles at multiple sites in the Seattle area, Atm. Env., 42, 6047–6056, 2008.

Kranenburg, R., Segers, A.J., Hendriks, C., Schaap, M.: Source apportionment using LOTOS-EUROS: Module description and evaluation, Geosci. Model Dev., 6, 721-733, 2013.

Lanz, V. A., Alfarra, M. R., Baltensperger, U., Buchmann, B., Hueglin, C., Szidat, S., Wehrli, M. N., Wacker, L., Weimer, S., Caseiro, A., Puxbaum, H., and Prevot, A. S. H.: Source attribution of submicron organic aerosols during wintertime inversions by advanced factor analysis of aerosol mass spectra, Environ. Sci. Technol., 42, 214–220, 2008.

Lenschow, P., Abraham, H.-J., Kutzner, K., Lutz, M., Preu, J.-D., Reichenbacher, W.: Some ideas about the sources of PM10, Atmos. Environ., 35, 23–33, 2001.

Liao, H.-T., Chou, C.C.-K., Chow, J.C., Watson, J.G., Hopke, P.K., and Wu C.-F.: Source and risk apportionment of selected VOCs and PM2.5 species using partially constrained receptor models with multiple time resolution data, Environ Pollut. 205:121–30. doi:10.1016/j.envpol.2015.05.035, 2015.

Millán, M. M., Salvador, R., Mantilla, E., Kallos, G.: Photo-oxidant dynamics in the Mediterranean Basin in Summer: Results from European Research Projects. J. Geophys. Res., 102, D7, 8811-8823, 1997.

Millán, M. M., E. Mantilla, R. Salvador, A. Carratalá, Mª.J. Sanz, L. Alonso, G. Gangoiti, M. Navazo, 2000: Ozone cycles in the Western Mediterranean Basin: Interpretation of Monitoring Data in Complex Coastal Terrain. J. Appl. Meteor., 39, 487-508.

Mohr, C., DeCarlo, P. F., Heringa, M. F., Chirico, R., Slowik, J. G., Richter, R., Reche, C., Alastuey, A., Querol, X., Seco, R., Peñuelas, J., Jiménez, J. L., Crippa, M., Zimmermann, R., Baltensperger, U., and Prévôt, A. S. H.: Identification and quantification of organic aerosol from cooking and other sources in Barcelona using aerosol mass spectrometer data, Atmos. Chem. Phys., 12, 1649-1665, https://doi.org/10.5194/acp-12-1649-2012, 2012.

Mooibroek, D., Schaap, M., Weijers, E.P., Hoogerbrugge, R.: Source apportionment and spatial variability of PM2.5 using measurements at five sites in the Netherlands, Atm. Env., 45, 4180-4191, 2011.

Mooibroek, D., Staelens, J., Cordell, R., Panteliadis, P., Delaunay, T., Weijers, E., Vercauteren, J., Hoogerbrugge, R., Dijkema, M., Monks, P.A., Roekens, E.: PM10 source apportionment in Five North Western European Cities – Outcome of the Joaquin Project, in Issues in Environmental Science and Technology No 42, Airborne Particulate Matter: Sources, Atmospheric Processes and Health, Edited by R.E. Hester, R.M. Harrison and X. Querol, The Royal Society of Chemistry, ISNN 1350-7583, 2016.

Paatero, P. and Tapper, U.: Positive matrix factorization: A nonnegative factor model with optimal utilization of error estimates of data values, Environmetrics, 5, 111–126, 1994.

Paatero, P.: Least squares formulation of robust non-negative factor analysis. Chemometrics and Intelligent Laboratory Systems, 37, 23–35, 1997.

Paatero, P.: The multilinear engine – a table-driven least squares program for solving multilinear problems, including the n-way parallel factor analysis model, J. Comput. Graph. Stat., 8, 854–888, 1999.

Paatero, P., Hopke, P. K., Song, X., and Ramadan, Z.: Understanding and controlling rotations in factor analytic models, Chemometr. Intell. Lab., 60, 253–264, 2002.

Paatero, P. and Hopke, P. K.: Discarding or downweighting high noise variables in factor analytic models, Anal. Chim. Acta, 490, 277–289, 2003.

Paatero, P.: User's guide for positive matrix factorization programs PMF2 and PMF3, Part 1: tutorial, University of Helsinki, Helsinki, Finland, 2004.

Paatero, P. and Hopke, P. K.: Rotational tools for factor analytic models implemented by using the multilinear engine, Chemometrics, 23, 91–100, 2008.

Paatero, P., Eberly, S., Brown, S.G., Norris, G.A., Methods for estimating uncertainty in factor analytic solutions. Atmos. Meas. Tech. 7, 781–797, 2014.

Pandolfi, M., Cusack, M., Alastuey, A., and Querol, X.: Variability of aerosol optical properties in the Western Mediterranean Basin, Atmos. Chem. Phys., 11, 8189–8203, https://doi.org/10.5194/acp-11-8189-2011, 2011.

Pandolfi, M., Gonzalez-Castanedo, Y., Alastuey, A., de la Rosa, J., Mantilla, E., Sanchez de la Campa, A., Querol, X., Pey, J., Amato, F., Moreno, T.: Source apportionment of PM10 and PM2.5 at multiple sites in the strait of Gibraltar by PMF: impact of shipping emissions, Environ. Sci. Pollut. Res., 18, 260–269, 10.1007/s11356-010-0373-4, 2011a.

Pandolfi, M., Amato, F., Reche, C., Alastuey, A., Otjes, R. P., Blom, M. J., and Querol, X.: Summer ammonia measurements in a densely populated Mediterranean city, Atmos. Chem. Phys., 12, 7557-7575, https://doi.org/10.5194/acp-12-7557-2012, 2012.

Pandolfi, M., et al.: Effects of sources and meteorology on particulate matter in the Western Mediterranean Basin: An overview of the DAURE campaign, J. Geophys. Res. Atmos., 119, 4978–5010, doi:10.1002/2013JD021079, 2014.

Pandolfi, M., Ripoll, A., Querol, X., and Alastuey, A.: Climatology of aerosol optical properties and black carbon mass absorption cross section at a remote high-altitude site in the western Mediterranean Basin, Atmos. Chem. Phys., 14, 6443-6460, https://doi.org/10.5194/acp-14-6443-2014, 2014a.

Pandolfi, M., Alastuey, A., Pérez, N., Reche, C., Castro, I., Shatalov, V., and Querol, X.: Trends analysis of PM source contributions and chemical tracers in NE Spain during 2004–2014: a multi-exponential approach, Atmos. Chem. Phys., 16, 11787-11805, https://doi.org/10.5194/acp-16-11787-2016, 2016.

Pérez, N., Pey, J., Castillo, S., Viana, M., Alastuey, A., and Querol, X.: Interpretation of the variability of levels of regional background aerosols in the Western Mediterranean, Sci. Total Environ., 407, 527–540, 2008.

Petetin, H., Beekmann, M., Sciare, J., Bressi, M., Rosso, A., Sanchez, O., and Ghersi, V.: A novel model evaluation approach focusing on local and advected contributions to urban PM2.5 levels – application to Paris, France, Geosci. Model Dev., 7, 1483–1505, https://doi.org/10.5194/gmd-7-1483-2014, 2014.

Petit, J.-E., Pallarès, C., Favez, O., Alleman, L.Y., Bonnaire, N., Rivière, E.: Sources and Geographical Origins of PM10 in Metz (France) Using Oxalate as a Marker of Secondary Organic Aerosols by Positive Matrix Factorization Analysis, Atmosphere, 10(7), 370; https://doi.org/10.3390/atmos10070370, 2019.

Pey, J., Pérez, N., Querol, X., Alastuey, A., Cusack, M., and Reche, C.: Intense winter atmospheric pollution episodes affecting the Western Mediterranean, Sci. Total Environ., 408, 1951–1959, 2010.

Pey, J., Querol, X., Alastuey, A., Forastiere, F., and Stafoggia, M.: African dust outbreaks over the Mediterranean Basin during 2001–2011: PM10 concentrations, phenomenology and trends, and its relation with synoptic and mesoscale meteorology, Atmos. Chem. Phys., 13, 1395-1410, https://doi.org/10.5194/acp-13-1395-2013, 2013.

Pisoni, E., Clappier, A., Degraeuwe, B., Thunis, P.: Adding spatial flexibility to source-receptor relationships for air quality modeling, Environ.l Mod. & Soft., 90, 68-77, https://doi.org/10.1016/j.envsoft.2017.01.001, 2017.

Polissar, A. V., Hopke, P. K., Paatero, P., Malm, W. C., and Sisler, J. F.: Atmospheric aerosol over Alaska 2. Elemental composition and sources, J. Geophys. Res.-Atmos., 103, 19045–19057, 1998.

Pokorná, P., Hovorka, J., Hopke, P.K., Kroužek, J.: PM1-10 source apportionment in a village situated in industrial region of Central Europe, J. Air Waste Manage. Assoc., 63, 1412-1421, 2013.

Pokorná, P., Hovorka, J., Klán, M., Hopke, P.K.: Source apportionment of size resolved particulate matter at a European air pollution hot spot, , Sci. of the Tot. Environ., 502, 172–183, 2015.

Pope, F. D., Gatari, M., Ng'ang'a, D., Poynter, A., and Blake, R.: Airborne particulate matter monitoring in Kenya using calibrated low-cost sensors, Atmos. Chem. Phys., 18, 15403–15418, https://doi.org/10.5194/acp-18-15403-2018, 2018.

Querol, X., Viana, M., Alastuey, A., Amato, F., Moreno, T., Castillo, S., Pey, J., de la Rosa, J., Artíñano, B., Salvador, P., García Dos Santos, S., Fernández-Patier, R., Moreno-Grau, S., Negral, L., Minguillón, M. C., Monfort, E., Gil, J. I., Inza, A., Ortega, L. A., Santamaría, J. M., and Zabalza, J.: Source origin of trace elements in PM from regional background, urban and industrial sites of Spain, Atmos. Environ., 41, 7219–7231, 2007.

Querol, X., Alastuey, A., Lopez-Soler, A., Plana, F; Puicercus, J.A., Mantilla, E., Palau, J.L.: Daily evolution of sulphate aerosols in a rural area, northeastern Spain-elucidation of an atmospheric reservoir effect, Environ. Poll., 105, 397-407, 1999.

Querol, X., Viana, M., Alastuey, A., Amato, F., Moreno, T., Castillo, S., Pey, J., de la Rosa, J., Artíñano, B., Salvador, P., García Dos Santos, S., Fernández-Patier, R., Moreno-Grau, S., Negral, L., Minguillón, M. C., Monfort, E., Gil, J. I., Inza, A., Ortega, L. A., Santamaría, J. M., and Zabalza, J.: Source origin of trace elements in PM from regional background, urban and industrial sites of Spain, Atmos. Environ., 41, 7219–7231, 2007.

Querol, X., Alastuey, A., Moreno, T., Viana, M.M., Castillo, S., Pey, J., Rodríguez, S., Artiñano, B., Salvador, P., Sánchez, M., Garcia Dos Santos, S., Herce Garraleta, M. D., Fernandez-Patier, R., Moreno-Grau, S., Negral, L., Minguillón, M. C., Monfort, E., Sanz, M. J., Palomo-Marín, R., Pinilla-Gil, E., Cuevas, E., de la Rosa, J., and Sánchez de la Campa, A.: Spatial and temporal variations inairborne particulate matter (PM10 and PM2.5) across Spain 1999–2005, Atmos. Environ., 42, 3694–3979, 2008.

Querol, X., Pey, J., Pandolfi, M., Alastuey, A., Cusack, M., Pérez, N., Moreno, T.,Viana, M., Mihalopoulos, N., Kallos, G., Kleanthous, S.: African dust contributions to mean ambient PM10 mass-levels across the Mediterranean Basin, Atm. Env., 43, 4266–4277, 2009.

Reche, C., Viana, M., Pandolfi, M., Alastuey, A., Moreno, T., Amato, F., Ripoll, A., and Querol, X.: Urban NH3 levels and sources in a Mediterranean environment, Atmos. Environ., 57, 153–164, 2012

Ripoll, A., Pey, J., Minguillón, M. C., Pérez, N., Pandolfi, M., Querol, X., and Alastuey, A.: Three years of aerosol mass, black carbon and particle number concentrations at Montsec (southern Pyrenees, 1570 m a.s.l.), Atmos. Chem. Phys., 14, 4279-4295, https://doi.org/10.5194/acp-14-4279-2014, 2014.

Sanz, M. J., Palomo-Marín, R., Pinilla-Gil, E., Cuevas, E., de la Rosa, J., and Sánchez de la Campa, A.: Spatial and temporal variations inairborne particulate matter (PM10 and PM2.5) across Spain 1999–2005, Atmos. Environ., 42, 3694–3979, 2008.

Seibert P., Kromp-Kolb H., Baltensperger U., Jost D.T., Schwikowski M.: Trajectory Analysis of High-Alpine Air Pollution Data, in: Gryning SE., Millán M.M. (eds) Air Pollution Modeling and Its Application X. NATO · Challenges of Modern Society, vol 18. Springer, Boston, MA, 1994.

Sofowote, U. M., Su, Y., Dabek-Zlotorzynska, E., Rastogi, A. K., Brook, J., and Hopke, P. K.: Sources and temporal variations of constrained PMF factors obtained from multiple-year receptor modeling of ambient PM2.5 data from five speciation sites in Ontario, Canada, Atmos. Environ., 108, 140–150, 2015.

Szidat, S., Jenk, T.M., Synal, H.A., Kalberer, M., Wacker, L., Hajdas, I., Kasper-Giebl, A., Baltensperger, U.: Contributions of fossil fuel, biomass-burning, and biogenic emissions to carbonaceous aerosols in Zurich as traced by C-14, Journal of Geophysical Research-Atmospheres 111, 12, 2006.

Thunis, P.: On the validity of the incremental approach to estimate the impact of cities on air quality, Atmos. Environ., 173, 210-222, 2018.

UNECE: Towards Cleaner Air. Scientific Assessment Report. EMEP Steering Body and Working Group on Effects of the Convention on Long-Range Transboundary Air Pollution, Oslo, 50 pp., edited by: Maas, R. and Grennfelt, P., www.unece.org/environmental-policy/conventions/envlrtapwelcome/publications.html (last access: 16 April 2019), 2016.

van Pinxteren, D., Fomba, K. W., Spindler, G., Mueller, K., Poulain, L., Iinuma, Y., Loschau, G., Hausmann A., and Herrmann, H.: Regional air quality in Leipzig, Germany: detailed source apportionment of size resolved aerosol particles and comparison with the year 2000, Faraday Discuss., 189, 291-315, 2016.

Van Damme, M., Clarisse, L., Whitburn, S., Hadji-Lazaro, J., Hurtmans, D., Clerbaux, C., Coheur, P.F.: Industrial and agricultural ammonia point sources exposed, Nature 564, 99–103, 2018.

Waked, A., Favez, O., Alleman, L. Y., Piot, C., Petit, J.-E., Delaunay, T., Verlinden, E., Golly, B., Besombes, J.-L., Jaffrezo, J.-L., and Leoz-Garziandia, E.: Source apportionment of PM10 in a north-western Europe regional urban background site (Lens, France) using positive matrix factorization and including primary biogenic emissions, Atmos. Chem. Phys., 14, 3325-3346, https://doi.org/10.5194/acp-14-3325-2014, 2014.

Zhang, X., Zhang, Y., Liu, Y., Zhao, J., Zhou, Y., Wang, X., Yang, X., Zou, Z., Zhang, C., Fu, Q., Xu, J., Gao, W., Li, N., and Chen, J.: Changes in the SO_2 level and $PM_{2.5}$ components in Shanghai driven by implementing the ship emission control policy, Environ. Sci. Technol., 53, 11580–11587, https://doi.org/10.1021/acs.est.9b03315, 2019.

Supplement of

Long range and local air pollution: what can we learn from chemical speciation of particulate matter at paired sites?

Marco Pandolfi [a,*], Dennis Mooibroek [b], Philip Hopke [c], Dominik van Pinxteren [d], Xavier Querol [a], Herrmann Hartmut [d], Andrés Alastuey [a], Olivier Favez [e], Christoph Hüglin [f], Esperanza Perdrix [g], Véronique Riffault [g], Stéphane Sauvage [g], Eric van der Swaluw [b], Oksana Tarasova [h], and Augustin Colette [e]

[a] Institute of Environmental Analysis and Water Research (IDAEA-CSIC), c/ Jordi-Girona 18-26, Barcelona, Spain

[b] Centre for Environmental Monitoring, National Institute of Public Health and the Environment (RIVM), A. van Leeuwenhoeklaan 9, P.O. Box 1, 3720 BA, Bilthoven, The Netherlands

[c] Center for Air Resources Engineering and Science, Clarkson University, Potsdam, NY, USA

[d] Leibniz Institute for Tropospheric Research (TROPOS), Atmospheric Chemistry Department (ACD), Permoserstr. 15, 04318 Leipzig, Germany

[e] National Institute for Industrial Environment and Risks (INERIS), Verneuil-en-Halatte, 60550, France

[f] Empa, Swiss Federal Laboratories for Materials Science and Technology, 8600 Dübendorf, Switzerland

[g] IMT Lille Douai, Univ. Lille, SAGE – Département Sciences de l'Atmosphère et Génie de l'Environnement, 59000 Lille, France

[h] World Meteorological Organization, Research Department, Geneva, Switzerland

* Corresponding author: Marco Pandolfi (marco.pandolfi@idaea.csic.es)

Table S1: PMF bootstrapping resampling results for ES, FR and CH. MM: mineral matter; IND: primary industrial; NSA: nitrate-rich aerosols; V-Ni: residual oil combustion; SS: aged sea salt; SSA: sulfate-rich aerosols; RT: primary road traffic ; FSS: fresh sea salt; LB: land biogenic; BB: biomass burning; MB: marine biogenic.

Country		sources									
		MM	IND	NSA	V-Ni	SS	SSA	RT			unmapped
	Boot MM	100	0	0	0	0	0	0			0
	Boot IND	0	99	0	0	0	0	1			0
	Boot NSA	0	0	100	0	0	0	0			0
ES	**Boot V-Ni**	0	0	0	95	0	4	1			0
	Boot SS	0	0	0	0	100	0	0			0
	Boot SSA	0	0	0	0	0	100	0			0
	Boot RT	0	0	0	0	0	7	93			0
		FSS	LB	SSA	RT	BB	NSA	SS	MM	MB	unmapped
	Boot FSS	100	0	0	0	0	0	0	0	0	0
	Boot LB	0	99	0	0	0	0	0	1	0	0
	Boot SSA	0	0	100	0	0	0	0	0	0	0
FR	**Boot RT**	0	0	0	96	0	0	0	4	0	0
	Boot BB	0	0	0	0	100	0	0	0	0	0
	Boot NSA	0	0	0	0	0	100	0	0	0	0
	Boot SS	0	0	0	0	0	0	100	0	0	0
	Boot MM	0	0	0	1	0	0	0	99	0	0
	Boot MB	0	0	0	0	0	1	0	2	97	0
		NSA	SSA	RT	BB	SS	MM				unmapped
	Boot NSA	100	0	0	0	0	0				0
	Boot SSA	0	100	0	0	0	0				0
CH	**Boot RT**	0	0	100	0	0	0				0
	Boot BB	1	0	0	99	0	0				0
	Boot SSA	0	0	0	0	100	0				0
	Boot MM	0	0	0	0	0	100				0

Table S2: Chemical PM_{10} data sampled at Barcelona (BCN; UB), Montseny (MSY; RB) and Montsec (MSA; CB) (Spain) and used in the PMF model (2010 – 2014). Specie concentrations are reported in $\mu g/m^3$.

Chemical specie	BCN			MSY			MSA			
[$\mu g/m^3$]	mean	SD	median	mean	SD	median	mean	SD	median	
PM_{10}	24.5719	10.1681	23.0796	16.3678	9.2712	15.0258	9.3843	7.8660	7.4151	
Al	0.2611	0.2306	0.1880	0.2773	0.5118	0.1441	0.2493	0.5356	0.1176	
Ca	0.6699	0.4680	0.5431	0.2887	0.3444	0.1937	0.3517	0.4216	0.2049	
K	0.2129	0.1471	0.1915	0.1420	0.1432	0.1060	0.1105	0.1508	0.0863	
Na	0.7847	0.6495	0.6153	0.3048	0.2704	0.2162	0.1711	0.1729	0.1143	
Mg	0.1661	0.0999	0.1389	0.1013	0.1163	0.0724	0.0760	0.1149	0.0476	
Fe	0.5097	0.2823	0.4394	0.2052	0.3401	0.1022	0.1368	0.2874	0.0671	
Mn	0.0101	0.0061	0.0088	0.0040	0.0044	0.0029	0.0041	0.0058	0.0026	
Ti	0.0183	0.0135	0.0148	0.0149	0.0267	0.0076	0.0148	0.0342	0.0066	
V	0.0056	0.0043	0.0046	0.0020	0.0018	0.0015	0.0012	0.0015	0.0007	
Ni	0.0027	0.0023	0.0021	0.0012	0.0015	0.0009	0.0006	0.0011	0.0004	
Cu	0.0189	0.0119	0.0163	0.0029	0.0018	0.0026	0.0011	0.0010	0.0009	
As	0.0004	0.0002	0.0004	0.0002	0.0001	0.0002	0.0001	0.0001	0.0001	
Rb	0.0005	0.0003	0.0004	0.0004	0.0005	0.0002	0.0003	0.0006	0.0002	
Sr	0.0024	0.0020	0.0020	0.0013	0.0021	0.0008	0.0016	0.0025	0.0009	
Sb	0.0024	0.0016	0.0020	0.0003	0.0002	0.0003	0.0001	0.0002	0.0000	
Pb	0.0083	0.0114	0.0061	0.0023	0.0019	0.0020	0.0012	0.0009	0.0009	
SO_4^{2-}	2.6322	1.6846	2.2756	1.8946	1.4842	1.6141	1.3343	1.1454	1.0266	
NO_3^-	2.4192	2.1829	1.7304	1.0455	1.0382	0.7587	0.7540	0.8747	0.4910	
Cl^-	0.6844	0.7647	0.4260	0.2488	0.2979	0.1662	0.1382	0.1762	0.1022	
NH_4^+	0.7736	0.8742	0.4737	0.4976	0.4713	0.3674	0.4482	0.4605	0.2983	
EC	1.1545	0.6589	1.0129	0.2318	0.1291	0.2089	0.1071	0.0811	0.0930	
OC	2.9088	1.4308	2.6011	1.8983	0.8589	1.7894	1.5188	0.8708	1.4112	

Table S3: Chemical PM_{10} data sampled at Zurich (ZUE; UB) and Payerne (PAY; RB) (Switzerland) and used in the PMF model (2008-2009). Specie concentrations are reported in $\mu g/m^3$.

Chemical specie	ZUE			PAY			
[$\mu g/m^3$]	mean	SD	median	mean	SD	median	
PM_{10}	20.41303	11.52026	15.77000	18.45809	11.84675	14.90000	
OC	3.70135	2.14696	3.09000	3.51303	2.23133	3.10000	
EC	1.26427	0.74653	1.06000	0.66292	0.46896	0.55000	
NO_3^-	3.78748	4.30968	1.98800	3.80962	4.64906	1.77700	
SO_4^{2-}	2.36776	1.53784	1.99100	1.91618	1.27660	1.68200	
Na^+	0.15094	0.16235	0.10100	0.12454	0.12452	0.09200	
NH_4^+	1.61817	1.54775	1.06000	1.57806	1.58461	0.92600	
K^+	0.20227	0.19533	0.12400	0.17213	0.16706	0.11100	
Mg_2^+	0.02904	0.02118	0.02400	0.02048	0.01686	0.01800	
Ca_2^+	0.31661	0.28609	0.19600	0.17528	0.13329	0.13800	
Al	0.07053	0.06501	0.04381	0.06521	0.06854	0.04636	
Ti	0.00195	0.00133	0.00158	0.00171	0.00155	0.00124	
V	0.00067	0.00046	0.00058	0.00056	0.00052	0.00039	
Cr	0.00198	0.00161	0.00154	0.00066	0.00071	0.00048	
Mn	0.00537	0.00318	0.00445	0.00264	0.00165	0.00229	
Fe	0.46942	0.27748	0.41346	0.11914	0.07740	0.09687	
Cu	0.02069	0.01165	0.01809	0.00415	0.00272	0.00338	
Zn	0.02849	0.02162	0.02359	0.01958	0.01611	0.01735	
Ga	0.00016	0.00011	0.00012	0.00008	0.00007	0.00006	
As	0.00052	0.00106	0.00032	0.00050	0.00058	0.00037	
Rb	0.00049	0.00042	0.00035	0.00056	0.00040	0.00051	
Sr	0.00076	0.00062	0.00054	0.00051	0.00048	0.00037	
Y	0.00004	0.00003	0.00003	0.00003	0.00003	0.00002	
Mo	0.00116	0.00070	0.00099	0.00024	0.00017	0.00022	
Cd	0.00012	0.00008	0.00010	0.00009	0.00007	0.00007	
Sb	0.00225	0.00129	0.00192	0.00059	0.00040	0.00053	
Ba	0.00370	0.00228	0.00310	0.00162	0.00188	0.00116	
La	0.00008	0.00005	0.00007	0.00005	0.00005	0.00004	
Ce	0.00014	0.00008	0.00013	0.00008	0.00007	0.00006	
Nd	0.00004	0.00003	0.00003	0.00003	0.00003	0.00002	
Pb	0.00533	0.00387	0.00396	0.00383	0.00311	0.00298	

Table S4: Chemical $PM_{2.5}$ data sampled at Schiedam (SCH; UB) and Hellendoorn (HEL; RB) (The Netherlands) and used in the PMF model (2007-2008). The concentration of major elements is reported in mg/m^3 and the concentration of trace elements in ng/m^3.

Chemical specie	**SCH**		**HEL**	
[μg/m^3]	mean	SD	mean	SD
$PM_{2.5}$	17.2	11.6	14.0	6.9
OC	2.1	1.1	2.0	0.8
EC	2.2	1.6	1.7	1.1
NH_4^+	1.2	1.5	1.6	1.4
NO_3^-	2.8	3.4	3.7	3.1
SO_4^{2-}	2.6	1.4	2.6	1.8
Cl	0.3	0.3	0.3	0.3
[ng/m^3]				
Al	61.9	131.7	35.6	74.3
As	0.7	0.6	0.4	0.4
Ba	11.0	56.3	5.5	16.5
Ca	87.5	76.8	61.7	55.8
Cd	0.3	0.3	0.3	0.2
Co	0.3	0.2	0.2	0.1
Cr	2.9	1.3	2.7	1.2
Cu	5.5	9.9	2.5	3.3
Fe	115.9	117.5	71.5	76.5
K	134.2	529.5	84.0	124.7
Mg	64.9	86.9	44.6	33.0
Mn	4.0	3.4	2.6	2.3
Mo	0.6	0.4	0.5	0.4
Na	339.9	311.4	173.8	201.0
Ni	5.4	4.0	1.9	1.2
P	90.0	37.7	80.1	36.3
Pb	9.1	11.9	8.3	12.5
Sb	1.0	1.0	0.6	0.5
Se	2.7	5.8	0.8	0.6
Si	93.2	171.3	84.5	12.5
Sn	4.2	11.2	0.9	0.8
Sr	2.2	12.4	0.9	2.2
Ti	2.5	2.9	1.5	2.0
V	9.0	7.7	2.0	1.9
Zn	95.3	36.7	90.5	31.7

Table S5: Chemical PM_{10} data sampled at Lens (LENS; UB) and Revin (REV; UB) (France) and used in the PMF model (2013-2014). Specie concentrations are reported in $\mu g/m^3$.

Chemical specie	**LENS**			**REV**			
[$\mu g/m^3$]	mean	SD	median	mean	SD	median	
PM_{10}	20.5193	12.7126	16.0000	16.3038	9.6521	15.0000	
EC	0.6029	0.5851	0.4462	0.1742	0.0993	0.1537	
OC	3.2052	2.6364	2.5157	2.1603	1.2652	1.8912	
Cl -	0.7378	0.9006	0.3797	0.3037	0.5599	0.0777	
NO_3^-	5.0508	5.5206	2.5376	3.2520	4.0694	1.8593	
SO_4^{2-}	2.3309	2.2417	1.6347	2.0347	1.7630	1.5002	
Na^+	0.6213	0.5690	0.4616	0.3787	0.4537	0.2097	
NH_4^+	1.8741	2.1916	0.9945	1.2723	1.4603	0.7491	
K^+	0.1294	0.0982	0.1064	0.0503	0.0413	0.0399	
Mg^{2+}	0.0796	0.0640	0.0611	0.0408	0.0398	0.0278	
MSA	0.0728	0.0805	0.0503	0.0395	0.0508	0.0210	
Levoglucosan	0.1906	0.2729	0.0940	0.1003	0.0994	0.0719	
Polisac	0.0304	0.0684	0.0125	0.0117	0.0143	0.0061	
Alcohols	0.0239	0.0347	0.0116	0.0242	0.0305	0.0126	
Al	0.1566	0.2059	0.0993	0.1192	0.2519	0.0539	
Fe	0.2713	0.2757	0.1696	0.1675	0.1891	0.1108	
Ca	0.3682	0.4660	0.2266	0.2543	0.3906	0.1705	
As	0.0007	0.0008	0.0004	0.0007	0.0007	0.0004	
Cd	0.0002	0.0002	0.0002	0.0002	0.0003	0.0002	
Co	0.0002	0.0002	0.0001	0.0001	0.0001	0.0001	
Cu	0.0121	0.0167	0.0072	0.0045	0.0042	0.0032	
La	0.0002	0.0002	0.0001	0.0001	0.0001	0.0001	
Mn	0.0066	0.0060	0.0045	0.0061	0.0055	0.0042	
Pb	0.0087	0.0092	0.0056	0.0082	0.0061	0.0065	
Rb	0.0005	0.0005	0.0003	0.0005	0.0004	0.0003	
Sb	0.0012	0.0011	0.0009	0.0006	0.0004	0.0005	
Se	0.0011	0.0009	0.0007	0.0012	0.0010	0.0010	
Sr	0.0019	0.0019	0.0015	0.0014	0.0017	0.0011	
Ti	0.0102	0.0107	0.0069	0.0098	0.0121	0.0066	
Zn	0.0302	0.0374	0.0183	0.0363	0.0405	0.0246	

Table S6: Main features of the sources from both the single-site PMF and the multi-site PMF (shaded background) for each country. EV: explained variation of the main markers of the sources for each PMF run; K: ratios between specific tracers in each source profile; CV: coefficient of variation of the ratios for each source. Ratio: ratios used to calculate K. CV values above 25% are highlighted in bold.

Source	**Country**	**Paired sites**	**base run EV**	**K**	**CV [%]** [(a)]	**Ratio**
SSA	Spain	BCN	SO_4^{2-} (48%), NH_4^+(41%)	0.233	13.7	$[NH_4^+]/[SO_4^{2-}]$
		MSY	SO_4^{2-} (35%), NH_4^+ (66%)	0.307		
		MSA	SO_4^{2-} (57%), NH_4^+ (51%)	0.280		
		BCN+MSY+MSA	SO_4^{2-} (49%), NH_4^+ (53%)	0.279		
	Switzerland	ZUE	SO_4^- (47%), NH_4^+ (27%)	0.389	9.3	
		PAY	SO_4^- (49%), NH_4^+ (26%)	0.444		
		ZUE+PAY	SO4- (56%), NH4+ (29%)	0.393		
	France	LEN	SO_4^{2-} (64%), NH_4^+ (28%)	0.348	0.2	
		REV	SO_4^{2-} (59%), NH_4^+ (33%)	0.347		
		LEN+REV	SO42- (74%), NH4+ (35%)	0.331		
NSA	Spain	BCN	NO_3^- (75%), NH_4^+ (59%)	0.207	13.0	$[NH_4^+]/[NO_3^-]$
		MSY	NO_3^- (73%), NH_4^+ (34%)	0.256		
		MSA	NO_3^- (75%), NH_4^+ (35%)	0.266		
		BCN+MSY+MSA	NO3- (82%), NH4+ (47%)	0.177		
	Switzerland	ZUE	NO_3^- (50%), NH_4^+ (52%)	0.400	20.4	
		PAY	NO_3^- (76%), NH_4^+ (55%)	0.299		
		ZUE+PAY	NO3- (65%), NH4+ (58%)	0.373		
	France	LEN	NO_3^- (66%), NH_4^+ (50%)	0.286	5.1	
		REV	NO_3^- (80%), NH_4^+ (54%)	0.266		
		LEN+REV	NO3- (78%), NH4+ (58%)	0.266		
Mineral	Spain	BCN	Al (85%), Ca (75%), Ti (71%), Rb (69%)	490	20.0	[Al+Ca]/[La+Rb]
		MSY	Al (87%), Ca (63%), Ti (84%), Rb (66%)	382		
		MSA	Al (89), Ca (51%), Ti (84%), Rb (68%)	333		
		BCN+MSY+MSA	Al (90%), Ca (59%), Ti (77%), Rb (70%)	365		
	Switzerland	ZUE	Al (71%), Ti (58%), Sr (75%)	28.5	15.9	[Al]/[Ti+Sr]
		PAY	Al (71%), Ti (61%), Sr (61%)	35.7		
		ZUE+PAY	Al (80%), Ti (65%), Sr (72%)	32.9		
	France	LEN	Al (84%), Ca (73%), La (49%), Rb (39%)	1590	2.4	[Al+Ca]/[La+Rb]
		REV	Al (80%), Ca (80%), La (42%), Rb (28%)	1644		
		LEN+REV	Al (81%), Ca (68%), La (46%), Rb (47%)	1484		
Primary Road	Spain	BCN	EC (73%), Cu (77%), Sb (79%)	9.35	18.7	[Cu]/[Sb]

Traffic		MSY	EC (58%), Cu (48%), Sb (46%)	13.51		
		MSA	EC (81%), Cu (40%), Sb (35%)	12.76		
		BCN+MSY+MSA	EC (75%), Cu (81%), Sb (80%)	9.31		
	Switzerland	ZUE	EC (46%), Cr (56%), Cu (47%), Sb(48%)	9.22	**31.1**	
		PAY	EC (36%), Cr (54%), Cu (38%), Sb(49%)	5.90		
		ZUE+PAY	EC (42%), Cr (60%), Cu (74%), Sb(69%)	9.39		
	France	LEN	EC (52%), Cu (51%), Sb (42%)	10.09	20.1	
		REV	EC (40%), Cu (53%), Sb (50%)	7.58		
		LEN+REV	EC (72%), Cu (60%), Sb (63%)	10.25		
Aged sea salt	Spain	BCN	Na^+ (80%), Mg_2^+ (41%), Cl^- (81%)	1.32	**35.9**	$[Na^+]/[Cl^-]$
		MSY	Na^+ (82%), Mg_2^+ (35%), Cl^- (61%)	2.19		
		MSA	Na^+ (72%), Mg_2^+ (25%), Cl^- (38%)	2.83		
		BCN+MSY+MSA	Na+ (83%), Mg2+ (38%), Cl- (83%)	1.34		
	Switzerland	ZUE	Na^+ (83%), Mg_2^+ (40%)	10.76	16.6	$[Na^+]/[Mg_2^+]$
		PAY	Na^+ (86%), Mg_2^+ (63%)	8.50		
		ZUE+PAY	Na+ (80%), Mg2+ (47%)	9.63		
	France	LEN	Na^+ (36%), Mg_2^+ (33%)	8.66	13.3	$[Na^+]/[Mg_2^+]$
		REV	Na^+ (45%), Mg_2^+ (38%)	10.46		
		LEN+REV	Na+ (58%), Mg2+ (52%)	9.33		
Fresh sea salt	France	LEN	Cl^- (84%), Na^+ (55%), Mg_2^+ (49%)	0.547	2.5	$[Na^+]/[Cl^-]$
		REV	Cl^- (90%), Na^+ (44%), Mg_2^+ (40%)	0.567		
		LEN+REV	Cl- (87%), Na+ (42%), Mg2+ (36%)	0.508		
Biomass burning	Switzerland	ZUE	EC (21%), K^+ (56%)	0.430	16.1	$[K^+]/[EC]$
		PAY	EC (29%), K^+ (41%)	0.342		
		ZUE+PAY	EC (32%), K+ (51%)	0.301		
	France	LEN	K^+(28), Levo. (82%), Polys. (85%)	7.15	23.5	[Levo.]/[Polys.]
		REV	K^+(33), Levo. (84%), Polys. (83%)	10.00		
		LEN+REV	K+(28), Levo. (89%), Polys. (85%)	8.58		
Residual Oil	Spain	BCN	V (69%), Ni (62%)	2.58	13.9	[V]/[Ni]
		MSY	V (61%), Ni (54%)	2.43		

		MSA (**)	V (42%), Ni (42%)	1.96		
		BCN+MSY+MSA	V (70%), Ni (62%)	2.57		
Primary industrial	Spain	BCN	Zn (75%), Pb (59%)	0.107	**48.8**	[Pb]/[Zn+As]
		MSY	Zn (75%), Pb (64%)	0.309		
		MSA	Zn (53%), Pb (52%)	0.205		
		BCN+MSY+MSA	Zn (75%), Pb (65%)	0.140		
Marine biogenic	France	LEN	Mg_2^+ (9%), MSA (74%)	0.114	**31.9**	[Mg_2^+]/[MSA]
		REV	Mg_2^+ (6%), MSA (81%)	0.072		
		LEN+REV	Mg2+ (3%), MSA (86%)	0.035		
Land biogenic		LEN	OC (10%), Alcohols (87%)	0.074	0.9	[Alcohol]/[OC]
		REV	OC (13%), Alcohols (82%)	0.075		
		LEN+REV	OC (9%), Alcohols (89%)	0.080		

(a) CV = (Standard Deviation / Mean) x 100

(**) Mixed with SSA in the single MSA PMF.

- **Source profiles from multi-site PMF for Spain.**

Figure S1 shows the chemical profiles of the sources detected at BCN, MSY and MSA from the multi-site PMF. A total of 7 common sources were identified at the three sites, namely:

- *Heavy-Oil combustion* (V-Ni), traced mainly by V, Ni and SO_4^{2-} and representing the direct emissions from heavy oil combustion sources, mostly shipping in the area under study during the period considered, but also long range transport. The sulfate associated with this source also includes primary sulfate from shipping (Ref.)

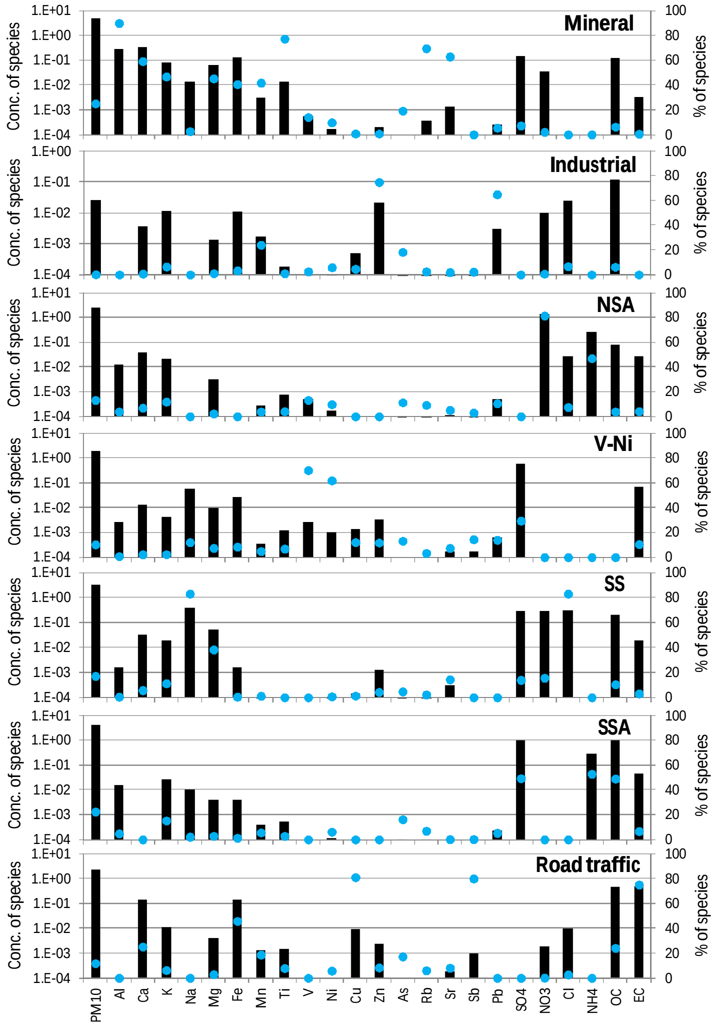

Figure S1: Chemical profiles of the sources detected at Barcelona (BCN; UB), Montseny (MSY; RB) and Montsec (MSA; CB) (Spain).

- *Mineral (MM),* traced by typical crustal elements such as Al, Ca, Ti, Rb, and Sr;
- *Aged sea salt (SS)*, traced by Na and Cl mainly with contributions from SO_4^{2-} and NO_3^- suggesting some aging of marine aerosols;
- *Secondary sulfate (SSA)*, secondary inorganic source traced by SO_4^{2-} and NH_4^+ with relatively high contents of OC which have been attributed to the condensation

of semi-volatile compounds on the high specific surface area of ammonium sulfate particles (Amato et al., 2009);

- *Primary Industrial (IND)*, traced by Pb and As representing mostly emissions from metallurgy;
- *Primary Road Traffic (RT)*, traced mainly by EC, OC, Cu, Sb and Fe;
- *Secondary nitrate (NSA)*, secondary inorganic source traced by NO_3^- and NH_4^+.

- **Source profiles from multi-site PMF for Switzerland.**

Figure S2 shows the chemical profiles of the sources from multi-site PMF for Switzerland. A total of 6 sources were identified at the two sites. A description of the sources is given below. The number and type of sources is the same as in Gianini et al. (2012):

- *Primary Road Traffic (RT)*, explaining large fractions of EC, OC and of the road traffic related elements (Mn, Cr, Fe, Cu, Mo, Sb);

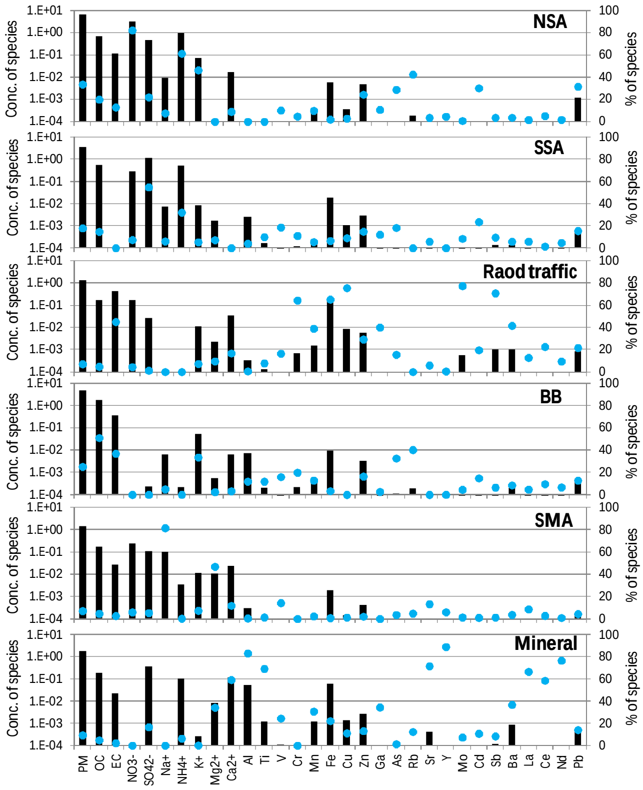

Figure S2: Chemical profiles of the sources detected at Zurich-Kaserne (ZUE; UB) and Payerne (PAY; RB).

- *Mineral (MM)*, dominated by Ca^{2+}, Fe, Al and Mg^{2+}, representing the main components of crustal matter. The mineral dust factors account moreover for a large mass fraction of crustal elements such as Ti, Sr, Y, La, Ce and Nd;
- *Na-Mg rich* (*SS*), contributing to high fractions of Na^+ and Mg^{2+}. The contributions of the *Na-Mg rich* factor did not show a clear annual cycle with elevated values during winter, thus suggesting a low contribution from the de-icing road salt. This

source was mostly related to the transport of sea spray aerosol particles (Gianini et al., 2012).

- *Secondary sulfate* (SSA), characterized by high concentrations of SO_4^{2-} and NH_4^+. Moreover, a relevant fraction of measured OC is also explained by the SSA factors; secondary OC is expected to be in receptor modelling studies largely associated with the secondary SO_4^{2-} because of similar temporal variation of these constituents of atmospheric PM (Kim et al., 2003). Relatively high contents of OC in secondary sulfate factors have been attributed to the condensation of semi-volatile compounds on the high specific surface area of ammonium sulfate (Amato et al., 2009);
- *Secondary nitrate* (*NSA*), secondary inorganic source traced by NO_3^- and NH_4^+;
- *Biomass burning* (*BB*), traced by high concentrations of OC, EC and K^+. This factor also explains a relevant mass fraction of Rb, an element related to biomass combustion emissions (Godoy et al., 2005);

- **Source profiles from multi-site PMF for France.**

Figure S3 shows the chemical profiles of the sources from multi-site PMF for France. A total of 9 sources were identified at the French paired sites. A description of the sources is given below.

- *Fresh sea salt*, traced by Na^+ and Cl^- this source represents mainly fresh marine aerosols;
- *Land (or Primary) biogenic (LB)*, traced by alcohols (arabitol and mannitol);
- *Secondary sulfate* (*SSA*)*,* secondary inorganic aerosol traced by SO_4^{2-} and NH_4^+;
- *Primary Road traffic (RT)*, traced by EC, OC, Fe, Cu, Sb;
- *Biomass burning (BB)*, traced mostly by levoglucosan and polysaccharides;
- *Secondary nitrate (NSA),* secondary inorganic aerosol traced by NO_3^- and NH_4^+;
- *Aged sea salt (SS),* representing aged sea salt. Lack of Cl^- in the chemical profiles and presence of Na^+ and NO_3^-;
- *Mineral (MM),* traced mainly by typical crustal elements such as Fe, Ca, Al, Sr and Ti;
- *Marine biogenic (MB),* traced mainly by methane sulphonic acid, a product of DMS oxidation.

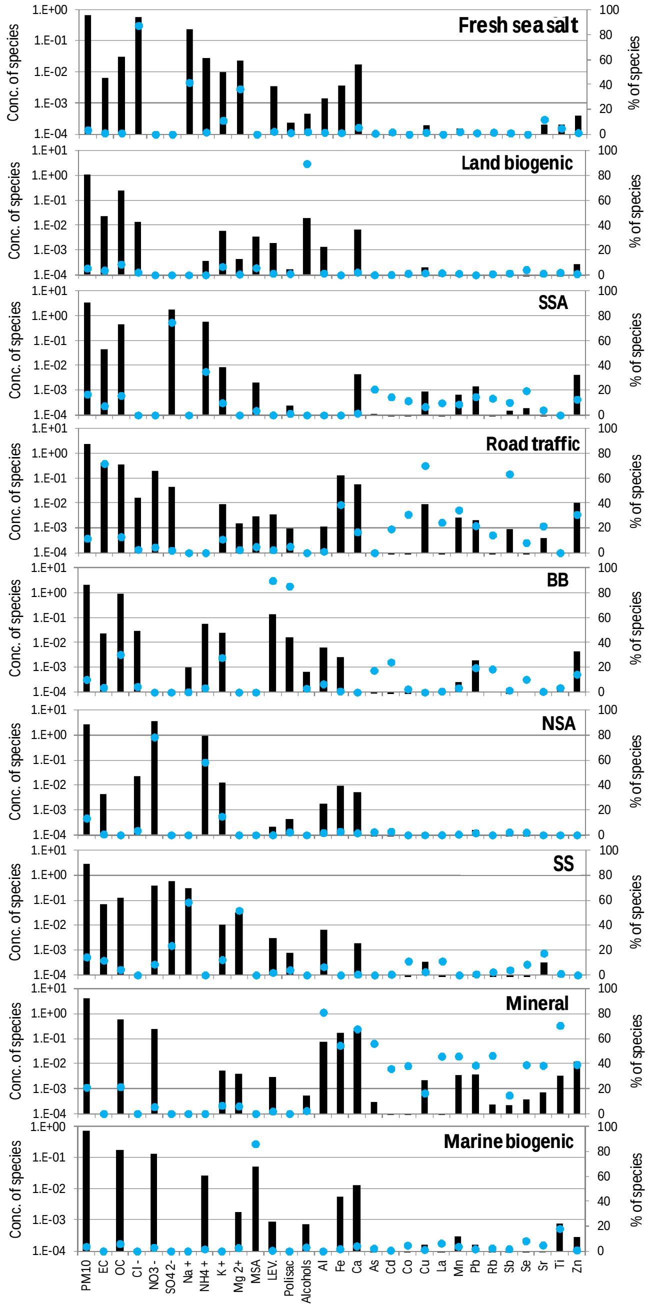

Figure S3: Chemical profiles of the sources detected at Lens (LENS; UB) and Revin (REV; RB).

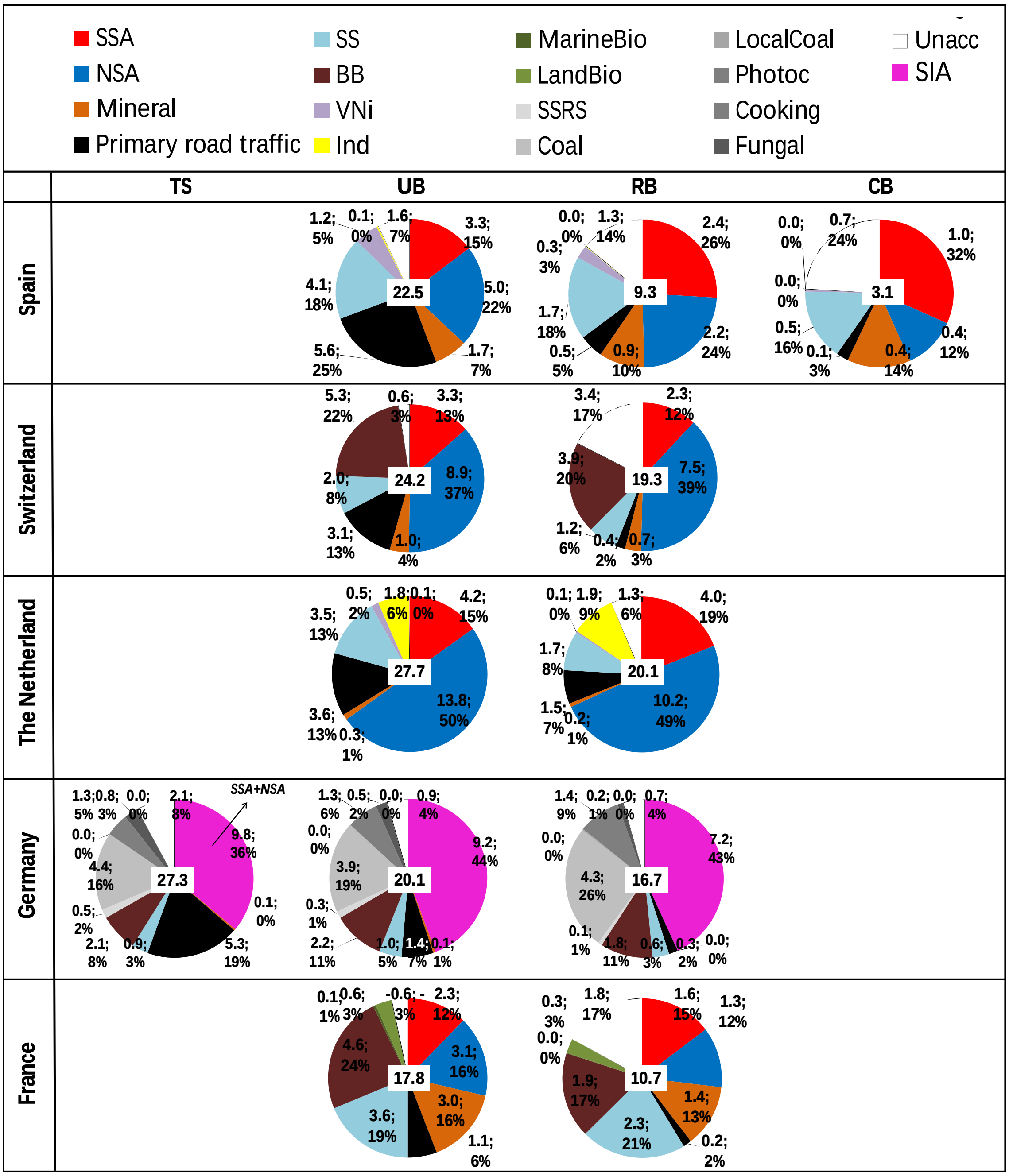

Figure S4: Source contributions to PM_{10} ($PM_{2.5}$ for The Netherlands) in winter (DJF) from the multi-site PMF for each country. The number in the white box at the center of the pie chart is the measured mass of PM (in $\mu g/m^3$). TS: traffic site; UB: urban background; RB: regional background; CB: continental background.

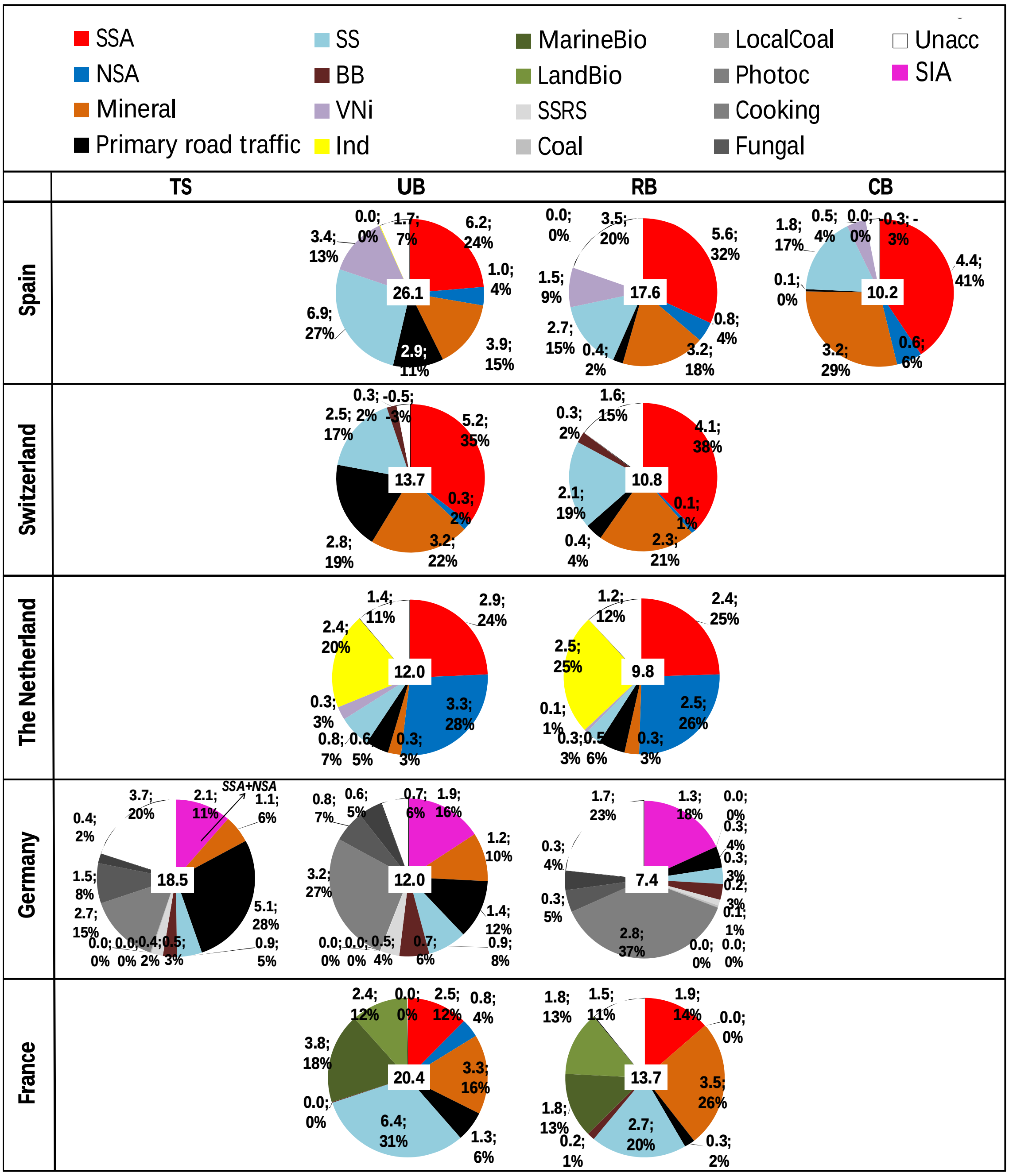

Figure S5: Source contributions to PM_{10} ($PM_{2.5}$ for The Netherlands) in summer (JJA) from the multi-site PMF for each country. The number in the white box at the center of the pie chart is the measured mass of PM (in $\mu g/m^3$). TS: traffic site; UB: urban background; RB: regional background; CB: continental background.

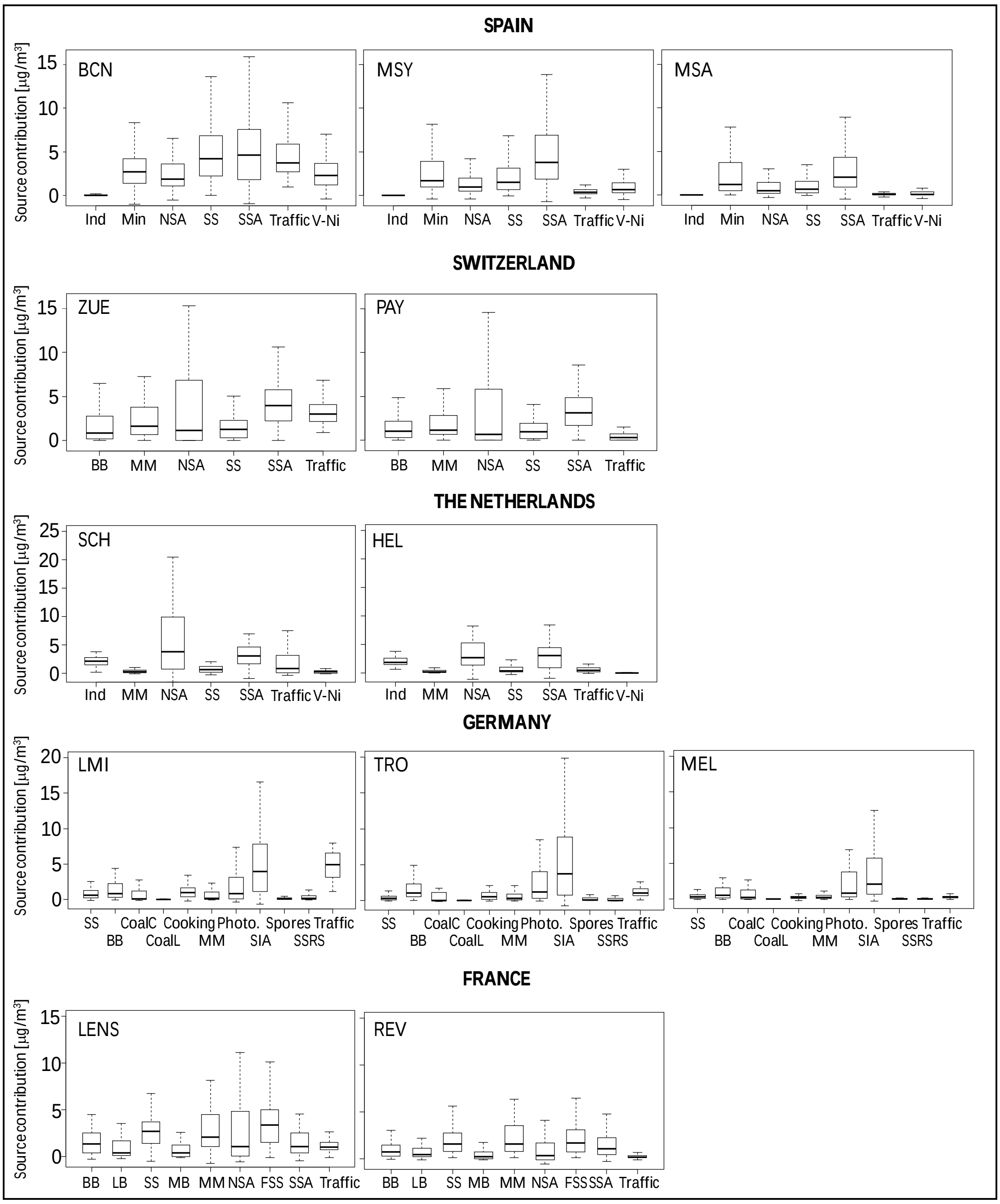

Figure S6: Mean annual source contributions to PM_{10} ($PM_{2.5}$ for The Netherlands) from the multi-site PMF for each site and country. IND: Industrial; MM: Mineral matter; NSA: nitrate-rich particles; SS: Aged sea Salt; SSA: sulfate-rich particles; RT: Road traffic; V-Ni: Residual oil combustion; BB: Biomass burning; Photo: Photochemistry; CoalL: Coal local; SIA: Secondary inorganic aerosols; SSRS: Sea salt/Road dust; LB: Land biogenic; FSS: Fresh sea salt; MB: Marine biogenic.

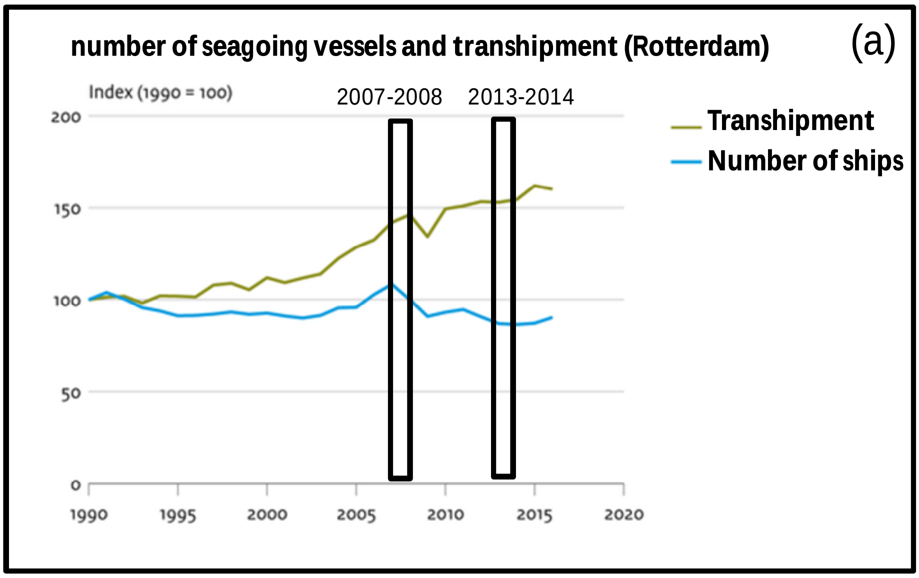

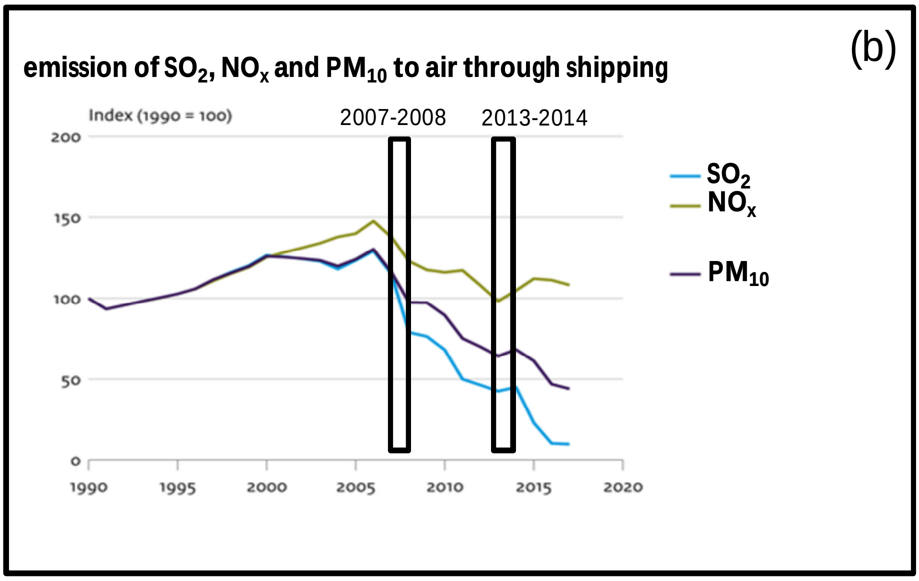

Figure S7: Number of seagoing vessels in Rotterdam (a), and emissions of SO_2, NO_x and PM_{10} through maritime shipping (b) from 1990 to 2017 (adapted from Environmental Data Compendium, Government of the Netherlands, https://www.clo.nl/en.)

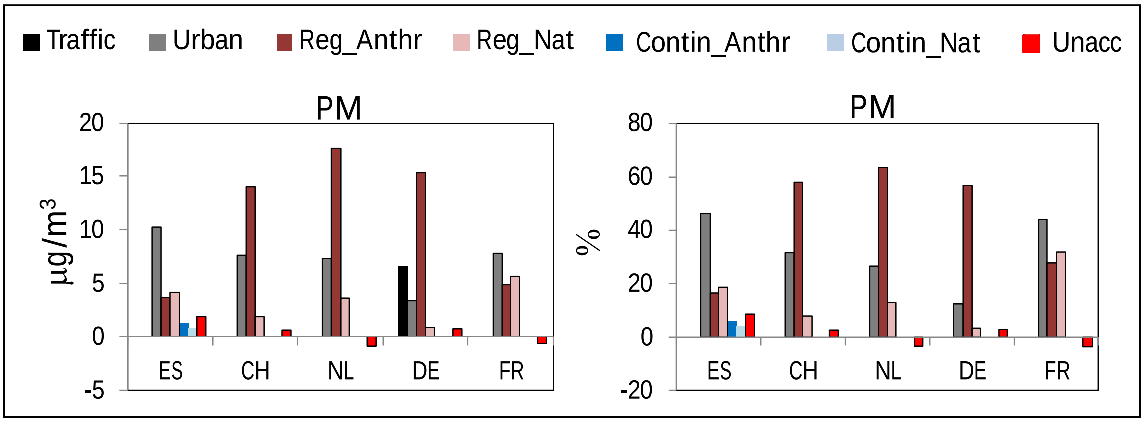

Figure S8: Lenschow's approach applied to the concentrations of PM. Average values for winter (DJF) are reported. ES: Spain; CH: Switzerland; NL: The Netherlands; DE: Germany; FR: France. In all countries with the exception of Spain, Reg_Anthr and Reg_Nat are the sum of regional+continental.

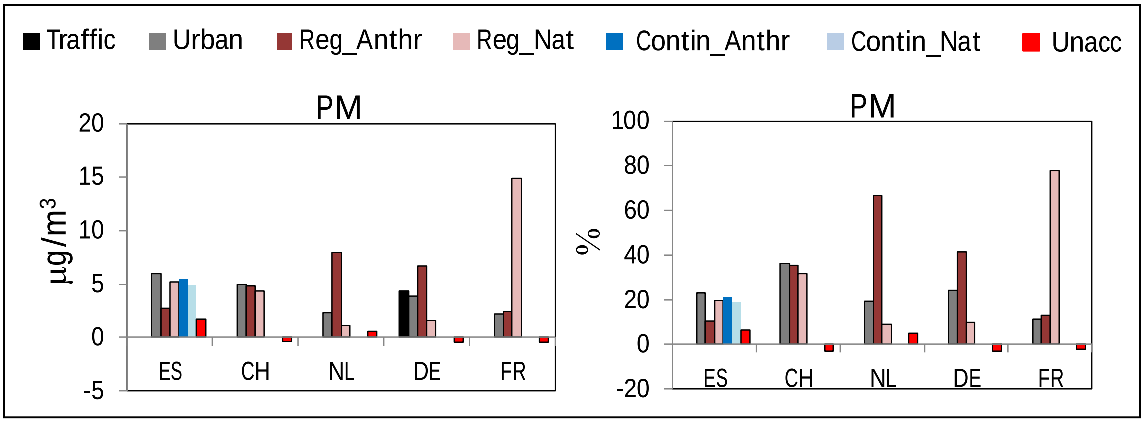

Figure S9: Lenschow's approach applied to the concentrations of PM. Average values for summer (JJA) are reported. ES: Spain; CH: Switzerland; NL: The Netherlands; DE: Germany; FR: France. In all countries with the exception of Spain, Reg_Anthr and Reg_Nat are the sum of regional+continental.

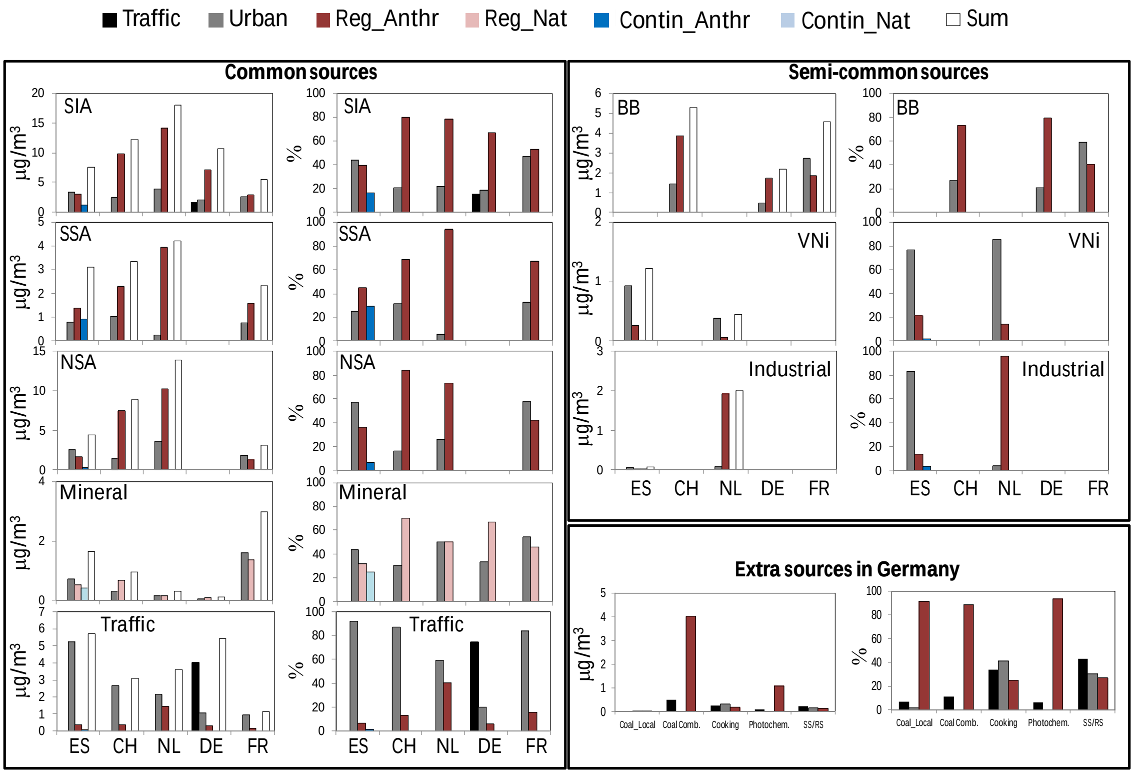

Figure S10: Lenschow's approach applied to the PMF source contributions. Average values for winter (DJF) are reported. ES: Spain; CH: Switzerland; NL: The Netherlands; DL: Germany; FR: France. In all countries with the exception of Spain, Reg_Anthr and Reg_Nat are the sum of regional+continental.

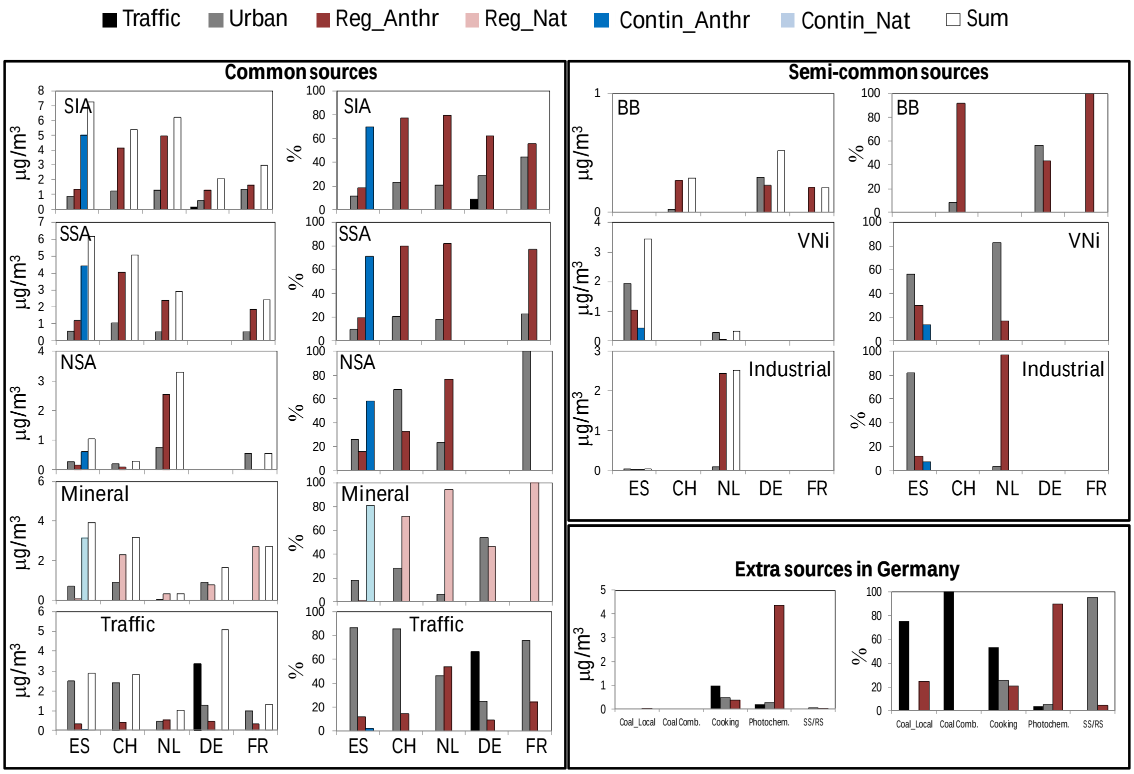

Figure S11: Lenschow's approach applied to the PMF source contributions. Average values for summer (JJA) are reported. ES: Spain; CH: Switzerland; NL: The Netherlands; DL: Germany; FR: France. In all countries, with the exception of Spain, Reg_Anthr and Reg_Nat are the sum of regional+continental.

Table S7: Allocation of PM to different sources and origin in each country. Annual means and winter (DJF) and summer (JJA) averages are reported.

		Annual mean					
Country	Contribution to PM [(A)] [μg/m^3; % of PM mass]	Traffic [μg/m^3; %]	Urban [μg/m^3; % of PM mass]	Regional [μg/m^3; % of PM mass]		Continental [μg/m^3; % of PM mass]	
		Anthr.	Anthr.	Natural	Anthr.	Natural	Anthr.
Spain	24.4; 100		8.5; 35.0	4.6; 18.8	3.4; 13.8	3.3; 13.5	4.3; 17.8
Switzerland	19.3; 100		6.5; 33.7	3.3; 17.0	10.0; 51.9		
The Netherlands	16.8; 100		4.3; 25.5	2.0; 12.1	10.5; 62.1		
Germany	21.6; 100	5.4; 24.8	3.5; 16.3	1.1; 5.0	10.8; 50.0		
France	20.7; 100		6.7; 32.6	9.1; 43.9	4.6; 22.5		
		Winter					
	Contribution to PM [μg/m^3; % of PM mass]	Traffic [μg/m^3; %]	Urban [μg/m^3; % of PM mass]	Regional [μg/m^3; % of PM mass]		Continental [μg/m^3; % of PM mass]	
		Anthr.	Anthr.	Natural	Anthr.	Natural	Anthr.
Spain	22.3; 100		10.3; 46.1	4.2; 18.8	3.7; 16.5	0.9; 4.0	1.3; 6.0
Switzerland	24.2; 100		7.6; 31.5	1.9; 7.9	14.0; 58.0		
The Netherlands	27.7; 100		7.4; 26.6	3.6; 13.1	17.6; 63.5		
Germany	27.0; 100	6.6; 24.3	3.4; 12.5	0.9; 3.4	15.4; 56.9		
France	17.8; 100		7.8; 44.0	5.7; 31.9	4.9; 27.6		
		Summer					
	Contribution to PM [μg/m^3; % of PM mass]	Traffic [μg/m^3; %]	Urban [μg/m^3; % of PM mass]	Regional [μg/m^3; % of PM mass]		Continental [μg/m^3; % of PM mass]	
		Anthr.	Anthr.	Natural	Anthr.	Natural	Anthr.
Spain	26.1; 100		6.0; 23.1	5.2; 19.7	2.7; 10.4	5.0; 19.1	5.5; 21.2
Switzerland	13.7; 100		5.0; 36.3	4.3; 31.7	4.8; 35.1		
The Netherlands	12.0; 100		2.3; 19.3	1.1; 9.2	8.0; 66.6		
Germany	16.0; 100	4.3; 27.3	3.9; 24.2	1.6; 9.8	6.6; 41.6		
France	19.1; 100		2.2; 11.5	14.9; 77.9	2.5; 12.9		

(A) PM concentrations measured in Barcelona (BCN; Spain), Zurich (ZUE; Switzerland), Schiedam (SCH; The Netherlands), Leipzig-Mitte (LMI; Germany) and Lens (LENS; France).

Table S8: Allocation of PMF source contributions in each country. Annual means are reported.

	Source contribution (A)	**Annual mean**					
	SIA [μg/m^3; % of PM mass]	Traffic [μg/m^3; % of SIA]	Urban [μg/m^3; % of SIA]	Regional [μg/m^3; % of SIA]		Continental [μg/m^3; % of SIA]	
		Anthr.	Anthr.	Natural	Anthr.	Natural	Anthr.
Spain	8.2; 33.6		1.9; 23.8		2.2; 27.4		4.0; 48.8
Switzerland	9.1; 46.9		1.7; 18.6		7.7; 85.4		
The Netherlands	9.8; 58.2		2.1; 21.0		7.7; 79.0		
Germany	6.2; 26.9	0.8; 13.5	1.3; 20.6		4.4; 71.7		
France	5.8; 28.2		2.5; 43.5		3.3; 56.5		
		Annual mean					
	SSA [μg/m^3; % of PM mass]	Traffic [μg/m^3; % of SSA]	Urban [μg/m^3; % of SSA]	Regional [μg/m^3; % of SSA]		Continental [μg/m^3; % of SSA]	
		Anthr.	Anthr.	Natural	Anthr.	Natural	Anthr.
Spain	5.2; 21.4		0.5; 8.7		1.8; 33.8		3.0; 57.5
Switzerland	4.6; 23.7		1.1; 23.7		3.5; 76.8		
The Netherlands	3.6; 21.2		0.7; 18.8		2.9; 81.2		
Germany							
France	2.2; 10.6		0.4; 17.4		1.8; 82.6		
		Annual mean					
	NSA [μg/m^3; % of PM mass]	Traffic [μg/m^3; % of NSA]	Urban [μg/m^3; % of NSA]	Regional [μg/m^3; % of NSA]		Continental [μg/m^3; % of NSA]	
		Anthr.	Anthr.	Natural	Anthr.	Natural	Anthr.
Spain	3.0; 12.2		1.5; 50.3		0.5; 16.1		1.0; 33.6
Switzerland	4.5; 23.2		0.6; 13.5		4.2; 94.2		
The Netherlands	6.2; 36.9		1.4; 22.2		4.8; 77.8		
Germany							
France	3.6; 17.5		2.1; 59.3		1.5; 40.7		
		Annual mean					
	Mineral [μg/m^3; % of PM mass]	Traffic [μg/m^3; % of Mineral]	Urban [μg/m^3; % of Mineral]	Regional [μg/m^3; % of Mineral]		Continental [μg/m^3; % of Mineral]	
		Anthr.	Anthr.	Natural	Anthr.	Natural	Anthr.
Spain	3.3; 13.6		0.7; 20.5	0.4; 13.2		2.2; 66.3	
Switzerland	2.6; 13.4		0.9; 33.1	1.9; 73.7			
The Netherlands	0.5; 3.2		0.1; 27.5	0.4; 72.5			
Germany	0.6; 2.4	0.0; 0.0	0.4; 70.4	0.3; 57.7			
France	5.0; 24.3		1.8; 35.3	3.2; 64.7			
		Annual mean					
	Road traffic [μg/m^3; % of PM mass]	Traffic [μg/m^3; % of RT]	Urban [μg/m^3; % of RT]	Regional [μg/m^3; % of RT]		Continental [μg/m^3; % of RT]	
		Anthr.	Anthr.	Natural	Anthr.	Natural	Anthr.
Spain	4.7; 19.1		4.2; 90.0		0.4; 8.1		0.1; 1.9
Switzerland	3.6; 18.5		3.0; 84.3		0.5; 13.4		
The Netherlands	2.0; 11.9		1.2; 62.2		0.7; 36.1		
Germany	5.2; 22.6	3.8; 73.0	1.1; 20.9		0.3; 6.1		
France	1.2; 5.6		0.9; 79.2		0.2; 20.8		
		Annual mean					
	SS [μg/m^3; % of PM mass]	Traffic [μg/m^3; % of SS]	Urban [μg/m^3; % of SS]	Regional [μg/m^3; % of SS]		Continental [μg/m^3; % of SS]	
		Anthr.	Anthr.	Natural	Anthr.	Natural	Anthr.
Spain	5.2; 21.5			5.2; 100			
Switzerland	1.7; 9.0			1.7; 100			

The Netherlands	1.6; 9.7			1.6; 100			
Germany	0.9; 4.0			0.9; 100			
France	3.7; 17.7			3.7; 100			
		Annual mean					
	Biomass burning [μg/m³; % of PM mass]	Traffic [μg/m³; % of BB]	Urban [μg/m³; % of BB]	Regional [μg/m³; % of BB]		Continental [μg/m³; % of BB]	
		Anthr.	Anthr.	Natural	Anthr.	Natural	Anthr.
Spain							
Switzerland	2.3; 12.0		0.6; 25.4		1.8; 78.1		
The Netherlands							
Germany	1.4; 6.0	0.0; 0.0	0.3; 23.2		1.1; 76.9		
France	2.6; 12.8		1.5; 57.6		1.1; 42.4		
		Annual mean					
	V-Ni [μg/m³; % of PM mass]	Traffic [μg/m³; % of V-Ni]	Urban [μg/m³; % of V-Ni]	Regional [μg/m³; % of V-Ni]		Continental [μg/m³; % of V-Ni]	
		Anthr.	Anthr.	Natural	Anthr.	Natural	Anthr.
Spain	2.7; 10.9		1.7; 62.9		0.7; 27.5		0.3; 9.6
Switzerland							
The Netherlands	0.3; 1.7		0.2; 83.8		0.1; 16.2		
Germany							
France							
		Annual mean					
	Industrial [μg/m³; % of PM mass]	Traffic [μg/m³; % of Ind]	Urban [μg/m³; % of Ind]	Regional [μg/m³; % of Ind]		Continental [μg/m³; % of Ind]	
		Anthr.	Anthr.	Natural	Anthr.	Natural	Anthr.
Spain	0.05; 0.2		0.04; 79.1		0.01; 13.2		0.00; 7.8
Switzerland							
The Netherlands	2.1; 12.7		0.3; 13.6		2.0; 91.3		
Germany							
France							
		Annual mean					
	Germany [μg/m³; % of PM mass]	Traffic [μg/m³; %]	Urban [μg/m³; %]	Regional [μg/m³; %]		Continental [μg/m³; %]	
		Anthr.	Anthr.	Natural	Anthr.	Natural	Anthr.
Coal_Local	0.02; 0.09	0.0; 12.6	0.0; 4.9		0.0; 82.5		
Coal	2.3; 10.0	0.3; 11.4	0.0; 0.0		2.3; 98.8		
Cooking	1.1; 5.0	0.5; 44.3	0.4; 32.8		0.3; 22.9		
Photochemistry	2.0; 8.6	0.1; 4.7	0.0; 0.3		1.9; 96.9		
SS/RS	0.5; 2.0	0.1; 20.6	0.3; 55.0		0.1, 24.4		
Fungal spores	0.2; 0.8			0.2; 0.8			
		Annual mean					
	France [μg/m³; % of PM mass]	Traffic [μg/m³; %]	Urban [μg/m³;%]	Regional [μg/m³; %]		Continental [μg/m³; %]	
		Anthr.	Anthr.	Natural	Anthr.	Natural	Anthr.
Marine bio	1.0; 4.8			1.0; 100			
Land bio	1.2; 5.7			1.2; 100			

(A) Source contributions calculated for Barcelona (BCN; Spain), Zurich (ZUE; Switzerland), Schiedam (SCH; The Netherlands), Leipzig-Mitte (LMI; Germany) and Lens (LENS; France).

Table S9: Allocation of PMF source contributions in each country. Mean values for the winter period (DJF) are reported.

	Source contribution [(A)]	Winter mean					
	SIA [μg/m^3; % of PM mass]	Traffic [μg/m^3; % of SIA]	Urban [μg/m^3; % of SIA]	Regional [μg/m^3; % of SIA]		Continental [μg/m^3; % of SIA]	
		Anthr.	Anthr.	Natural	Anthr.	Natural	Anthr.
Spain	8.3; 37.0		3.3; 40.0		3.0; 36.1		1.2; 14.8
Switzerland	12.2; 50.2		2.5; 20.3		9.8; 80.4		
The Netherlands	18.0; 65.1		3.9; 21.6		14.1; 78.4		
Germany	9.9; 36.1	1.6; 16.0	2.0; 20.1		6.4; 65.3		
France	5.5; 30.6		2.6; 47.1		2.9; 52.9		
		Winter mean					
	SSA [μg/m^3; % of PM mass]	Traffic [μg/m^3; % of SSA]	Urban [μg/m^3; % of SSA]	Regional [μg/m^3; % of SSA]		Continental [μg/m^3; % of SSA]	
		Anthr.	Anthr.	Natural	Anthr.	Natural	Anthr.
Spain	3.3; 14.7		0.8; 23.7		1.6; 47.8		0.9; 27.8
Switzerland	3.3; 13.5		1.0; 32.1		2.3; 70.6		
The Netherlands	4.2; 15.2		0.3; 6.1		4.0; 93.9		
Germany							
France	2.3; 13.1		0.8; 32.6		1.6; 67.4		
		Winter mean					
	NSA [μg/m^3; % of PM mass]	Traffic [μg/m^3; % of NSA]	Urban [μg/m^3; % of NSA]	Regional [μg/m^3; % of NSA]		Continental [μg/m^3; % of NSA]	
		Anthr.	Anthr.	Natural	Anthr.	Natural	Anthr.
Spain	5.0; 22.3		3.0; 60.9		1.6; 32.4		0.3; 6.2
Switzerland	8.9; 36.8		1.4; 16.0		7.5; 83.9		
The Netherlands	13.8; 50.0		3.6; 26.3		10.2; 73.7		
Germany							
France	3.1; 17.5		1.8; 58.0		1.3; 42.0		
		Winter mean					
	Mineral [μg/m^3; % of PM mass]	Traffic [μg/m^3; % of Mineral]	Urban [μg/m^3; % of Mineral]	Regional [μg/m^3; % of Mineral]		Continental [μg/m^3; % of Mineral]	
		Anthr.	Anthr.	Natural	Anthr.	Natural	Anthr.
Spain	1.7; 7.3		0.7; 43.2	0.5; 31.5		0.4; 24.3	
Switzerland	1.0; 4.1		0.3; 28.7	0.7; 66.7			
The Netherlands	0.3; 1.1		0.16; 49.7	0.16; 50.3			
Germany	0.09; 0.3	0.0; 0.0	0.03; 39.9	0.06; 68.3			
France	3.0; 16.7		1.6; 54.1	1.4; 45.9			
		Winter mean					
	Road traffic [μg/m^3; % of PM mass]	Traffic [μg/m^3; % of RT]	Urban [μg/m^3; % of RT]	Regional [μg/m^3; % of RT]		Continental [μg/m^3; % of RT]	
		Anthr.	Anthr.	Natural	Anthr.	Natural	Anthr.
Spain	5.6; 25.1		5.2; 92.9		0.4; 7.1		0.1; 1.4
Switzerland	3.1; 12.8		2.7; 86.5		0.4; 12.9		
The Netherlands	3.6; 13.0		2.1; 59.4		1.5; 40.6		
Germany	5.3; 19.2	4.0; 76.2	1.1; 20.5		0.3; 5.9		
France	1.1; 6.3		0.9; 84.0		0.2; 16.0		
		Winter mean					
	SS [μg/m^3; % of PM mass]	Traffic [μg/m^3; % of SS]	Urban [μg/m^3; % of SS]	Regional [μg/m^3; % of SS]		Continental [μg/m^3; % of SS]	
		Anthr.	Anthr.	Natural	Anthr.	Natural	Anthr.
Spain	4.1; 18.0			4.1; 100			

Switzerland	2.0; 8.4			2.0; 100			
The Netherlands	3.5; 12.5			3.5; 100			
Germany	0.9; 3.2			0.9; 100			
France	3.6; 20.1			3.6; 100			
		Winter mean					
	Biomass burning [μg/m^3; % of PM mass]	Traffic [μg/m^3; % of BB]	Urban [μg/m^3; % of BB]	Regional [μg/m^3; % of BB]		Continental [μg/m^3; % of BB]	
		Anthr.	Anthr.	Natural	Anthr.	Natural	Anthr.
Spain							
Switzerland	5.3; 21.9		1.4; 26.8		3.9; 73.1		
The Netherlands							
Germany	2.1; 7.8	0.0; 0.0	0.5; 21.2		1.7; 77.8		
France	4.6; 25.7		2.7; 59.4		1.9; 40.6		
		Winter mean					
	V-Ni [μg/m^3; % of PM mass]	Traffic [μg/m^3; % of V-Ni]	Urban [μg/m^3; % of V-Ni]	Regional [μg/m^3; % of V-Ni]		Continental [μg/m^3; % of V-Ni]	
		Anthr.	Anthr.	Natural	Anthr.	Natural	Anthr.
Spain	1.2; 5.3		0.9; 78.8		0.2; 20.9		0.0; 0.4
Switzerland							
The Netherlands	0.5; 1.6		0.4; 85.6		0.1; 14.4		
Germany							
France							
		Winter mean					
	Industrial [μg/m^3; % of PM mass]	Traffic [μg/m^3; % of Ind]	Urban [μg/m^3; % of Ind]	Regional [μg/m^3; % of Ind]		Continental [μg/m^3; % of Ind]	
		Anthr.	Anthr.	Natural	Anthr.	Natural	Anthr.
Spain	0.1; 0.3		0.1; 83.7		0.01; 13.9		0.00; 3.5
Switzerland							
The Netherlands	1.8; 6.3		0.1; 4.5		1.7; 95.3		
Germany							
France							
		Winter mean					
	Germany [μg/m^3; % of PM mass]	Traffic [μg/m^3; % of Ind]	Urban [μg/m^3; % of Ind]	Regional [μg/m^3; % of Ind]		Continental [μg/m^3; % of Ind]	
		Anthr.	Anthr.	Natural	Anthr.	Natural	Anthr.
Coal_Local	0.03; 0.12	0.00; 6.6	0.00; 1.6		0.03; 86.7		
Coal	4.4; 15.9	0.5; 11.4	0.0; 0.0		3.9; 90.0		
Cooking	0.8; 2.9	0.3; 33.7	0.3; 41.1		0.2; 24.7		
Photochemistry	1.3; 4.7	0.1; 5.9	0.0; 0.0		1.2; 94.6		
SS/RS	0.5; 1.9	0.12; 44.8	0.2; 31.8		0.1, 28.1		
Fungal spores	0.0; 0.0			0.0; 0.0			
		Winter mean					
	France [μg/m^3; % of PM mass]	Traffic [μg/m^3; %]	Urban [μg/m^3;%]	Regional [μg/m^3; %]		Continental [μg/m^3; %]	
		Anthr.	Anthr.	Natural	Anthr.	Natural	Anthr.
Marine bio	0.1; 0.6			0.1; 100			
Land bio	0.6; 3.6			0.6; 100			

(A) Source contributions calculated for Barcelona (BCN; Spain), Zurich (ZUE; Switzerland), Schiedam (SCH; The Netherlands), Leipzig-Mitte (LMI; Germany) and Lens (LENS; France).

Table S10: Allocation of PMF source contributions in each country. Mean values for the summer period (JJA) are reported.

	Source contribution (A)	**Summer mean**					
	SIA [μg/m³; % of PM mass]	Traffic [μg/m³; % of SIA]	Urban [μg/m³; % of SIA]	Regional [μg/m³; % of SIA]		Continental [μg/m³; % of SIA]	
		Anthr.	Anthr.	Natural	Anthr.	Natural	Anthr.
Spain	7.2; 27.7		0.9; 11.9		1.3; 18.7		5.0; 69.4
Switzerland	5.4; 39.5		1.2; 22.7		4.1; 76.5		
The Netherlands	6.2; 51.9		1.3; 20.6		4.9; 79.4		
Germany	2.1; 11.4	0.2; 8.5	0.6; 28.5		1.3; 61.8		
France	3.3; 16.3		1.3; 39.6		2.0; 60.0		
		Summer mean					
	SSA [μg/m³; % of PM mass]	Traffic [μg/m³; % of SSA]	Urban [μg/m³; % of SSA]	Regional [μg/m³; % of SSA]		Continental [μg/m³; % of SSA]	
		Anthr.	Anthr.	Natural	Anthr.	Natural	Anthr.
Spain	6.2; 23.7		0.6; 9.5		1.2; 19.2		4.4; 71.3
Switzerland	5.2; 37.7		1.0; 20.1		4.1; 78.5		
The Netherlands	2.9; 24.3		0.3; 17.8		2.6; 82.2		
Germany							
France	2.5; 12.5		0.6; 21.9		1.9; 77.3		
		Summer mean					
	NSA [μg/m³; % of PM mass]	Traffic [μg/m³; % of NSA]	Urban [μg/m³; % of NSA]	Regional [μg/m³; % of NSA]		Continental [μg/m³; % of NSA]	
		Anthr.	Anthr.	Natural	Anthr.	Natural	Anthr.
Spain	1.0; 4.0		0.3; 26.1		0.2; 15.8		0.6; 58.1
Switzerland	0.3; 1.9		0.2; 76.5		0.1; 33.5		
The Netherlands	3.3; 27.5		0.8; 23.1		2.5; 76.9		
Germany							
France	0.8; 3.9		0.8; 100.0		0.0; 0.0		
		Summer mean					
	Mineral [μg/m³; % of PM mass]	Traffic [μg/m³; % of Mineral]	Urban [μg/m³; % of Mineral]	Regional [μg/m³; % of Mineral]		Continental [μg/m³; % of Mineral]	
		Anthr.	Anthr.	Natural	Anthr.	Natural	Anthr.
Spain	3.9; 15.0		0.7; 18.0	0.1; 1.4		3.2; 80.6	
Switzerland	3.2; 23.1		0.9; 28.4	2.3; 72.1			
The Netherlands	0.3; 2.7		0.02; 6.0	0.3; 94.0			
Germany	1.1; 5.8	0.0; 0.0	1.1; 92.0	0.0; 8.0			
France	3.3; 16.3		0.3; 8.9	3.0; 90.1			
		Summer mean					
	Road traffic [μg/m³; % of PM mass]	Traffic [μg/m³; % of RT]	Urban [μg/m³; % of RT]	Regional [μg/m³; % of RT]		Continental [μg/m³; % of RT]	
		Anthr.	Anthr.	Natural	Anthr.	Natural	Anthr.
Spain	2.9; 11.0		2.5; 86.5		0.3; 11.7		0.1; 1.8
Switzerland	2.8; 20.4		2.4; 86.6		0.4; 14.5		
The Netherlands	0.6; 4.8		0.5; 88.8		0.0; 11.2		
Germany	5.1; 27.5	3.4; 66.2	1.3; 25.0		0.5; 8.9		
France	1.3; 6.3		1.0; 77.9		0.3; 23.2		
		Summer mean					
	SS [μg/m³; % of PM mass]	Traffic [μg/m³; % of SS]	Urban [μg/m³; % of SS]	Regional [μg/m³; % of SS]		Continental [μg/m³; % of SS]	
		Anthr.	Anthr.	Natural	Anthr.	Natural	Anthr.
Spain	6.9; 26.5			6.9; 100			

Switzerland	2.5; 18.1			2.5; 100			
The Netherlands	0.8; 6.7			0.8; 100			
Germany	0.9; 5.1			0.9; 100			
France	6.4; 31.5			6.4; 100			
		Summer mean					
	Biomass burning [μg/m^3; % of PM mass]	Traffic [μg/m^3; % of BB]	Urban [μg/m^3; % of BB]	Regional [μg/m^3; % of BB]		Continental [μg/m^3; % of BB]	
		Anthr.	Anthr.	Natural	Anthr.	Natural	Anthr.
Spain							
Switzerland	0.3; 2.2		0.02; 7.8		0.3; 88.2		
The Netherlands							
Germany	0.5; 2.8	0.0; 0.0	0.5; 96.2		0.0; 3.8		
France	0.0; 0.0		0.0; 0.0		0.0; 0.0		
		Summer mean					
	V-Ni [μg/m^3; % of PM mass]	Traffic [μg/m^3; % of V-Ni]	Urban [μg/m^3; % of V-Ni]	Regional [μg/m^3; % of V-Ni]		Continental [μg/m^3; % of V-Ni]	
		Anthr.	Anthr.	Natural	Anthr.	Natural	Anthr.
Spain	3.4; 13.2		1.9; 56.4		1.0; 30.3		0.5; 13.4
Switzerland							
The Netherlands	0.3; 2.9		0.3; 83.0		0.1; 17.0		
Germany							
France							
		Summer mean					
	Industrial [μg/m^3; % of PM mass]	Traffic [μg/m^3; % of Ind]	Urban [μg/m^3; % of Ind]	Regional [μg/m^3; % of Ind]		Continental [μg/m^3; % of Ind]	
		Anthr.	Anthr.	Natural	Anthr.	Natural	Anthr.
Spain	0.03; 0.1		0.03; 81.5		0.00; 11.6		0.00; 6.9
Switzerland							
The Netherlands	2.4; 19.9		0.1; 3.4		2.3; 95.7		
Germany							
France							
		Summer mean					
	Germany [μg/m^3; % of PM mass]	Traffic [μg/m^3; % of Ind]	Urban [μg/m^3; % of Ind]	Regional [μg/m^3; % of Ind]		Continental [μg/m^3; % of Ind]	
		Anthr.	Anthr.	Natural	Anthr.	Natural	Anthr.
Coal_Local	0.01; 0.03	0.00; 73.7	0.00; 0.0		0.00; 24.1		
Coal	0.03; 0.2	0.02; 67.1	0.0; 0.0		0.01; 33.3		
Cooking	1.5; 8.2	1.0; 65.1	0.5; 31.0		0.0; 4.0		
Photochemistry	2.7; 14.6	0.2; 7.4	0.3; 10.1		2.2; 83.0		
SS/RS	0.5; 2.4	0.0; 8.0	0.5; 91.0		0.0, 0.0		
Fungal spores	0.4; 2.0			0.0; 0.0			
		Summer mean					
	France [μg/m^3; % of PM mass]	Traffic [μg/m^3; %]	Urban [μg/m^3;%]	Regional [μg/m^3; %]		Continental [μg/m^3; %]	
		Anthr.	Anthr.	Natural	Anthr.	Natural	Anthr.
Marine bio	3.8; 18.4			3.8; 100			
Land bio	2.4; 12.0			2.4; 100			

(A) Source contributions calculated for Barcelona (BCN; Spain), Zurich (ZUE; Switzerland), Schiedam (SCH; The Netherlands), Leipzig-Mitte (LMI; Germany) and Lens (LENS; France).